

**STRENGTH COMPARISON OF MASONRY WALL MADE
OF CLAY BURNT BRICK WITH FROG MARK AND
MACHINE MADE BRICK WITHOUT FROG MARK**

A Thesis

by

Mohammad Rafiqul Islam

MASTER OF SCIENCE IN CIVIL ENGINEERING (STRUCTURAL)



**DEPARTMENT OF CIVIL ENGINEERING
BANGLADESH UNIVERSITY OF ENGINEERING AND TECHNOLOGY
DHAKA, BANGLADESH**

July, 2017

**STRENGTH COMPARISON OF MASONRY WALL MADE
OF CLAY BURNT BRICK WITH FROG MARK AND
MACHINE MADE BRICK WITHOUT FROG MARK**

by

Mohammad Rafiqul Islam

A thesis submitted to the Department of Civil Engineering of Bangladesh University of Engineering and Technology, Dhaka, in partial fulfillment of the requirements for the degree

of

MASTER OF SCIENCE IN CIVIL ENGINEERING (STRUCTURAL)



DEPARTMENT OF CIVIL ENGINEERING
BANGLADESH UNIVERSITY OF ENGINEERING AND TECHNOLOGY
DHAKA, BANGLADESH

July, 2017

CERTIFICATE OF APPROVAL

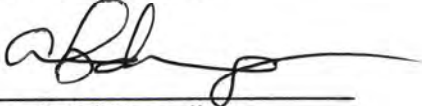
This thesis titled “Strength Comparison of Masonry Wall Made of Clay Burnt Brick With Frog Mark and Machine Made Brick Without Frog Mark”, submitted by Mohammad Rafiqul Islam, Student Number 0413042329(F) Session: April 2013, has been accepted as satisfactory in partial fulfillment of the requirements for the degree of **Master of Science in Civil Engineering (Structural)** on 03 July, 2017.

BOARD OF EXAMINERS



Dr. Raquib Ahsan
Professor
Department of Civil Engineering
BUET, Dhaka-1000

Chairman
(Supervisor)



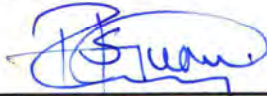
Dr. Abdul Muqtadir
Professor and Head
Department of Civil Engineering
BUET, Dhaka-1000

Member
(Ex-officio)



Dr. Mahbuba Begum
Professor
Department of Civil Engineering
BUET, Dhaka-1000

Member



Dr. Major Md. Soebur Rahman
Instructor Class B
Department of Civil Engineering
MIST, Mirpur Cantonment, Dhaka

Member
(External)

DEDICATION

This thesis is dedicated to my parents and teachers

DECLARATION

It is hereby declared that, except where specific references are made, the work embodied in this thesis is the result of investigation carried out by the author under the supervision of Dr. Raquib Ahsan, Professor, Department of Civil Engineering, BUET.

Neither the thesis nor an part of it is concurrently submitted elsewhere for the award of any degree or diploma.



(Signature of the Student)

Mohammad Rafiqul Islam

ACKNOWLEDGEMENT

First and foremost, I would like to admit the blessings of almighty, merciful, gracious Allah who enables me to accomplish this thesis successfully.

I would like to take this opportunity to express my profound gratitude and deep regard to my thesis supervisor Professor Dr. Raquib Ahsan, Department of Civil Engineering, Bangladesh University of Engineering and Technology (BUET) for his exemplary guidance, quick response and constant encouragement throughout the duration of the research. His valuable suggestions and enthusiastic supervision were of immense help throughout my research work. Working under him was an extremely knowledgeable experience for me.

I wish to express my gratitude and heartiest thanks to respected defence committee members Prof. Dr. Abdul Muqtadir, Prof. Dr. Mahbuba Begum and Instructor Dr. Major Md. Soebur Rahman for their valuable advice and help in reviewing this thesis.

I would like to thank Tonmoy Das and all laboratory members for their advice and technical support throughout the experimental program.

The author also appreciatively remembers the assistance and encouragement of his friends and well wishers and everyone related to carry out and complete this study. Finally, the author wishes to express his deep gratitude to his family members, parents and sisters for their constant support, encouragement and sacrifice throughout the research work.

.

ABSTRACT

Compressive strength, shear strength and Modulus of elasticity of masonry are significant parameters when considering structural masonry design. For simulation of structural behavior of masonry buildings, performance of embedded joint is important from the point of view of seismic design. Masonry structures of Bangladesh are mostly designed for vertical loads. The structural elements such as walls which were designed for vertical loads only, have to carry lateral load as well during an earthquake. Important masonry parameters are compressive strength, flexural strength, shear strength, modulus of elasticity etc. An attempt has been made in this study to correlate compressive strength, shear strength and wall stiffness, for clay burnt bricks with frog mark and machine made bricks without frog mark.

In this experimental study, eight prisms and eight (10") URM wall specimens with a size of $5' \times 3'$ were constructed with two different types of bricks, i.e clay burnt brick with frog mark and machine made brick without frog mark. Two types of mortar thicknesses $1/2''$ and $3/4''$ were used in the test specimens.

The prism specimens were tested under axial compression normal to the bed joints and the wall specimens were tested under horizontal incremental cyclic loading along with constant axial compressive load. Lateral loading was applied using a loading control pattern. The specimens were tested under cyclic loading conditions displacing them laterally, along the axis of the walls and their load-deformation behavior was measured by dial gauges. It is observed that, increasing mortar thickness prism ultimate strength increases 18.0% for clay burnt brick and with increasing mortar thickness prism ultimate strength increases 1.3% for machine made brick. On the other hand, with the increasing mortar thickness ultimate shear strength decreases 9.6% for clay burnt brick with frog mark and with increasing mortar thickness ultimate shear strength decreases 8.0% for machine made bricks without frog mark. In clay burnt brick shear strength is 12.5% more than machine made brick. Increasing mortar thickness ductility decreases 22.0% for clay burnt brick and 20.0% for machine made bricks.

TABLE OF CONTENTS

ACKNOWLEDGEMENT	iv
ABSTRACT	v
TABLE OF CONTENTS	vi
LIST OF FIGURES	x
LIST OF TABLES	xiv
LIST OF NOTATIONS	xv
CHAPTER 1 INTRODUCTION	
1.1 General	1
1.2 Background of the Study	2
1.3 Objectives	4
1.4 Scope of Work	4
1.5 Organization of the Thesis	5
CHAPTER 2 LITERATURE REVIEW	
2.1 Introduction	6
2.2 Types of Masonry Wall	7
2.3 Joints of Masonry Wall	8
2.4 Bond of Brick Wall	8
2.5 Mechanical Properties of Masonry Materials	10
2.5.1 Masonry units	10
2.5.2 Mortars	10
2.5.3 Masonry	12
2.6 Behavior of Masonry Prisms	12
2.6.1 Previous research-masonry compressive strength	14
2.6.2 Code guide lines	17
2.7 Masonry Shear Strength	18
2.7.1 Why the shear bond strength is important	20
2.7.2 Applied loads that cause shear bond failure	20
2.7.3 Factors affecting the shear bond strength in masonry	21
2.8 Failure Modes of URM Walls	21

2.9 Factors affecting Shear Wall Response	23
2.9.1 Aspect ratio (H/L)	23
2.9.2 Pre-compression	24
2.9.3 Material properties	25
2.10 Previous Research – Masonry Shear Strength	26
CHAPTER 3 EXPERIMENTAL PROGRAMME	
3.1 General	31
3.2 Material Properties	31
3.2.1 Compressive strength of machine made bricks	31
3.2.2 Compressive strength of clay burnt bricks	32
3.2.3 Properties of sand	32
3.2.4 Properties of coarse aggregate	33
3.2.5 Cement	34
3.2.6 Properties of Mortar	34
3.3 Specimen Preparation	35
3.3.1 Scaffolding preparation	35
3.3.2 Reinforcement placement on formwork	36
3.3.3 Casting	37
3.3.4 Curing	37
3.3.5 Construction of test specimen (Masonry wall)	38
3.3.6 Construction of test specimen (Masonry prism)	39
3.4 Prism Test Setup	40
3.5 Experimental Shear Test Setup	42
3.6 Experimental Setup of wall Stiffness	45
3.6.1 Load selection	47
3.6.2 Testing procedure	48
CHAPTER 4 EXPERIMENTAL RESULTS AND DISCUSSION	
4.1 General	49
4.2 Failure Modes of Prism Test Specimen	49
4.2.1 Clay burnt brick prism with mortar thickness 1/2"	49
4.2.2 Clay burnt brick prism with mortar thickness 3/4"	50

4.2.3 Machine made brick prism with mortar thickness 1/2"	51
4.2.4 Machine made brick prism with mortar thickness 3/4"	52
4.3 Prism Strength	54
4.3.1 Properties of machine made brick prism	54
4.3.2 Properties of clay burnt brick prism	54
4.4 Failure Modes of Shear Test Specimen	55
4.4.1 Clay burnt brick with mortar thickness 1/2"	55
4.4.2 Clay burnt brick with mortar thickness 3/4"	56
4.4.3 Machine made brick with mortar thickness 1/2"	56
4.4.4 Machine made brick with mortar thickness 3/4"	57
4.5 Shear Strength	58
4.6 Failure Modes of wall Stiffness	59
4.6.1 Crack patterns of specimen wall C-1/2	59
4.6.2 Crack patterns of specimen wall C1-1/2	60
4.6.3 Crack patterns of specimen wall C-3/4	61
4.6.4 Crack patterns of specimen wall C1-3/4	62
4.6.5 Crack patterns of specimen wall M-1/2	63
4.6.6 Crack patterns of specimen wall M1-1/2	65
4.6.7 Crack patterns of specimen wall M-3/4	66
4.7 Load – Deformation Response	68
4.8 Summary of Test Results of Seven Specimens	73
4.9 Characteristics of First Crack Formation	74
4.10 Stiffness of Specimens	75
4.11 Load Characteristics	78
4.12 Maximum Displacement	79
4.13 Residual Displacement	80
4.14 Ductility of the Specimen Wall	82
4.15 Stiffness Degradation Calculation	84
4.16 Energy Dissipation Calculation	88
4.17 Hysteresis Damping	92
4.18 Relationship between Prism Strength and Shear Strength	95

4.19 Relationship between Lateral Load vs Shear Force	100
4.20 Relationship between Lateral Load vs Prism Strength	105
4.21 Relationship between Lateral Load vs Shear Strength	110
4.22 Relationship between Calculated Lateral load vs Tested Lateral Load	115
CHAPTER 5 SUMMARY, CONCLUSIONS AND RECOMMENDATIONS	
5.1 Summary	118
5.2 Conclusion	119
5.3 Recommendations	121
REFERENCES	122
APPENDIX-A	
APPENDIX-B	

LIST OF FIGURES

Figure 1.1 Severe damages at URM buildings after an earthquake	3
Figure 2.1 Stretcher bond	8
Figure 2.2 Header bond	8
Figure 2.3 English bond	9
Figure 2.4 Flemish bond	9
Figure 2.5 Schematic diagram of a prism test specimen	13
Figure 2.6 Diagrammatical explanation of the shear bond strength in masonry	19
Figure 2.7 Shear bond failure caused by foundation settlement	20
Figure 2.8 Shear bond failure caused by applied loads	21
Figure 2.9 Modes of failure of unreinforced masonry shear walls	23
Figure 2.10 Masonry shear walls	25
Figure 3.1 Grain size analysis of sand	33
Figure 3.2 Grain size analysis of coarse aggregate	33
Figure 3.3 Reinforcement placement on formwork	36
Figure 3.4 Compaction of fresh concrete into formwork using vibrator	37
Figure 3.5 Casted specimens with formwork	37
Figure 3.6 Curing of sample	38
Figure 3.7 Construction of brick wall specimen	39
Figure 3.8 Construction of masonry prisms	40
Figure 3.9 Test setup of masonry prisms	42
Figure 3.10 Hand grinding machine	42
Figure 3.11 Hammer and chisel	42
Figure 3.12 Experimental setup of shear test	44
Figure 3.13 Schematic diagram of loading condition during test	47
Figure 3.14 Experimental setup before starting test	48
Figure 4.1 Failure pattern of prism test specimen C-1/2	49
Figure 4.2 Failure pattern of prism test specimen C1-1/2	50
Figure 4.3 Failure pattern of prism test specimen C-3/4	51
Figure 4.4 Failure pattern of prism test specimen C1-3/4	51
Figure 4.5 Failure pattern of prism test specimen M-1/2	52

Figure 4.6 Failure pattern of prism test specimen M1-1/2	52
Figure 4.7 Failure pattern of prism test specimen M-3/4	53
Figure 4.8 Failure pattern of prism test specimen M1-3/4	53
Figure 4.9 Failure pattern of shear test specimen C-1/2	55
Figure 4.10 Failure pattern of shear test specimen C1-1/2	55
Figure 4.11 Failure pattern of shear test specimen C-3/4	56
Figure 4.12 Failure pattern of shear test specimen C1-3/4	56
Figure 4.13 Failure pattern of shear test specimen M-1/2	57
Figure 4.14 Failure pattern of shear test specimen M1-1/2	57
Figure 4.15 Failure pattern of shear test specimen M-3/4	57
Figure 4.16 Failure pattern of shear test specimen M1-3/4	58
Figure 4.17 Initial crack (flexure) pattern of specimen C-1/2	59
Figure 4.18 2nd crack (shear) pattern of specimen C-1/2	59
Figure 4.19 Final crack pattern of specimen wall C-1/2	59
Figure 4.20 Initial crack (flexure) pattern of specimen C1-1/2	60
Figure 4.21 2nd crack (shear) pattern of specimen C1-1/2	60
Figure 4.22 3rd crack (shear) pattern of specimen C1-1/2	61
Figure 4.23 Final crack pattern of specimen C1-1/2	61
Figure 4.24 Initial crack (flexure) patterns at base of specimen C-3/4	62
Figure 4.25 2nd cracks (shear) patterns of specimen C-3/4	62
Figure 4.26 3rd cracks (shear) patterns of specimen C-3/4	62
Figure 4.27 Final crack pattern of specimen C-3/4	62
Figure 4.28 Initial crack (flexure) patterns at specimen C1-3/4	63
Figure 4.29 2nd cracks (shear) patterns of specimen C1-3/4	63
Figure 4.30 Final crack pattern of specimen C1-3/4	63
Figure 4.31 Initial crack (flexure) patterns at specimen M-1/2	64
Figure 4.32 2 nd and 3 rd cracks patterns of specimen M-1/2	64
Figure 4.33 Final crack pattern of specimen M-1/2	64
Figure 4.34 Initial crack (flexure) patterns at specimen M1-1/2	65
Figure 4.35 2nd and 3rd cracks patterns of specimen M1-1/2	65
Figure 4.36 Final crack pattern of specimen M1-1/2	66

Figure 4.37 Initial crack (flexure) patterns at specimen M-3/4	67
Figure 4.38 2nd cracks patterns of specimen M-3/4	67
Figure 4.39 Final crack pattern of specimen M-3/4	67
Figure 4.40 Load- deformation response of specimen wall C-1/2	69
Figure 4.41 Load- deformation response of specimen wall C1-1/2	69
Figure 4.42 Load- deformation response of specimen wall C-3/4	70
Figure 4.43 Load- deformation response of specimen wall C1-3/4	70
Figure 4.44 Load- deformation response of specimen wall M-1/2	71
Figure 4.45 Load- deformation response of specimen wall M1-1/2	71
Figure 4.46 Load- deformation response of specimen wall M-3/4	72
Figure 4.47 Hysteresis loop envelopes of all types of specimens	72
Figure 4.48 Load at first crack formation of seven specimens	75
Figure 4.49 Secant stiffness of each cycle for seven samples	76
Figure 4.50 Degradation of stiffness of each cycle for seven specimens	76
Figure 4.51 Stiffness after 1st cycle of seven samples	77
Figure 4.52 Stiffness after final cycle of seven samples	77
Figure 4.53 The load of the specimens at every cycle	78
Figure 4.54 Maximum load of seven specimens	79
Figure 4.55 Maximum displacement of seven specimens	80
Figure 4.56 Residual displacement of seven specimens	81
Figure 4.57 Bilinear approximation for displacement ductility parameter	82
Figure 4.58 Ductility of the specimens	84
Figure 4.59 Stiffness degradation of specimen C-1/2	84
Figure 4.60 Stiffness degradation of specimen C1-1/2	85
Figure 4.61 Stiffness degradation of different types of walls	85-87
Figure 4.62 Energy dissipation calculation sample specimen (C-1/2)	88
Figure 4.63 Energy dissipation calculation sample specimen (C-3/4)	89
Figure 4.64 Energy dissipation of different types of walls	89-91
Figure 4.65 Equivalent viscous damping ratio for symmetric hysteresis loops	92
Figure 4.66 Equivalent viscous damping ratio for asymmetric hysteresis loops	93
Figure 4.67 Hysteresis damping percentage for wall assemblies	94

Figure 4.68 Relationship between shear strength & prism compressive strength of C-1/2"	96
Figure 4.69 Relationship between shear strength & prism compressive strength of C-3/4"	97
Figure 4.70 Relationship between shear strength & prism compressive strength of M-1/2"	98
Figure 4.71 Relationship between shear strength & prism compressive strength of M-3/4"	99
Figure 4.72 Relationship between lateral load vs shear force of C-1/2"	101
Figure 4.73 Relationship between lateral load vs shear force of C-3/4"	102
Figure 4.74 Relationship between lateral load vs shear force of M-1/2"	103
Figure 4.75 Relationship between lateral load vs shear force of M-3/4"	104
Figure 4.76 Relationship between horizontal load vs prism strength of different types of wall	106-109
Figure 4.77 Relationship between horizontal load vs shear strength of different types of wall	111-114
Figure 4.78 Relationship between calculated lateral load vs tested lateral load of different types of wall	116-117

LIST OF TABLES

Table 3.1 Compressive strength of machine made bricks	32
Table 3.2 Compressive strength of clay burnt bricks	32
Table 3.3 Compressive strength of mortar (7-days)	34
Table 3.4 Compressive strength of mortar (14-days)	34
Table 3.5 Compressive strength of mortar (28-days)	35
Table 3.6 Applied loading histories	46
Table 4.1 Compressive strength of machine made brick prism 1/2" mortar thickness	54
Table 4.2 Compressive strength of machine made brick prism 3/4" mortar thickness	54
Table 4.3 Compressive strength of clay burnt brick prism 1/2" mortar thickness	54
Table 4.4 Compressive strength of clay burnt brick prism 3/4" mortar thickness	55
Table 4.5 Shear strength value	58
Table 4.6 Test results of seven specimens	73
Table 4.7 Secant stiffness (average of L/D) of seven specimens at each cycle	73
Table 4.8 Characteristics of first crack of seven specimens	74
Table 4.9 Maximum displacement of each specimen during test	79
Table 4.10 Residual displacement of each specimen during test	80

NOTATIONS

A = Effective area of masonry

A_g = Gross area of wall

E_d = Energy dissipation per cycle

E_s = Elastic strain energy

f_v = Computed shear stress due to design load

f_m' = Specified compressive strength of masonry at the age of 28 days

F_a = Allowable average axial compressive stress for centroidally applied axial load only

F_b = Allowable flexural compressive stress if members were carrying bending load only

h' = Effective height of a wall or column

H = Height of wall

K = Effective stiffness

L = Length of a wall or segment

t = Effective thickness of a wythe, wall or column

μ = The friction coefficient between the interfaces

τ_u = Average stress

τ_o = Initial stress without any pre-compression applied

σ_n = The applied pre-compression, i.e. the vertical load applied to the specimen before testing

σ_{pc} = Pre-compression

μ_Δ = Displacement ductility

Δ = Deformation at given response level

Δ_y = Deformation at ideal yield

ξ_{eq} = Equivalent viscous damping ratio

CHAPTER 1

INTRODUCTION

1.1 General

Masonry has been used as a common construction material worldwide for many centuries. However, the vulnerability of unreinforced masonry systems was highlighted during past and recent earthquakes (K.C Voon and J.M Ingham, 2013). Old masonry buildings are integral and very important part of housing infrastructure in Bangladesh. Old masonry buildings are generally exposed to a very high seismic risk due to high seismic vulnerability inherent in such buildings. For simulation of structural behavior of such buildings, performance of embedded joint is important from the point of view of seismic design. Masonry structures of Bangladesh are mostly designed only for vertical loads. The structural elements such as walls which were designed for vertical loads only, have to carry lateral load as well during an earthquake. Important masonry parameters are compressive strength, flexural strength, shear strength, modulus of elasticity, creep and thermal expansion etc.

Compressive strength test of masonry prism is to be conducted according to ASTM C1314. Compressive strength of masonry is dependent on numerous factors such as mortar strength, unit strength, relative value of units and mortar strength, aspect ratio of the units (ratio of height to least horizontal dimension), and orientation of the units in relation to the direction of the applied load. Those factors give indications of the complexity of making an accurate assessment of masonry strength.

The masonry shear walls are the main seismic load resisting elements in unreinforced masonry buildings. The in-plane shear resistance and the out-of-plane bending capacity of the walls are their main lines of defense against earthquake loads. Shear strength of masonry mortar joint is to be determined in accordance with ASTM C1531. The shear and bending capacities of brick walls are dependent on the ability of the horizontal mortar joints (bed joints) and the vertical mortar joints (head joints) to transfer the loads through the brick units; they also depend on the mode of failure of the wall. A number of investigators have studied the behaviour of the mortar bed joints and head joints and their effects on the global strength and response of the wall. The prevalent view of the behaviour of the mortar joint, models the response on a - Columb shear failure mechanism assigning bond strength and friction for bed joints. In an earlier study, Stafford-

Smith and Carter (1971) questioned this model and proposed that the failure of mortar bed joints occurs in tension and therefore it may be predicted more rationally by comparing the actual tensile stresses in the mortar layer with its tensile strength. El-Sakhawy, et-al (2002) also investigated the behaviour of mortar joints in masonry walls under shear.

1.2 Background of the Study

Masonry construction was very common from the beginning of the civil construction technique over the whole world. Clay bricks have been employed for at least 10,000 years. They were made from sun-dried bricks and widely used in Babylon, Egypt, Spain, South American, United States and elsewhere (Drysdale et al. 1994). Older buildings mostly consist of unreinforced masonry (URM) walls. The URM elements are constructed from hand-placed units of natural or manufactured material such as clay-brick etc. and one stacked atop another and jointed to each other with mortar. The properties of bricks are influenced by the nature of the clays, methods of molding and the firing. Pure clays are useless for brick making unless they are mixed with a non-plastic material and this is different for every country or region. As the properties of clays vary throughout the world, it will be apparent that different kinds of bricks predominate in different regions. Most of the masonry buildings are designed primarily to resist gravity loads only since the provision for earthquake loading codes are not established. It was observed in frequent earthquakes that older masonry structures perform poorly and most of those buildings would collapse in a major earthquake. The clay brick material is relatively heavy, brittle, of low tensile strength and show low ductility when subjected to seismic excitation. Some historical performance of unreinforced masonry buildings throughout past earthquakes are shown on Figure 1.1. A number of common failures of URM buildings have been observed from around the world. Bruneau (1994), regrouped the failure performances as follows: lack of anchorage, anchor failure, in-plane failures, out-of-plane failure, combined in-plane and out-of-plane effects and diaphragm-related failures. Many older URM-buildings lack positive anchorage of the floors and roof to the URM-walls, which contribute to sudden failure under seismic excitation. The in-plane failure characterized by a shear crack pattern, where cracks are primarily along the mortar bed joints; some inclined cracks may also be developed.



(a) Armenia earthquake December 7, 1988



(b) Northridge earthquake January 17, 1994



(c) Bengkulu earthquake –Indonesia
June 4, 2000



(d) Nisqually earthquake February 28, 2001

Figure 1.1. Severe damages at URM buildings after an earthquake

The exact crack pattern will, of course, depend on the wall boundary conditions and the aspect ratio of the URM elements. Seismic actions are bidirectional and the URM can perform in both in-plane and out-of-plane direction. The in-plane failure characterized by a shear crack pattern, where cracks are primarily along the mortar bed joints; some inclined cracks may also be developed.

1.3 Objectives

The objectives of the study is

- i. To determine the compressive strength of masonry prism by prism test.
- ii. To determine the shear strength of masonry by shear test.
- iii. To find out the shear behavior of unreinforced masonry (URM) wall constructed with clay burnt brick and machine made brick with variables mortar thickness. Mortar thickness was varied 1/2" and 3/4".
- iv. To develop a relation between compressive strength measured by prism test and shear strength measured by shear test of clay burnt brick with frog mark and machine made brick without frog mark.

1.4 Scope of Work

To achieve the objectives mentioned above experimental studies were conducted. Experimental program consisted of eight prisms for two different types of bricks. Out of eight prisms four prisms were made of clay burnt brick with two mortar thicknesses 1/2" and 3/4" respectively. Four prisms were made of machine made bricks with two mortar thicknesses 1/2" and another two mortar thickness 3/4". Eight (10 inch) URM wall with a size of 5' × 3' were constructed for shear test and wall stiffness test. Out of eight URM wall four walls were made of clay burnt brick and another four walls were made of machine made bricks with two mortar thickness 1/2" and another two with mortar thickness 3/4". No bond wrench test was done.

1.5 Organization of the Thesis

This thesis is divided into five chapters. An introduction to the study is presented in Chapter 1. It includes the research background, objectives and the scope of the study. Chapter 2 presents a brief review on the literature related to masonry structure, prism test, shear test and stiffness of masonry structure. Chapter 3 presented the experimental test program where includes material properties, specimens preparation and experimental setup of masonry walls to be examined. This chapter presents the step by step construction procedure of specimens and adopted procedure for testing under cyclic loading in detail. It includes the details of the casting procedures, test setups, and test instrumentation. Chapter 4 presents the results from the experimental program of this research. The experimental results and observation for different loading conditions were also included in this chapter. A summary of the methodology and conclusions regarding the achievements of this research work were included in Chapter 5, along with the recommendations for future research.

CHAPTER 2

LITERATURE REVIEW

2.1 Introduction

Masonry units form the main part of masonry structure. Units are produced from clay, concrete and calcium silicate. All units have broadly similar uses although their properties differ depending on the raw materials and the method of manufacture. The selection of a particular type of unit for any given structure is also dependent on strength, durability, adhesion, fire resistance, thermal properties, acoustic properties and aesthetics. Bricks and blocks are produced in many formats: solid, perforated, and hollow. The specifications for the sizes of clay brick and machine made brick are given in BNBC respectively. The standard work sizes for individual clay brick units are 225 mm length x 105 mm width x 70 mm height and machine made bricks are 250 mm length x 120 mm width x 75 mm height. Masonry can be regarded as an assemblage of structural units which are bonded together in a particular pattern by mortar or grout. It is well known as being strong in compression but weak in tension. Parameters which are most significant when considering structural masonry design relate to strength and elastic properties; e.g. compressive strength, flexural strength, shear strength, modulus elasticity, coefficient of friction, creep, moisture moment and thermal expansion. Tensile strength is generally ignored in masonry. Compressive strength of masonry is dependent on numerous factors such as mortar strength, unit strength, relative value of units and mortar strength, aspect ratio of the units (ratio of height to least horizontal dimension), and orientation of the units in relation to the direction of the applied load. Those factors give indications of the complexity of making an accurate assessment of masonry strength.

The main objective of this study is to investigate the behavior and strength of masonry prisms with the focus on the effect of the loading direction. The findings are incorporated in evaluating the in-plane strength of masonry infills. The following literature review attempts to summarize the existing research on behavior and strength of masonry prisms and the in-plane strength of masonry infills.

This chapter presents review of different studies incorporating the performances of unreinforced masonry walls. Not much research on unreinforced masonry walls has been conducted in Bangladesh. Studies have also been undertaken to analyze the response of URM walls due to

gravity loading and lateral loading. This section will briefly summarize previous research relating to the material components of masonry and in-plane performance of URM walls.

This study also provides a brief review of literature regarding the unreinforced masonry shear walls. Conventional and high bond strength masonry shear walls are reviewed with particular focus on their modes of failure. Experimental investigations and numerical modelling strategies reported in the literature are included. The gaps in the literature with particular reference to high bond strength, thin layer mortared masonry are also identified and discussed.

2.2 Types of Masonry Wall

- **Cavity Wall:** A wall comprising two limbs each built up as single or multi wythe units and separated by a 50 - 115 mm wide cavity. The limbs are tied together by metal ties or bonding units for structural integrity.
- **Curtain Wall:** A non load bearing self supporting wall subject to transverse lateral loads, and laterally supported by vertical or horizontal structural member where necessary.
- **Faced Wall:** A wall in which facing and backing of two different materials are bonded together to ensure common action under load.
- **Load Bearing Wall:** A wall designed to carry an imposed vertical load in addition to its own weight, together with any lateral load.
- **Partition Wall:** An interior non load bearing wall, one story or part story in height.
- **Panel Wall:** An exterior non load bearing wall in framed structure, supported at each story but subject to lateral loads.
- **Shear Wall:** A load bearing wall designed to carry horizontal forces acting in its own plane with or without vertical imposed loads.
- **Veneered Wall:** A wall in which the facing is attached to the backing but not so bonded as to result in a common action under load.

2.3 Joints on Masonry Wall

- Bed joints: the mortar joint that is horizontal at the time the masonry units are placed.
- Collar joints: the vertical, longitudinal, mortar or grouted joints.
- Head joints: the mortar joint having a vertical transverse plane.

2.4 Bond of Brick Wall

- Stretcher Bond: The length of the brick its along with the face of the wall.

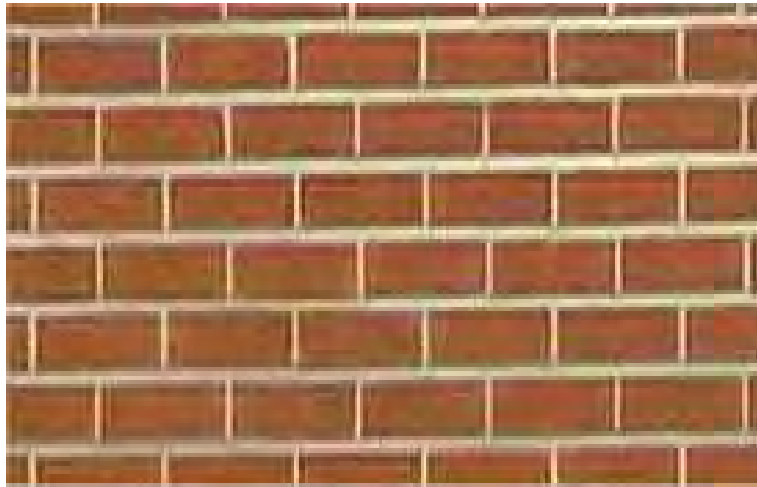


Figure 2.1 Stretcher Bond

- Header Bond: The width of the bricks are thus along the direction of the wall.

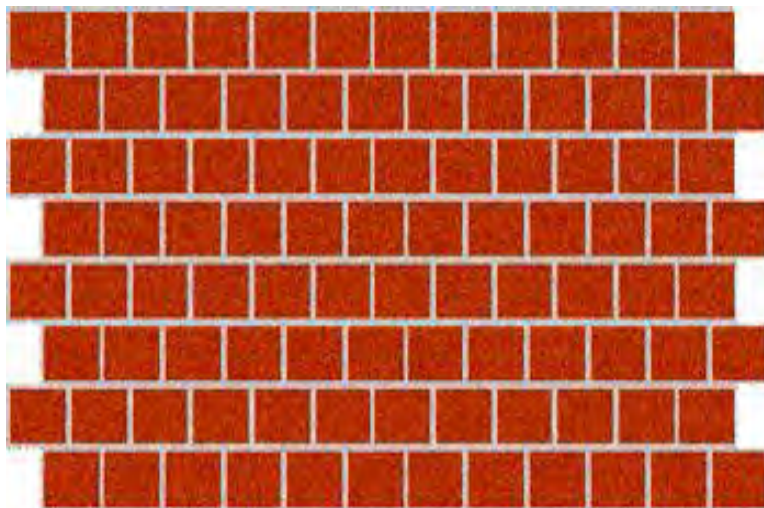


Figure 2.2 Header Bond

- English Bond: It is the most commonly used methods, this bond is considered to be the strongest. This bond consists of alternate course of stretchers and headers.



Figure 2.3 English Bond

- ▶ Flemish Bond :In this type of course is comprised of alternative headers and stretchers



Figure 2.4 Flemish Bond

2.5 Mechanical Properties of Masonry Materials

Masonry is a nonhomogeneous material consisting of bricks and mortar in filled joints. Both have certain strengths and deformation capabilities. Only a proper balance between the right type of mortar and the right type of brick can give a good result for bearing walls. The strength value of brick work is also strongly influenced by the workmanship. This section will discuss the properties of the brick units, the mortar and their behaviour in masonry walls.

2.5.1 Masonry Units

Currently there are various types of masonry units produced from a variety of raw materials such as clay, calcium silicate (sand lime brick), stone and concrete and by a variety of production methods. Regarding its shape, however, clay brick is still produced in a rectangular shape for easy handling. In this research programme only clay brick material will be investigated. Clay brick as a building element is made of clay with or without a mixture of other substances, burned at an adequately high temperature to prevent it from crumbling again when soaked in water. Bricks can be classified as solid or hollow. Most building codes define a brick as solid if the net cross-sectional area in every plane parallel to a bearing surface is 75% or more of its gross cross-sectional area measured in the same plane. The hollow brick is defined if the cores, cells, or hollow spaces within the total cross-sectional area exceed 25% of the cross section of the unit.

2.5.2 Mortars

Although mortars form only a small proportion of brickwork as a whole, their characteristics have a big influence on the quality of the brickwork. Batching and mixing are also an essential factor that has a great influence on both strength and workability of mortars. Mortar is used as a means of sticking or bonding bricks together and to take up all irregularities in the bricks. To do this the mortar must be well workable so that all joints are filling completely. There are two things of importance for the workability, stiffness and plasticity. The stiffness is dependent upon how much water there is added to the mortar. How much water to add depends on what one is to use the mortar for, and does not say anything about the quality, but it is a characteristic of the condition. The plasticity is a term for how easy the mortar can be formed. A binder rich mortar has a better plasticity than a binder poor mortar. The grading of the aggregate also has a certain influence on the plasticity, the closer the grading is to the ideal curve the better the plasticity.

The water content is calculated after the water is added to the dry mortar. The moisture in the aggregate is not considered in this calculation. The water content in the aggregate was about 20% by weight.

According to BNBC (1993), Mortar shall consist of a mixture of cementitious material and aggregates to which sufficient water and approved additives, if any, have been added to achieve a workable, plastic consistency. Cementitious materials for mortar shall be one or more of the following: lime, masonry cement, Portland cement and mortar cement. Mortar for masonry construction other than the installation of ceramic tile shall conform to the requirements of ASTM C270, Mortar for Unit Masonry.

Curing of mortar cubes : according to ASTM C-270, should be stored as follows : Mortars where cement is the main binder, cubes must be cured in a relative humidity of 90 % or more and kept in the moulds for from 48 – 52 hours, in such a manner that the upper surfaces shall be exposed to the moist air. Different mortar strengths are obtained by changing the aggregate ratio. Mortars, which only contain lime as a binder normally, have a strength of 0.5 to 1 MPa, cement-lime mortars strength varies from 1 to 10 MPa and pure cement mortar strengths ranges from 10 to 20 MPa.

Various types of cement can be used for mortar, such as ordinary Portland cement or Masonry cement. Ordinary Portland cement should conform to ASTM C-150 standard and Masonry cement should conform to ASTM C-207 standard.

The sand for mortar should be clean, sharp and free from salt and organic contamination (Hendry et al., 1997). Most natural sand contains a small quantity of silt or clay. A small quantity of silt improves the workability. Specifications of sand should conform to ASTM C- 144 standard, prescribe grading limits for the particle size distribution. Mixing water for mortar should be clean and free from contaminants either dissolved or in suspension. Ordinary water will be suitable.

2.5.3 Masonry

Clay-brick material with a relatively heavy specific gravity is capable of resisting axial load force but is weak in resisting tensile and shear load. In accordance with its character clay brick becomes a structural element of low ductility. In the event of an earthquake an unreinforced masonry building often experiences damage so that unreinforced masonry construction is no longer recommended for buildings in seismic prone regions.

The tensile strength of masonry is very low, in the order of 1.5 to 2 % of its compressive strength. Normally brickwork strength is strongly correlated to the strength of the mortar. It mortar strength when the elasticity modulus of brick and mortar are approximately equal appears that masonry strength may vary between the $1/3$ power and the $2/3$ power of the of the mortar strength when the elasticity modulus of brick and mortar are approximately equal (Sahlin, 1971). Because of specific characteristics of each constituent masonry materials, especially the masonry unit, it is not easy to predict the mechanical characteristics of a specific masonry construction type by knowing only the characteristics of its constituent materials, mortar and masonry units. It is therefore of relevant importance that, for each type of masonry, experiments to correlate the strength characteristics of constituent materials with the characteristics of masonry are carried out.

2.6 Behavior of Masonry Prisms

A masonry prism is an assemblage of masonry units and mortar that is constructed to serve as a test specimen for determining properties of masonry assemblages. In this research, prisms were constructed by assembling of bricks, one on top of the other, using mortar as the bonding material.

Masonry has been used primarily as the gravity load bearing material to resist compression. For example, masonry walls and columns are designed to resist vertical loads. Therefore, the compressive strength of masonry prisms is the most important property required in the design of structural masonry. In this case, the compressive forces are applied normal to the bed joint and thus the masonry compressive strength f_m' is obtained by subjecting the masonry prisms in compression normal to the bed joint in the experimentation. However, there are other masonry members, such as beams and flexural walls spanning horizontally which rely on the compressive strength of masonry parallel to bed joints.

Masonry prism behavior and strength under vertical loading has been a fundamental research topic for the past six decades and many influential parameters on the prism strength have been researched in the form of experimentation and numerical modeling. A detailed literature review is provided in Section 2.6.1. The following gives a basic understanding of the behavior of masonry prisms. Figure 2.5 shows a schematic diagram of a prism test specimen.

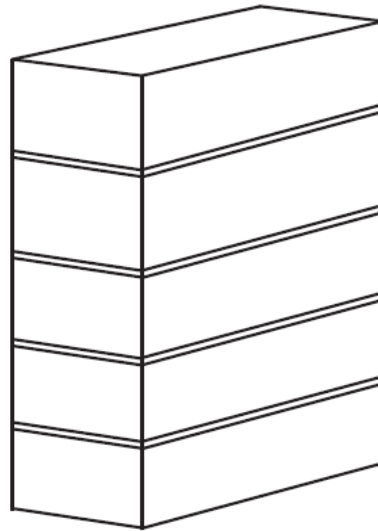


Figure 2.5 Schematic diagram of a prism test specimen.

It has been established that the compressive strength of the masonry assemblage differs from the compressive strength of individual components of the prism. Typical compressive strength of masonry units is relatively high but the compressive strength of mortar is low. The resulted prism strength is found to be somewhere in between.

Two types of failure modes are commonly observed for masonry prisms in compression. One is masonry crushing for weak units and the other is the vertical cracking through either the face-shell or web of the prism. For the latter mode, the vertical compressive stresses applied are transferred to the mortar, which results in the mortar expanding laterally. The masonry unit resists the expansion of the mortar and thus creates lateral confined compressive stresses in the mortar and lateral tensile stresses in the unit. Due to the low tensile strength of the masonry, cracking through the flange or web of the units is formed which results in the final failure of the prism.

2.6.1 Previous Research - Masonry Compressive Strength

Hegemier et al. (1978) investigated the compressive strength of concrete masonry prisms normal to the bed joint. The authors found that prism strength was primarily a function of the number of bed joints and not the h/t ratio. Bond pattern was observed to have an effect on strength. The authors recommended that prisms be constructed from four or five courses with either three or four mortar bed joints.

Boult (1979) aimed to determine a relationship between the compressive strength and the height of concrete masonry prisms made of different types of masonry blocks. A series of stack bonded prisms with h/d (height-to-least lateral dimension) of 2 to 5 were constructed for each masonry unit type. Test results showed that the compressive strength decreased as the prism height increased and the rate of decline was dependent on the block type. Results also showed that the decrease in strength as height increased appeared to be insignificant between the 5- course high prisms and the 12- course high columns. Boult suggested that careful consideration of the material properties of the units and grout should be taken into account when assembling the prisms.

Drysdale and Hamid (1980) studied the failure modes and strength of both the concrete and brick masonry prisms when subjected to compression applied at designated angles in relation to the bed joint. Axial compression both parallel and normal to the bed joint was considered as well as θ of 15° , 45° and 75° . Regular flat ended concrete blocks, Type S mortar and a medium strength grout was used for all prisms. Results showed that grout had a maximum contribution for $\theta = 15^\circ$ and no significant contribution for $\theta = 75^\circ$. It was observed that two major failures were exhibited for both ungrouted and grouted prisms; a shear mode failure along the bed or head joint and a tensile failure of the prism. For $\theta = 15^\circ$, large shear stresses and small normal stresses were developed along the bed joint resulting into a shear-slip failure. For $\theta = 75^\circ$, high shear stresses and low normal stresses along the head joint resulted in a shear-tension failure. For $\theta = 45^\circ$, a mixed shear-tension mode of failures was developed since shear and normal stresses were balanced along the bed and head joints. The maximum prism strength was achieved when prisms were compressed at an angle normal to the bed joint. The authors underlined the importance of

considering the effects of the stress orientation along the bed joint when determining the strength of masonry in design.

Brown and Whitlock (1982) showed that high strength grout and mortar, high tensile strength brick and low brick coring percentage are several factors that increased prism strength. For most prisms tested, it was found that the simple superposition of the strength of grouted core and the hollow brick prisms overestimates the strength and the contribution from the grout.

Lee et al. (1984) tested 82 grouted and ungrouted concrete masonry prisms under compression both parallel and perpendicular to the bed joints. The effects of several parameters on the compressive strength in the two different loading orientations considered were the mortar and grout strength, and head mortar joint detail. The authors noted that for prisms loaded parallel to the bed joint, the head joint had a significant effect on the behavior of the prism and was recommended that the head joints be completely filled. The mortar strength was found to be an important parameter in affecting the strength of prisms loaded parallel to the bed joint; a maximum increase in prism strength of 52% is noted with the use of a stronger mortar. A significant increase in grout strength is found to have a small effect on prism strength.

Wong and Drysdale (1985) tested prisms made from hollow, solid and grouted concrete block units subjected to compression both normal and parallel to the bed joint. Prisms of 2 to 5 courses high were tested for both hollow and grouted concrete block units. Two types of blocks were used to build the prisms, a 190 mm two-cell stretcher unit and a solid 190 mm block. Type S mortar and a medium strength grout were used in all prisms. The authors found that the compression parallel to the bed joint is 25% lower than the compression normal to the bed joint. In addition, they confirmed that grouted and solid prisms exhibited 35% lower strength than hollow prisms and this is valid for both loading directions. Wong and Drysdale recommended that design standards should take into account the properties of the prisms for all directions of compression forces and treat the prisms separately.

Using experimental and numerical modeling Guo (1991) assessed various parameters and their influence on the mechanical properties of masonry units and assemblages under several loading

conditions. Guo found that prism strength is higher for prisms subjected to compression normal to the bed joint than parallel to the bed joint. Furthermore, the cracking load was also lower for compression parallel to the bed joint. For compression normal to the bed joint, typical prisms were laid in running bond with face shell mortar bedding using hollow concrete block units and type S mortar. For compression parallel to the bed joint, the author does not state whether or not the cross-sectional area was based on full or face shell mortar bedding, but indicates that ultimate strength calculation was based on minimum cross-sectional area. Guo noted that for compression parallel to the bed joint, the bed joint thickness is not a controlling factor affecting prism strength but the head joint thickness is. It was found that unit strength has a larger effect on prism strength when compression is parallel to the bed joint than normal to the bed joint. Increasing block strength from normal to strong increases the prism strength by 22% and 35% for compression normal and parallel to the bed joint, respectively.

Khalaf (1997) investigated the strength and behavior of grouted and ungrouted prisms and blocks when subjected to compression both normal and parallel to the bed joint. The author found that increasing mortar strength increased prism strength in both direction of loading. However, the effect of increasing mortar strength on prism strength was not significant for prisms compressed parallel to the bed joint. It was observed an increase in grout strength leads to an increase in compressive strength for prisms compressed normal to the bed joint; whereas prisms compressed parallel to the bed joint exhibited a decrease in strength for high strength grout. Khalaf (1997) found that strength of grouted block work masonry compressed parallel to the bed joint was in the range of 16-42% less than that when compressed normal to the bed face.

Bennett et al. (1997) conducted tests on 23 structural clay tile prisms subjected to axial compression. The force was applied at an angle θ of 0° , 22.5° , 45° , 67.5° and 90° with the bed joint. Mortar strength was observed to have little effect on prism strength. Prisms strength when loaded normal to the bed joint was estimated to be three-tenth the unit tile strength. Prisms loaded at $\theta = 0^\circ$, normal to the bed joint, showed maximum prism strength, while prisms loaded at $\theta = 67.5^\circ$ showed minimum strength.

Haach et al. (2010) investigated the compressive strength of concrete block masonry when subjected to uniaxial compression loads. When the specimens were loaded in compression

parallel to the bed joints, cracking along the mortar-block interface was observed due to the tensile stresses that are developed normal to the bed joint. The authors noted that the compressive strength parallel to the bed joint is about 55% of the compressive strength normal to the bed joint.

Drysdale and Hamid (1979) performed 146 axial compression tests on concrete block masonry prisms and established that a 3-course block prism is preferred to 2-course high block to represent the behavior close to a real wall. It was found that Type N mortar, which has lower strength than Type S mortar, only resulted in a 10% decrease in prism strength and a large increase in grout strength resulted in a relatively small increase in prism capacity.

Soon (2011) tested concrete masonry block prism subjected to loading either normal or parallel to the bed joint. Type S mortar was used and prisms were either grouted, partially grouted or fully grouted. When loaded parallel to the bed joint, hollow square prisms showed higher compressive strength than fully grouted square prisms. The compressive strength of the prisms when loaded normal to the bed joint was found to be approximately 50% higher than prisms loaded parallel to the bed joint.

2.6.2 Code Guide Lines

In Canada, the design of masonry structures is governed by CSA S304.1-04 (2004) and the masonry material testing methods and specifications are covered in various CSA standards. In the United States, the Masonry Structures Joint Committee (MSJC) is responsible for design provisions of masonry structures and the material testing methods and specifications are specified in various ASTM standards. CSA S304.1 provides requirements and procedures for determining the compressive strength of masonry prisms. These test methods are similar in many respects to corresponding ASTM standards (ASTM C1314, C1072 2011). In addition, ASTM E519 (2010) describes the test requirements to determine the tensile strength of masonry when loaded in diagonal compression. BNBC (1993) describes the test requirements to determine the prism compressive strength in article 4.3.3.1 and shear strength in article 4.3.5.

Strength of mortar and grout for engineered masonry shall be determined in accordance with the requirements of CSA A179 (2004). ASTM C270 and ASTM C476 provide similar requirements and proportioning procedures for both mortar and grout respectively.

The prism compressive strength is calculated by dividing the failure load at the 28-day age by the effective cross-sectional area, A_e . Both CSA S304.1-04 and ASTM C1314 specify a correction factor for specified f_m' to account for the height-to-thickness ratios, h/t , of prisms. These factors are considered to be conservative values for most prisms. The CSA S304.1-04 recommends the use of prisms with height-to-thickness ratio close to 5. For other values of ratio, correction factors which are less than unity are used. In ASTM C1314 (2011), the specified correction factors are different from CSA values and they are for a general masonry prism without stating type of masonry unit or the grouting condition.

The CSA S304.1-04 (2004) specifies a factor χ to be used in combination with f_m' to account for the effect of loading direction on the compressive stress. When the compressive forces are applied parallel to the bed joint and the grout is not horizontally continuous in the zone of compression, the factor χ is to be 0.5. When the compressive forces are applied parallel to the bed joint and the grout is horizontally continuous in the zone of compression, the factor χ is considered to be 0.7. The factor χ is considered to be unity when the compressive forces are applied normal to bed joint.

2.7 Masonry Shear Strength

The shear bond strength in masonry is the force in shear required to “separate the units from the mortar and each other”. This is as shown in Figure 2.2 below

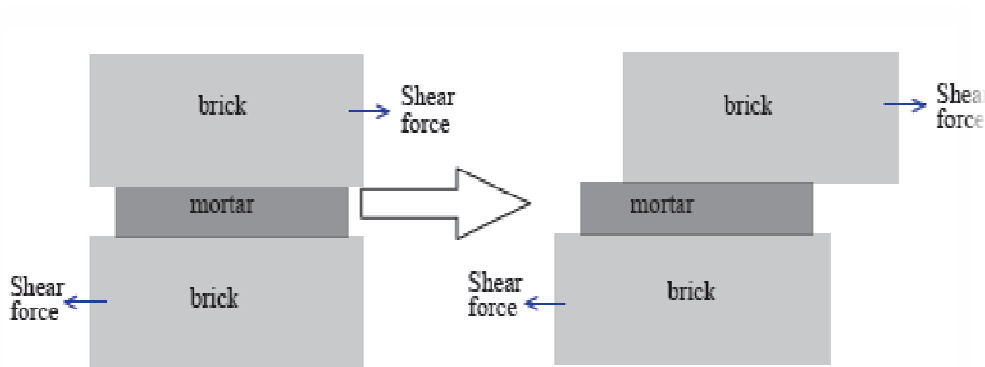


Figure 2.6 Diagrammatical explanation of the shear bond strength in masonry

The shear bond strength in masonry is the bond strength between the brick mortar interface.

The “Shear strength at the interface comes from friction due the asperities between the surface of mortar layer and the surface of the brick unit, and the chemical bond between mortar and brick units. Normal compression perpendicular to the interface further increases its shear strength because the asperities cannot easily slide over one another”. (Mosalam, 2009) “The bond development in masonry is due to mechanical interlocking of hydrated cement-products into the pores of the brick”. (Reddy, 2008).

According to (Mosalam, 2009) this phenomenon can be represented by the Mohr-Coulomb Criterion as stated in equation below

$$\tau_u = \tau_o + \mu \sigma_n$$

Where:

- τ_u -is the average stress
- τ_o - is the initial stress without any pre-compression applied
- μ – is the friction coefficient between the interfaces
- σ_n - is the applied pre-compression, i.e. the vertical load applied to the specimen before testing

According to (Riddington, 1994) the linear relationship of shear stress to normal stress (pre-compression) is valid up to approximately 2 N/mm² of applied pre-compression, i.e. above 2

N/mm² the Mohr Coulomb Criterion is no longer valid. “The bond between brick and mortar is derived from penetration of the mortar and hydration products, such as calcium silicate hydrates CSH, into the brick surface voids and pores” (Lawrence, 1987)

2.7.1 Why the Shear Bond Strength is Important

According to (Maheri, 2011) the shear strength in masonry is very important as it is the principle resisting force to seismic loads.

The shear bond strength is important as the strength of the masonry bricks is generally greater than that of the mortar so failure generally occurs at the joint. (Maheri, 2011 & Mosalam, 2009).

2.7.2 Applied Loads that Cause Shear Bond Failure

- Wind loads
- Seismic loads
- Normal loads
- Settlement of the foundations
- Impact loads
- Lateral earth pressures

An example of shear bond failure caused by foundation settlement is shown in the Figure 2.3 below.

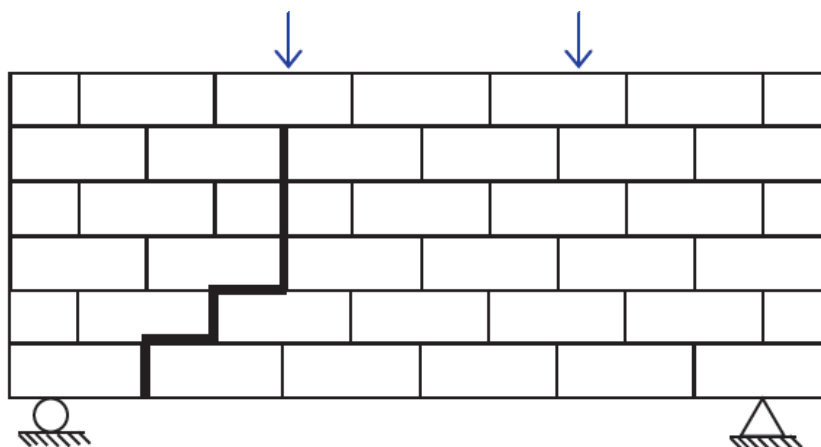


Figure 2.7 Shear bond failure caused by foundation settlement

An example of shear bond failure caused by wind or normal loading is shown in figure 2.4

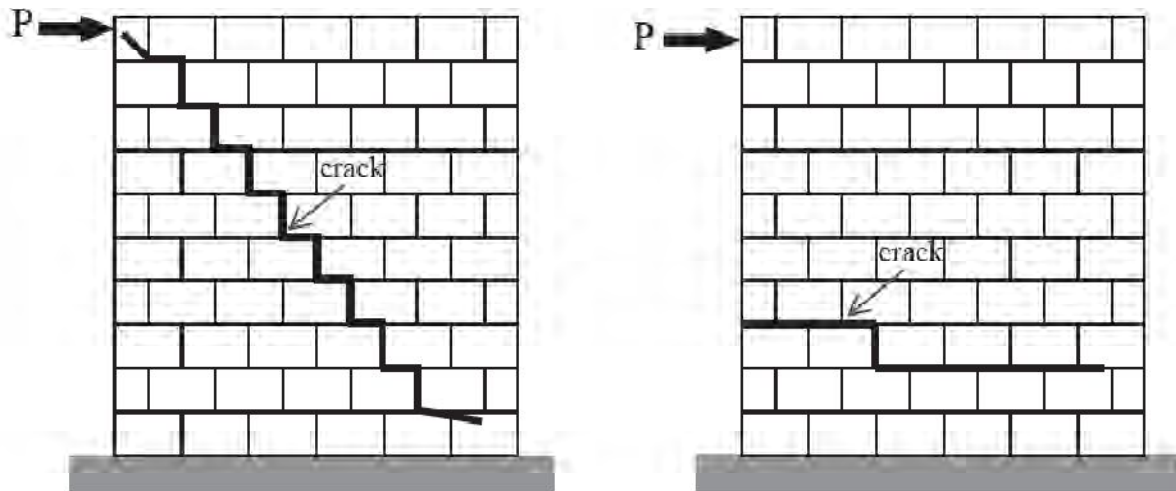


Figure 2.8 Shear bond failure caused by applied loads

2.7.3 Factors Affecting the Shear Bond Strength in Masonry

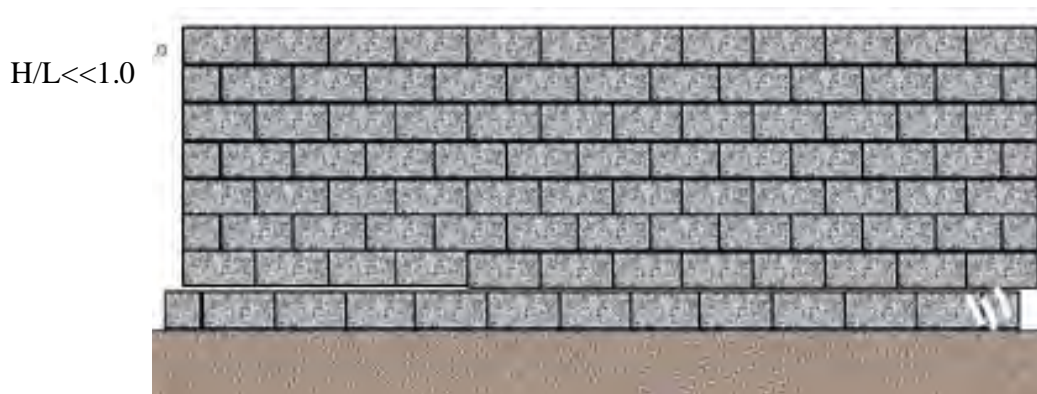
The shear bond strength in masonry is related to the bond strength in masonry. Greater the bond strength the greater the initial shear strength (τ_0). The bond strength can be affected by the

- Mortar Strength
- Mortar Shrinkage
- Brick Strength
- Joint Thickness
- Interface Morphology
- and Chemical Bond (Zhu, 1997)

2.8 Failure Modes of URM Walls

Masonry is a non-homogeneous and anisotropic composite structural material, consisting of masonry units and mortar. The behavior of masonry is complex. The accurate prediction of lateral load capacity of URM walls is difficult because of the complex brick block-mortar interaction behavior. The masonry units can be stone, calcium silicate, clay or concrete. This research program deals with clay units. The main in-plane failure mechanisms of URM walls subjected to earthquake actions are summarized as following:

- **Sliding mode:** In the case of low vertical loads or low friction coefficient, which may be due to poor quality mortar, horizontal cracks in the bed joints will form. These cracks can form a sliding plane extending along the wall length as shown in Figure 2.5(a).
- **Shear failure:** This takes place when the principal tensile stresses, developed in the wall under the combination of the horizontal and vertical loads, exceed the tensile resistance of masonry materials. Just before the attainment of maximum lateral load, diagonal cracks are developed in the wall. These cracks as shown in Figure 2.5(b) are stair stepped “strong bricks and 2 weak mortars”. They pass through the bricks in case of “weak bricks and strong mortars”. For high axial load explosive failure may happen.
- **Flexural (rocking) mode:** In case of high moment/shear ratio or improved shear resistance, crushing of the compressed zones at the edge of the wall may happen. Failure is obtained by overturning of the wall as shown in Figure 2.5(c).



(a) Sliding Shear Failure

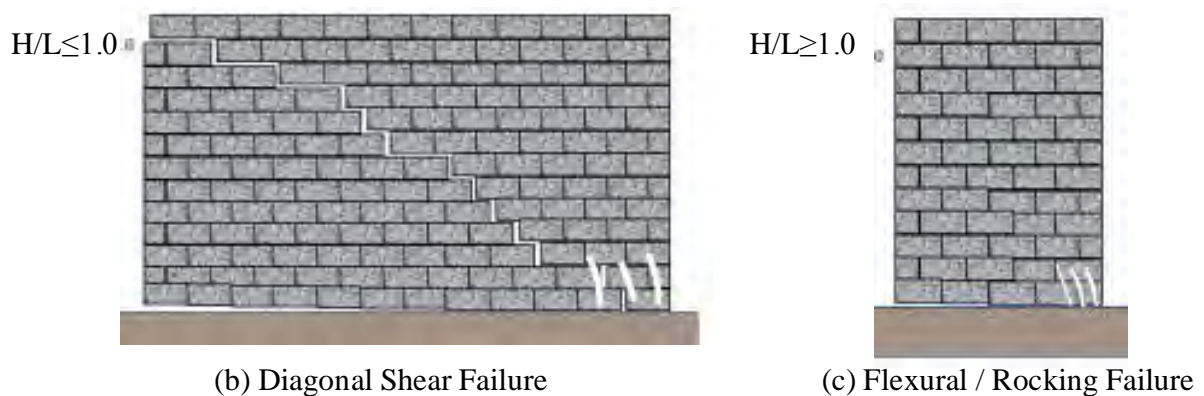


Figure 2.9 Modes of failure of unreinforced masonry shear walls

2.9 Factors Effecting Shear Wall Response

An unreinforced conventional masonry shear wall can initiate failure due to flexural uplift at heel or principal tensile cracking along the diagonal or sliding along the bottom courses depending on the aspect ratio (H/L), pre-compression (σ_{pc}) and the ratio of the bond strength to compressive strength of masonry. Crushing at toe or loaded corner defines ultimate stage of failure, but other stability criterion might take precedence over the crushing failure. Conventional masonry shear walls exhibiting low tensile and shear bond strengths typically fail through mortar joint or unit-mortar interface. There are three main factors that can influence the failure modes.

- a. Aspect Ratio (H/L), in which H and L are height and length of wall
- b. Pre-compression (σ_{pc})
- c. Material properties – in particular relative strengths of interfacing bond and unit compressive strengths; stiffness properties of joint and units also have some effect.

2.9.1 Influence of Aspect Ratio (H/L)

The ratio of wall height to its length is defined as the aspect ratio (H/L). Brunner and Shing (1996) have reported that the in-plane shear capacity of masonry shear wall that fails due to diagonal cracking is higher than those walls that fail due flexure (uplifting of heel followed by toe crushing). Failure modes of masonry shear wall are affected by the aspect ratio (H/L) to a large extent. For example a tall wall ($H \gg L$) tends to fail in flexure whilst a short wall ($H \ll L$)

tends to fail due to diagonal cracking (induced by the principal tension perpendicular to diagonal strut).

Shear failure, whether base sliding Figure 2.5a or diagonal cracking Figure 2.5b, is common in masonry walls where the aspect ratio (H/L) is less than one (height is less than the length of wall). Tensile uplift at heel and crushing at toe is common when aspect ratio of wall is greater than one, as shown in Figure 2.5c (Shing et al. 1989, Davidson and Brammer 1996, Haider 2007, Dhanasekar and Haider 2008, Haach et al. 2011).

A numerical study performed on unreinforced masonry shear walls by Haach et al. (2011) has shown that increase of aspect ratio from 0.64 to 2.33 (or, 3.6 fold) would cause nine fold reduction of the in-plane shear capacity when the pre-compression pressure (σ_{pc}) is kept constant. This change in aspect ratio also changes the failure mode from diagonal to flexural. For high bond strength masonry shear walls, in regards to aspect ratio, there are limited data available.

2.9.2 Influence of Pre-compression (σ_{pc})

Pre-compression (σ_{pc}) is another important factor that influences the failure mode of masonry shear wall and hence the in-plane shear capacity. It is reported that the precompression can change the mode of failure from flexural to diagonal shear for a square wall and correspondingly increase its shear capacity (Fattal 1993, Ghanem et al. 1993, Alcocer and Meli 1995, Haach et al. 2011). A change in pre-compression from $0.05 f_m'$ to $0.1 f_m'$ can cause an increase in in-plane shear capacity by 80% (Ghanem et al. 1993). Voon and Ingham (2006) reported that an increase in pre-compression from $0.02 f_m'$ MPa to $0.05 f_m'$ MPa on conventional masonry square walls can increase shear capacity of the wall by 13% and 22%.

Haach et al. (2011) reported that an increase in pre-compression (σ_{pc}) up to $0.40 f_m'$ increases the in-plane shear capacity of the wall and changes the failure mode from flexural rocking to diagonal shear cracking for square walls. Further increase in precompression can reduce the in-plane shear capacity causing compression failure.

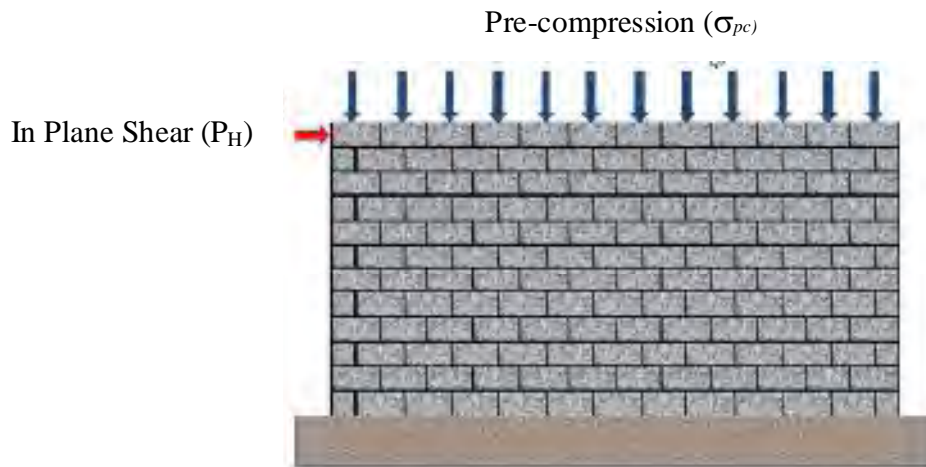


Figure 2.10 Masonry shear walls

Da Porto (2005) has performed studies on high bond strength masonry shear walls under high pre-compression ($> 0.17 f_m'$). For high bond strength masonry shear walls of aspect ratio (H/L) equal to one, the increase in pre-compression from $0.17 f_m'$ to $0.33 f_m'$ has shown to increase the in-plane shear capacity by 1.45 times. Furthermore, the failure occurred through the blocks more prominently than limited to the joints, therefore, high bond strength mortared masonry walls with pre-compression almost could eliminate the delamination type joint failure. The effect of pre-compression requires further investigate for high bond strength masonry shear walls in particular pre-compression lower than $0.17 f_m'$ for a reliable design information; this research focuses on low pre-compression.

2.9.3 Influence of Material Properties

Material property is another important parameter which affects the in-plane shear strength of masonry walls. The important material properties which affect the response of shear walls are the properties of masonry units and the unit-mortar adhesion and friction. Riddington and Naom (1994) have reported that tensile strength of masonry unit can increase the ultimate shear capacity of the wall. Zhuge (1998) has reported that the tensile and shear bond strengths of masonry have more influence when precompression is low. The strength properties of mortar has limited effect on shear capacity of the wall but mortar workability and block surface roughness can affect the tensile and the shear bond strengths, hence, the failure mode and the in-plane shear capacity (Riddington and Naom 1994, Hansen et al. 1998, Thamboo 2014). Dhanasekar (1985)

has reported that the increase in tensile and shear bond strength can increase in shear capacity of masonry walls while the compressive strength has relatively low influence.

2.10 Previous Research - Masonry Shear Strength

(Reddy, 2008), investigated the relationship between the shear bond strength and the compressive bond strength. In order to make this comparison for a certain masonry block and mortar mix without altering their respective compositions (Reddy, 2008) altered the texture of their masonry block specimens to increase the shear bond strength. “Brick–mortar bond development is generally attributed to the mechanical interlocking of cement hydration products into the surface pores of the bricks”, (Reddy, 2008) Therefore a rougher surface texture will give greater bond strength than a smooth surface due to the increase in size of surface pores. The results of the shear tests indicated that there was an increase of up to four times in shear strength comparing the specimens with a smoother surface texture to the ones with the rougher surface texture the range of results which they had achieved ranged from 0.21 MPa to 0.83 MPa. (Reddy, 2008) Noticed that failure of the interface generally occurred if the shear strength was lower than 0.25 MPa, if the shear strength was greater than 0.25 MPa then either the brick or the mortar will fail in shear.

Waon-Ho et al. (2004) constructed and tested seven unreinforced masonry wall specimens to study the shear behavior and capacity. From the investigation of test results it shows that, most test walls show the primary influence by rocking mode. Because of the load concentration in toe portion due to the rotation of the wall body, the crushing occurred at the toe portion. In case of the slender wall, sliding due to the bed-joint crack occurs. The relationship between shear stress and vertical axial stress is proportionate in square root pattern. The relationship between shear stress and aspect ratio shows the linear pattern. Shear stress and cross sectional area are not proportional. The proposed rocking strength/actual strength ratio of 1.03, and coefficient of correlation $R = 0.9889$ are proved to be more appropriately than FEMA 273 rocking strength formulas.

Churilov and Dumova-Jovanoska (2010) carried out experimental investigation of the behaviour of in-plane loaded unreinforced masonry panels. This study demonstrates the behaviour of

unstrengthened URM walls under cyclic loads, shows damage propagation and failure mechanisms, horizontal load-displacement hysteresis behaviour and diagrams, identification of the characteristic limit states, stiffness degradation and energy dissipation. Furthermore, the investigations will be enlarged with experimental testing of strengthened masonry panels with RC jacketing to compare with the behaviour of plain masonry walls.

Dowling et al. (2007) constructed and tested triplet unit characteristics both horizontal stack and running bond patterns. A modified soil mechanics shear box testing apparatus was used in the experiment. The horizontal application of load to the triplet unit is considered to more accurately represent the load distribution in actual wall units, and the slight increase in normal load is considered to be insignificant. The load was applied with a horizontal hydraulic jack at a constant rate of loading (1.2 mm/min) such that failure of the joint occurred between 45 seconds and 3 minutes after initial loading.

The shear strength of the horizontal stack (HS) specimens was generally slightly higher than the running bond (RB) specimens. This can be attributed to two main reasons firstly, the RB units possessed an additional plane of weakness in the vertical joint (crushing was evident in most RB specimens); and secondly, the RB specimen construction was more complex and difficult, resulting in less uniformity in triplet units. Comprehensive testing of conventional masonry with varying pre-compressive loads show monotonically increasing linear relationship between the applied pre-compressive stress and the average shear stress at failure. The results for horizontal stack (HS) units with 20 kPa pre-compression were unexpectedly higher than HS units with 30 kPa.

Ali et al. (2012) constructed and tested 108 mortar cubes, 96 masonry prisms for triplet tests, 48 masonry prisms for compression tests and 48 masonry wallets for diagonal tension tests.

The effect of various mortar types (cement-sand CS, cement-khaka CK and cement-sand-khaka CSK) and mix proportion on the mechanical properties are investigated. Simplified relationships are developed to relate the mortar strength, mortar types and mix proportion with the masonry basic mechanical properties. The study provided tools essential within the context of assessment and design verification of masonry walls subjected to lateral loads. The relationships mortar type and mix proportion to masonry bond strength and friction coefficient are first of its kind and of a

great importance for practical applications. From the study they found, masonry bond strength, compression strength, diagonal tension strength and elastic modulus decreases with increasing the relatively proportion of sand and khaka constituent in mortar.

Masonry friction coefficient increases with increasing the relatively proportion of sand and khaka constituent in mortar for CS and CSK mortar type whereas it decreases with increasing the relatively proportion of khaka constituent in mortar for CK mortar type.

The relationship between shear modulus and young modulus as specified by the Code appears to provide an over-conservative estimate for shear modulus for the considered masonry type.

The research study revealed that mortars with khaka either alone as the fine aggregate or in combination with sand, provide relatively high shear strength or stiffness as compared to mortars with only sand as fine aggregate. The positive aspects of use of khaka as a masonry constituent are the good mechanical characteristics besides being economical and more workable in construction work

Voon and Ingham investigated the effects of shear reinforcement, axial compression load, type of grouting, and wall aspect ratio on masonry shear strength. Axial compression load had a significant influence on the in-plane shear performance of masonry shear walls, mainly because it suppressed the tensile field in a material inherently weak in tension. Consequently, as the axial compression load increased, so did the ability of the walls to provide shear resistance. However, the post-cracking deformation capacities were observed to reduce with increasing axial load. This was because of the increasing brittleness of this failure type as the axial compression stress increased. It was observed that shear reinforcement not only provided additional shear resistance, but also improved the postcracking performance of the masonry walls when shear reinforcement was uniformly distributed up the height of the walls. The provision of closely spaced shear reinforcement enabled the distribution of stresses throughout the wall diagonals after the initiation of shear cracking. Accordingly, the initial diagonal cracks did not widen significantly under increasing lateral displacements, but instead new sets of diagonal cracks formed and gradually spread over the wall diagonals, accompanied by higher energy dissipation and more ductile behavior. The test results also demonstrated that partial grouting significantly reduced masonry shear strength. However, the effect of grouting became less significant when net shear stress was calculated accounting for the cross-sectional area of both the masonry units and

grouted cells. In addition, the test results indicated that masonry shear strength decreased inversely in relation to the H_e/L ratio.

Maheri et al. (2008) carried out a number of tests on half-scale of brick wall panels, having different material properties, with head joints and without head joints are presented. The walls are subjected to in-plane, as well as out-of-plane pushover loads to failure and their load displacement curves are established. It is found that, depending on the material properties and the modes of failure of the wall, the head joints contribute 40% to 50% to the in-plane shear capacity of the wall. Omitting the head joints also substantially reduces the out-of-plane yield strength and stiffness of the wall. Post the yield point, this omission has a reduced effect on the stiffness and the ultimate strength. In walls without head joints, the bed joints dominate the response of the wall to out-of-plane bending. Lack of mortar in head joints, causes a change in the performance of a wall subjected to biaxial bending from a relatively brittle response, to a largely ductile behaviour.

Maheri and Sherafati (1998) collected from field tests on brick walls of over 400 unreinforced brick buildings, situated in different parts of Iran, are comparatively analyzed to derive at quantitative results regarding the main factors affecting their shear strength. Some of the most important factors investigated include; type of brick units, type of mortar, date of construction and the environmental condition of the location of the building, including humidity and temperature. The results show the important effects of the humidity level of the environment on the shear strength of brick masonry walls. A nearly two folds increase in strength can be seen for walls constructed in wetter northern parts of the country compared to the drier central parts. It is, therefore, recommended that for assessing the vulnerability of unreinforced brick buildings, regionalization is considered and an appropriate 'region factor' is adopted. The type of bricks used in construction of the wall has a marked influence on the shear strength of that wall; the walls constructed using the manufactured, perforated brick units exhibiting much larger strength than the traditional solid brick units. This is not necessarily related to the strength weakness of the latter, but to the higher chemical and mechanical brick mortar bond strength achievable using the former type.

Schlegel (2004) numerically evaluated the effects of the head joints on the failure pattern of stone masonry. According to them, due to shrinkage of the head joints and the subsequent loss of bond between the stone and mortar, their contribution to the shear transfer is far less than the bed joints.

Maheri et al (2000) conducted experiments to determine the state of brick units' moisture content on the shear capacity of brick walls. They found that the in-plane shear capacity of brick walls are more than doubled if the bricks are used in a saturated, surface dry condition, compared with naturally dried (20% moisture) condition. Based on their laboratory test results, they recommended that for strength and seismic evaluation and retrofitting studies of existing brick structures in dry regions of the world, the shear capacity of the walls constructed with dry bricks should be considered as only half of the capacity of the walls constructed with pre-wetted brick units. Dry bricks and low consistency of mortar paste invariably result in a weak bond between the two and, as a result, a weak wall. In their study, Maheri et al also investigated the post-construction effects of moisture on the strength properties of brickwork and shear strength of brick walls. They cured the brickwork specimens and the brick wall test samples for a period of 28 days in a similar fashion to curing of concrete. Their test results showed that moisture curing of brickwork can enhance bond strength, mortar strength and, consequently, the shear and flexural strengths of masonry walls by around 50%. They recommended that such practice be applied to new constructions and highlighted the fact that the benefits of this practice in dry regions would naturally be higher than those in the wet regions. They also pointed out that; as in dry regions the air humidity and the moisture content of dry bricks are naturally low, different strength properties of brickwork are much lower than those of the brickwork in wet regions, and therefore, the empirical strength and seismic property relations and constitutive laws developed for brick masonry and enforced by codes of practice throughout the world may not be applicable in dry regions as they are generally based on tests results carried out in wet regions.

CHAPTER 3

EXPERIMENTAL PROGRAMME

3.1 General

The existence of a masonry structure depends not only on the form of the structure but ultimately on the properties of individual units and jointing material. It is therefore, necessary to determine the characteristics of the materials involved before considering the structural behaviour of the material in a structural element. The properties of brick work are influenced by variables such as type and physical properties of bricks, type of mortar, physical properties of the sand and lime used for the mortar, state of the bricks before laying, curing, workmanship etc. In order to keep the scope of this investigation within reasonable limits, the materials used were kept constant, and the properties of the component masonry materials are documented in this chapter.

This chapter presents material properties and the experimental program of this research consisting of sample preparation of one third scale models of masonry wall. The chapter describes the method of the research work, design specification, casting, curing and coloring. There is no general agreement on the shear behaviour, prism strength and wall stiffness of masonry wall. Beside these, there are very few experimental investigations on masonry wall. In this study shear test, prism compressive strength test and wall stiffness test have been carried out to correlate this parameter that is necessary for masonry structure design.

3.2 Material Properties

3.2.1 Compressive Strength of Machine Made Bricks

The compressive strength of machine made bricks quoted in Table 3.1 was evaluated using the standard code procedure. This involved loading the brick in compression with the brick located between the testing machine platens in the same manner as in a wall. It is recommended that average brick strengths will be used for design.

Table 3.1 Compressive Strength of Machine Made Bricks

Brick Type	Length (mm)	Width (mm)	Compressive Strength, Mpa (psi)	Compressive Strength, Mpa (psi)
Machine Made Bricks	250	120	22.88 (3318)	27.63 (4006)
			29.61 (4293)	
			30.40 (4408)	

3.2.2 Compressive Strength of Clay Burnt Bricks

The compressive strength of machine made bricks quoted in Table 3.2 was evaluated using the standard code procedure. This involved loading the brick in compression with the brick located between the testing machine platens in the same manner as in a wall. It is recommended that average brick strengths will be used for design.

Table 3.2 Compressive Strength of Clay Burnt Bricks

Brick Type	Length (mm)	Width (mm)	Compressive Strength, Mpa (psi)	Compressive Strength, Mpa (psi)
Clay Burnt Bricks	230	105	24.11 (3496)	25.27 (3664)
			25.54 (3704)	
			26.15 (3792)	

3.2.3 Properties of Sand

Sand is a naturally occurring granular material composed of finely divided rock and mineral particles. It is defined by size, being finer than gravel and coarser than silt. Sand can also refer to a textural class of soil or soil type; i.e. a soil containing more than 85% sand-sized particles (by mass). Physical and chemical properties of the sand influence the strength and durability of concrete. Local sand has been used for masonry wall constructions.. Figure 3.1 shows the gradation curve.

Sand (%)	Fines (%)	F.M	Cu	Cc
98	02	1.07	2.5	1.1

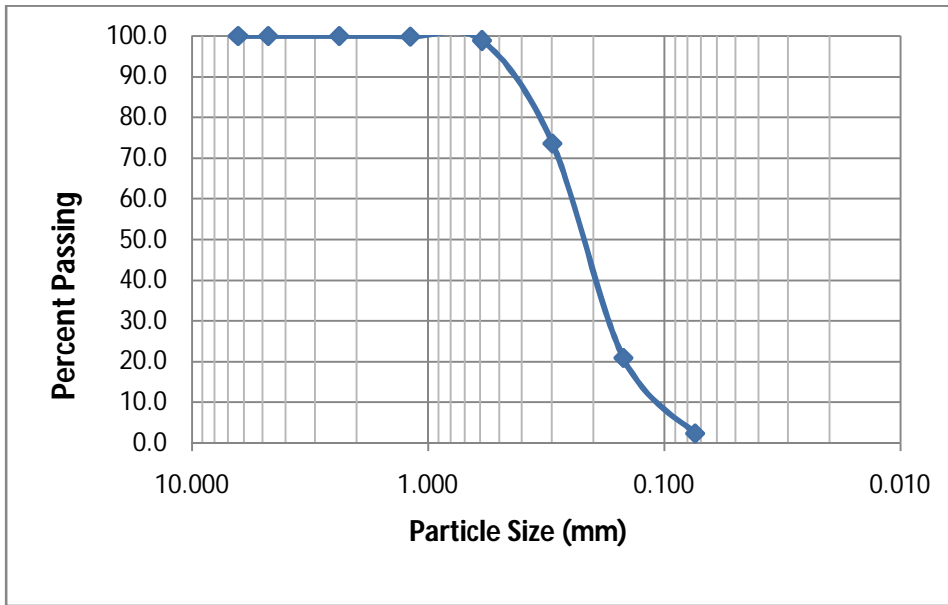


Figure: 3.1 Grain Size Analysis of Sand

3.2.4 Properties of Coarse Aggregate

Construction aggregate, or simply "aggregate", is a broad category of coarse particulate material used in construction, including sand, gravel, crushed stone, slag, recycled concrete and geosynthetic aggregates. Aggregates are the most mined materials in the world. Strength and durability of concrete depend on the type, quality and size of the aggregates. The gradation curve are shown in figure 3.2

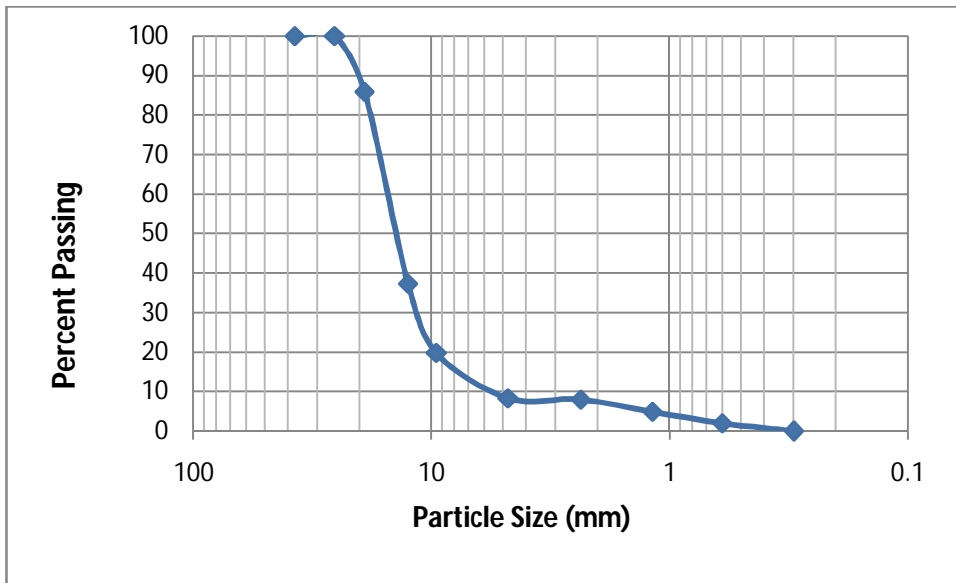


Figure: 3.2 Grain Size Analysis of Coarse Aggregate

3.2.5 Cement

Cement is a binder, a substance that sets and hardens and can bind other materials together. The most important uses of cement are as a component in the production of mortar in masonry, and of concrete, a combination of cement and an aggregate to form a strong building material.

3.2.6 Properties of Mortar

The average mortar compressive strength shall be determined by cube test of mortar. A mortar mix of 1:3 (cement: sand) was used throughout this investigation.

Cement: Ordinary Portland cement

Sand: Finely graded sand suitable for scaled mortar joints.

The dimensions and compressive strength of the mortar in different days are given in Table 3.3

Table: 3.3 Compressive Strength of Mortar (7-days)

Mortar Type	Block Area (mm ²)	Load (kN)	Average Load (kN)	Stress, (Mpa) (psi)	Stress, (Mpa) (psi)
7-days Strength (Set-1)	2500	32.23	33.54	13.41(1945)	13.01(1887)
		33.74			
		34.64			
7-days Strength (Set-2)	2500	31.62	31.54	12.62(1829)	
		29.41			
		33.59			

Table: 3.4 Compressive Strength of Mortar (14-days)

Mortar Type	Block Area (mm ²)	Load (kN)	Average Load (kN)	Stress, (Mpa) (psi)	Stress, (Mpa) (psi)
14-days Strength (Set-1)	2500	42.74	41.17	16.41 (2388)	15.99 (2318)
		41.00			
		39.77			
14-days Strength (Set-2)	2500	38.94	38.78	15.51(2249)	
		39.32			
		38.06			

Table: 3.5 Compressive Strength of Mortar (28-days)

Mortar Type	Block Area (mm ²)	Load (kN)	Average Load (kN)	Stress, (Mpa) (psi)	Stress, (Mpa) (psi)
28-days Strength (Set-1)	2500	42.48	42.99	17.20 (2493)	17.05(2472)
		42.13			
		44.36			
28-days Strength (Set-2)	2500	43.57	42.27	16.91 (2452)	
		42.43			
		40.82			

3.3 Specimen preparation

Eight specimens of different bricks and mortar thickness were prepared for research purposes.

3.3.1 Scaffolding Preparation

Timber as well as plywood was used to make this formwork. Formwork is used to support and control the shape of fresh concrete. The formwork must be capable of handling all of the loads imposed on it through the weight and pressure of the concrete as well as any other loads imposed by personnel, materials, equipment, or environmental loads. It must also support the concrete structure until the concrete has gained enough strength to support itself and all imposed loads.

Good formwork should satisfy the following requirements:

- a. It should be strong enough to withstand all types of dead and live loads.
- b. It should be rigidly constructed and efficiently propped and braced both horizontally and vertically, so as to retain its shape.
- c. The joints in the formwork should be water-tight against leakage of cement grout.
- d. The material of the formwork should be cheap, easily available and should be suitable for reuse.
- e. The formwork should be set accurately to the desired line and levels. It should have plane surface.
- f. Erection of formwork should permit removal of various parts in desired sequences without damage to the concrete.
- g. It should be as light as possible.

- h. The material of the formwork should not warp or get distorted when exposed to the elements.
- i. It should rest on firm base.

Eight wood formworks were prepared for construction of masonry wall on slab. Four formworks were prepared for clay burnt brick wall and four formworks were prepared for machine made brick wall.

3.3.2 Reinforcement Placement on Formwork

Reinforcement is the most vital factor in this research purposes, so great importance and carefulness was given for preparation of reinforcement. The reinforcement 12 mm Φ bars were used as main reinforcement of slab. 8 mm Φ bars @ 4" C/C were used as perpendicular to the main reinforcement.



Figure 3.3 Reinforcement Placement on formwork

3.3.3 Casting

After proper placement of reinforcement over the formwork fresh concrete was poured over it. In the slab 19 mm down grade brick chips were used as coarse aggregate and sylhet sand, 1:3 in proportion were used in concrete mix. The mixing ratio of concrete was kept 1:2:3 (by weight) having the water-cement ratio of 0.46 in order to obtain more concrete strength. A limited quantity of fresh concrete placed over the formwork and a vibrator machine was used to vibrate so that no air void existed at the concrete. A number of small mortar blocks were used on the inner base and on two sides of the formwork to maintain the clear cover and tamping rod was used for proper compaction. Compacted form of hardened concrete was gained for this effort. Figure 3.4 and 3.5 represent proper vibration of concrete and fresh concrete at formwork respectively.



Figure 3.4: Compaction of Fresh Concrete into Formwork using Vibrator



Figure 3.5 Casted Specimens with Formwork

3.3.4 Curing

Curing supplies required hydration and has significant influence to complete the reaction of cement. Thus, water curing method was applied after final setting of cement. Formwork attachment remained for 28 days curing period as it prevents the evaporation of the existing moisture of concrete. After casting several techniques such as pouring, spraying water, thick jute cloths and rice straw were adopted for the curing purpose. Figure 3.6 represent curing of sample.



Figure 3.6 Curing of Sample

3.3.5 Construction of Test Specimen (Masonry Wall)

There are eight masonry walls specimens are constructed for test. Four Masonry walls are constructed by clay burnt brick with two mortar thickness 1/2" and another two mortar thickness 3/4". And also another four masonry walls are constructed by machine made brick with two mortar thicknesses 1/2" and 3/4".



a. Construction of machine made brick wall with 1/2" mortar thickness



b. Construction of machine made brick wall with 3/4" mortar thickness



c. Construction of clay burnt brick wall with 1/2" mortar thickness



d. Construction of clay burnt brick wall with 3/4" mortar thickness

Figure: 3.7 Construction of Brick wall Specimens

3.3.6 Construction of Test Specimen (Masonry Prism)

There are eight masonry prisms are constructed for test. Four masonry prisms are constructed by clay burnt brick two with mortar thickness 1/2" and two with mortar thickness 3/4". Another four masonry prisms are constructed by machine made brick two with mortar thickness 1/2" and another two with mortar thickness 3/4".



a. Construction of machine made prism with mortar thickness 1/2".



b. Construction of machine made prism with mortar thickness 3/4".



c. Construction of clay burnt brick prism with mortar thickness 1/2".



d. Construction of clay burnt brick with mortar thickness 3/4".

Figure 3.8 Construction of Masonry Prisms

3.4 Prism Test Setup

After 28 days of casting of prism, the compressive strength of prisms was determined by compressive loading.



a. Clay burnt brick prism (C) with mortar thickness 1/2"



b. Clay burnt brick prism (C1) with thickness 1/2"



c. Clay burnt brick prism (C) with mortar thickness 3/4"



d. Clay burnt brick prism (C1) with mortar thickness 3/4"



e. Machine made brick prism (M) with mortar thickness 1/2"



f. Machine made brick prism (M1) with mortar thickness 1/2"



g. Machine made brick prism (M) with mortar thickness 3/4"



h. Machine made brick prism (M1) with mortar thickness 3/4"

Figure: 3.9 Test setup of Masonry Prisms

3.5 Experimental Shear Test Setup

There are four types, eight masonry walls constructed for shear test. Shear test was done with 5" wall. Shear test in two walls C-1/2 and C1-1/2, i.e Clay burnt brick wall with mortar thickness 1/2" was performed with three (3) ton vertical loads. Another six (6) walls was performed with 6 ton vertical loads. Out of 6 walls, two made of clay burnt bricks with mortar thickness 3/4" and other four made of machine made brick with mortar thickness 1/2" and 3/4". Hand grinding machine, hammer and chisel was used for cutting the wall and setup shear test arrangement.



Figure 3.10 Hand grinding machine



Figure 3.11 Hammer and Chisel



a. Shear test setup of clay burnt brick wall (C-1/2) with mortar thickness 1/2"



b. Shear test setup of clay burnt brick wall (C-1/2) with mortar thickness 1/2"



c. Shear test setup of clay burnt brick wall (C-3/4) with mortar thickness 3/4"



d. Shear test setup of clay burnt brick wall (C1-3/4) with mortar thickness 3/4"



e. Shear test setup of machine made brick wall (M-1/2) with mortar thickness 1/2"



f. Shear test setup of machine made brick wall (M1-1/2) with mortar thickness 1/2"



g. Shear test setup of machine made brick wall (M-3/4) with mortar thickness 3/4"



h. Shear test setup of machine made brick wall (M1-3/4) with mortar thickness 3/4"

Figure 3.12 Experimental Setup of Shear Test

3.6 Experimental Setup of wall Stiffness, Testing procedure, Data Acquisition:

The experiments were carried out in concrete laboratory of BUET. The models were placed on a steel base and laterally fixed by anchoring the wall. The base plate was fixed on a steel beam which was fixed with the concrete floor as shown in Figure 3.13. There are two hydraulic jacks manually operated to provide axial load on the top of the wall. And also another two hydraulic jacks leftward and rightward direction to provide lateral load on the wall.

The wall specimens were tested under horizontal incremental cyclic loading along with constant axial load. Lateral loading was applied using a loading control pattern. The specimens were tested under cyclic loading conditions displacing them laterally, along the axis of the walls. Loading and unloading was applied in 0.5 ton increments in the positive (leftward) and negative (rightward) direction for every cycle. Whereas 2 ton, 3ton, 4ton, 5 ton , 7 ton, 9 ton and 10 ton loading increments were maintained for 1st, 2nd , 3rd , 4th ,5th and 6th cycle. A constant loading rate per cycle was maintained until the specimens experienced significant loss of capacity. The loading history applied to the specimens is shown in Table 3.6.

Table 3.6 Applied Loading Histories

Wall Types	Cycle Name	Leftward		Rightward	
		Loading Condition (Ton)	Unloading Condition (Ton)	Loading Condition (Ton)	Unloading Condition (Ton)
C-1/2	Cycle-I	0 to 2	2 to 0	0 to -2	-2 to 0
	Cycle-II	0 to 3	3 to 0	0 to -3	-3 to 0
	Cycle-III	0 to 4	4 to 0	0 to -4	-4 to 0
	Cycle-IV	0 to 5	5 to 0	0 to -5	-5 to 0
C1-1/2	Cycle-I	0 to 2	2 to 0	0 to -2	-2 to 0
	Cycle-II	0 to 3	3 to 0	0 to -3	-3 to 0
	Cycle-III	0 to 4	4 to 0	0 to -4	-4 to 0
	Cycle-IV	0 to 5	5 to 0	0 to -5	-5 to 0
	Cycle-V	0 to 6	6 to 0	0 to -6	-6 to 0

Wall Types	Cycle Name	Leftward		Rightward	
		Loading Condition (Ton)	Unloading Condition (Ton)	Loading Condition (Ton)	Unloading Condition (Ton)
C-3/4	Cycle-I	0 to 2	2 to 0	0 to -2	-2 to 0
	Cycle-II	0 to 3	3 to 0	0 to -3	-3 to 0
	Cycle-III	0 to 4	4 to 0	0 to -4	-4 to 0
	Cycle-IV	0 to 5	5 to 0	0 to -5	-5 to 0
	Cycle-V	0 to 7	7 to 0	0 to -7	-7 to 0
	Cycle-VI	0 to 9	9 to 0	0 to -9	-9 to 0
C1-3/4	Cycle-I	0 to 2	2 to 0	0 to -2	-2 to 0
	Cycle-II	0 to 3	3 to 0	0 to -3	-3 to 0
	Cycle-III	0 to 4	4 to 0	0 to -4	-4 to 0
	Cycle-IV	0 to 5	5 to 0	0 to -5	-5 to 0
	Cycle-V	0 to 7	7 to 0	0 to -7	-7 to 0
	Cycle-VI	0 to 10	10 to 0	0 to -10	-10 to 0
M-1/2	Cycle-I	0 to 2	2 to 0	0 to -2	-2 to 0
	Cycle-II	0 to 3	3 to 0	0 to -3	-3 to 0
	Cycle-III	0 to 4	4 to 0	0 to -4	-4 to 0
	Cycle-IV	0 to 5	5 to 0	0 to -5	-5 to 0
	Cycle-V	0 to 6	6 to 0	0 to -6	-6 to 0
M1-1/2	Cycle-I	0 to 2	2 to 0	0 to -2	-2 to 0
	Cycle-II	0 to 3	3 to 0	0 to -3	-3 to 0
	Cycle-III	0 to 4	4 to 0	0 to -4	-4 to 0
	Cycle-IV	0 to 5	5 to 0	0 to -5	-5 to 0
	Cycle-V	0 to 6	6 to 0	0 to -6	-6 to 0
M-3/4	Cycle-I	0 to 2	2 to 0	0 to -2	-2 to 0
	Cycle-II	0 to 3	3 to 0	0 to -3	-3 to 0
	Cycle-III	0 to 4	4 to 0	0 to -4	-4 to 0
	Cycle-IV	0 to 5	5 to 0	0 to -5	-5 to 0
	Cycle-V	0 to 6	6 to 0	0 to -6	-6 to 0

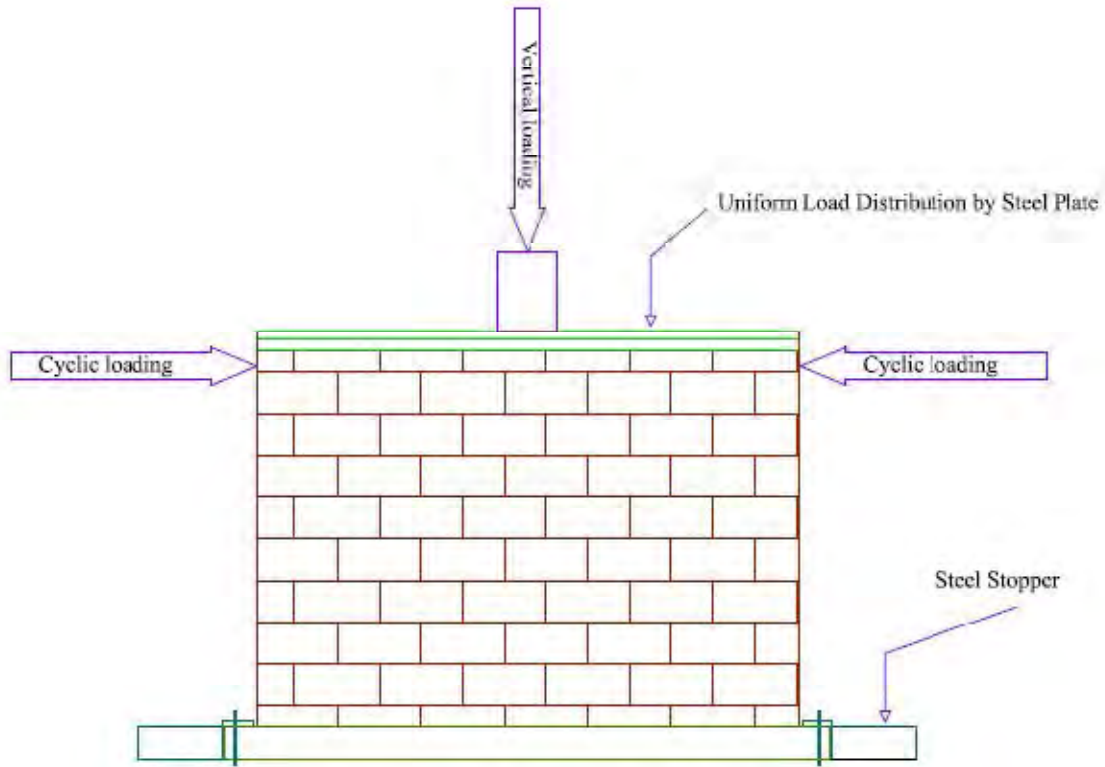


Figure 3.13 Schematic Diagram of Loading Condition During Test

3.6.1 Load Selection

The specimen walls were tested under incremental cyclic loading along with constant axial load of 6% of prism strength. The wall specimen of clay burnt brick with mortar thickness 1/2" was tested with 3 ton axial loads. Two wall specimen of clay burnt brick with mortar thickness 3/4" and another four specimen walls made of machine made bricks were tested with 6 ton axial loads. The axial load was kept constant throughout the experiment of each specimen. The static cyclic loading had been provided by two hydraulic jacks. The load had been controlled by measuring horizontal displacement of the wall for the cycle I, cycle II, cycle III, cycle IV, cycle-V and cycle VI respectively. The planned load cycle are shown in Table 3.6

3.6.2 Testing Procedure

Before testing all the specimens were all through white washed to find out the crack and their absolute location. Precautions were taken to avoid any potential damages during lifting and transporting of the specimens. The specimens had been lifted by series of pulleys and set on the base plate. One hydraulic jack was set in the position at the top of the column to apply constant axial loading. Another two hydraulic jacks were linked to the left side and right side of the specimen wall along its length to apply incremental cyclic loading. The dial gauges was set in position. At first 6 ton axial load was applied on the top of the wall and kept constant throughout the test. After applying the axial load, the initial dial gauges reading was taken as reference points to measure the deflections of the wall. Then the incremental cyclic loadings were applied by the left and right jacks simultaneously and progressive readings were taken. The loading and the unloading of the hydraulic jacks were controlled manually. Figure 3.14 shows the experimental setup before starting wall stiffness test.



Figure 3.14 Experimental Setup before Starting Test

CHAPTER 4

EXPERIMENTAL RESULTS AND DISCUSSION

4.1 General

This chapter summarizes the qualitative and quantitative experimental results from test specimens. All eight samples of wall were subjected to constant axial load throughout shear test and incremental cyclic loading in stiffness test of the wall. Eight prism test specimen were tested by compressive loading. Dial gauges were used to measure the deflection of the wall. The qualitative results include photographs of each specimen through the course of testing and displaying the crack patterns. Load corresponding to displacements and different crack history were recorded for producing the quantitative results.

4.2 Failure Modes of Prism Test Specimen

4.2.1 Clay Burnt Brick Prism with Mortar Thickness 1/2"

The cracks were marked by permanent black pen and the corresponding loadings were noted. The first crack initiated in the specimen C-1/2 when the applied load was 84 kN (Stress 3.56 Mpa) and in the specimen C1-1/2 when the applied load was 93 kN (Stress 3.68 Mpa). Then with the progress of loading the first crack was propagated. The ultimate load capacity of the prism specimen C-1/2 was 114.9 kN (Stress 4.86 Mpa) and in the prism specimen C1-1/2 was 135.5 kN (Stress 5.36 Mpa). The initial crack pattern and ultimate crack pattern of specimen C-1/2 and C1-1/2 have shown in Figure 4.1(a & b) and 4.2(a & b)



a. Appearance of first crack of prism C-1/2 b. Ultimate crack of prism C-1/2

Figure 4.1 Failure Pattern of Prism Test Specimen C-1/2



a. Appearance of first crack of prism C1-1/2

b. Ultimate crack of prism C1-1/2

Figure 4.2 Failure Pattern of Prism Test Specimen C1-1/2

4.2.2 Clay Burnt Brick Prism Test Specimen with Mortar Thickness 3/4"

The cracks were marked by permanent black pen and the corresponding loadings were note. The first crack initiated in the specimen C-3/4 when the applied load was 77 kN (Stress 3.15 Mpa) and in the specimen C1-3/4 when the applied load was 74 kN (Stress 3.06 Mpa). Then with the progress of loading the first crack was propagated. The ultimate load capacity of the prism specimen C-3/4 was 176.7 kN (Stress 7.24 Mpa) and in the prism specimen C1-3/4 was 180.7 kN (Stress 7.48 Mpa). The initial crack pattern and ultimate crack pattern of specimen C-3/4 and C1-3/4 have shown in Figure 4.3 (a & b) and 4.4 (a & b). It is observed that, with the increasing mortar thickness in clay burnt brick with frog mark prism cracking strength and ultimate strength increases.



a. Appearance of first crack of prism C-3/4



b. Ultimate crack of prism C-3/4

Figure 4.3 Failure Pattern of Prism Test Specimen C-3/4



a. Appearance of first crack of prism C1-3/4



b. Ultimate crack of prism C1-3/4

Figure 4.4 Failure Pattern of Prism Test Specimen C1-3/4

4.2.3 Machine Made Brick Prism Test Specimen with Mortar Thickness 1/2"

The cracks were marked by permanent black pen and the corresponding loadings were note. The first crack initiated in the specimen M-1/2 when the applied load was 64 kN (Stress 2.13 Mpa) and in the specimen M1-1/2 when the applied load was 67 kN (Stress 2.23 Mpa). Then with the progress of loading the first crack was propagated. The ultimate load capacity of the prism specimen M-1/2 was 255.3 kN (Stress 8.51 Mpa) and in the prism specimen M1-1/2 was 241.9

kN (Stress 8.06 Mpa). The initial crack pattern and ultimate crack pattern of specimen M-1/2 and M1-1/2 have shown in figure 4.5 (a & b) and 4.6 (a & b).



a. Appearance of first crack of prism M-1/2



b. Ultimate crack of prism M-1/2

Figure 4.5 Failure Pattern of Prism Test Specimen M-1/2



a. Appearance of first crack of prism M-1/2



b. Ultimate crack of prism M-1/2

Figure 4.6 Failure Pattern of Prism Test Specimen M1-1/2

4.2.4 Machine Made Brick Prism Test Specimen with Mortar Thickness 3/4"

The cracks were marked by permanent black pen and the corresponding loadings were note. The first crack initiated the specimen M-3/4 when the applied load was 69 kN (Stress 2.33 Mpa) and

in the specimen M1-3/4 when the applied load was 67 kN (Stress 2.28 Mpa). Then with the progress of loading the first crack was propagated. The ultimate load capacity of the prism specimen M-3/4 was 265.3 kN (Stress 8.95 Mpa) and in the prism specimen M1-3/4 was 249.9 kN (Stress 8.50 Mpa). The initial crack pattern and ultimate crack pattern of specimen M-3/4 and M1-3/4 have shown in figure 4.7 (a & b) and 4.8 (a & b). It is observed that, with the increasing mortar thickness in machine made brick without frog mark prism cracking strength and ultimate strength increases.



a. Appearance of first crack of prism M-3/4

b. Ultimate crack of prism M-3/4

Figure 4.7 Failure Pattern of Prism Test Specimen M-3/4



a. Appearance of first crack of prism M1-3/4

b. Ultimate crack of prism M1-3/4

Figure 4.8 Failure Pattern of Prism Test Specimen M1-3/4

4.3 Prism Strength

4.3.1 Properties of Machine made brick Prism

Table: 4.1 Compressive Strength of Machine made brick prism 1/2" Mortar thickness

Type	Length (mm)	Width (mm)	Area (mm ²)	Cracking Load (kN)	Ultimate Load (kN)	Cracking Stress, (Mpa), (psi)	Ultimate Stress, Mpa (psi)
Set-1 (M-1/2")	250	120	30000	64	255.3	2.13 (309)	8.51 (1234)
Set-2 (M1-1/2")	250	120	30000	67	241.85	2.23 (324)	8.06 (1169)

Table: 4.2 Compressive Strength of Machine made brick prism 3/4" Mortar thickness

Type	Length (mm)	Width (mm)	Area (mm ²)	Cracking Load (kN)	Ultimate Load (kN)	Cracking Stress, (Mpa), (psi)	Ultimate Stress, (Mpa) (psi)
Set-1 (M-3/4")	247	120	29641	69	265.26	2.33 (338)	8.95 (1298)
Set-2 (M1-3/4")	245	120	29400	67	249.90	2.28 (330)	8.50 (1233)

4.3.2 Properties of Clay Burnt Brick Prism

Table: 4.3 Compressive Strength of Clay burnt brick prism 1/2" Mortar thickness

Type	Length (mm)	Width (mm)	Area (mm ²)	Cracking Load (kN)	Ultimate Load (kN)	Cracking Stress, (Mpa), (psi)	Ultimate Stress, (Mpa) (psi)
Set-1 (C-1/2")	225	105	23625	88	114.91	3.72 (540)	4.86 (705)
Set-2 (C1-1/2")	230	110	25300	93	135.50	3.68 (533)	5.36 (777)

Table: 4.4 Compressive Strength of Clay burnt brick prism 3/4" Mortar thickness

Type	Length (mm)	Width (mm)	Area (mm ²)	Cracking Load (kN)	Ultimate Load (kN)	Cracking Stress, (Mpa), (psi)	Ultimate Stress, (Mpa) (psi)
Set-1 (C-3/4")	226	108	24408	77	176.70	3.15 (457)	7.24 (1050)
Set-2 (C1-3/4")	230	105	24150	74	180.70	3.06 (444)	7.48 (1085)

4.4 Failure Modes of Shear Test Specimen

4.4.1 Clay Burnt Brick with Mortar Thickness 1/2"

The cracks were marked by permanent black pen and the corresponding loadings were note. The first crack initiated in the specimen C-1/2 when the applied load was 63.9 kN (Stress 2.23 Mpa) and in the specimen C1-1/2 when the applied load was 61.1 kN (Stress 2.29 Mpa). Then with the progress of loading the first crack was propagated. The ultimate capacity of the specimen C-1/2 and C1-1/2 are 78.9 kN (Stress 2.75 Mpa) and 74.8 kN (Stress 2.80 Mpa) resaeactively. The crack pattern of shear test specimen C-1/2 and C1-1/2 have shown in figure 4.9 and 4.10.



Figure 4.9 Failure Pattern of Shear Test
Specimen C-1/2



Figure 4.10 Failure Pattern of Shear Test
Specimen C1-1/2

4.4.2 Clay Burnt Brick with Mortar Thickness 3/4"

The cracks were marked by permanent black pen and the corresponding loadings were note. The first crack initiated in the specimen C-3/4 when the applied load was 46.1 kN (Stress 1.73 Mpa) and in the specimen C1-3/4 when the applied load was 47.5 kN (Stress 1.77 Mpa). Then with the progress of loading the first crack was propagated. The ultimate capacity of the specimen C-3/4 and C1-3/4 are 59.7 kN (Stress 2.24 Mpa) and 62.5 kN (Stress 2.33 Mpa) respectively. The crack pattern of shear test specimen C-3/4 and C1-3/4 have shown in figure 4.11 and 4.12. It is observed that, with the increasing mortar thickness in clay burnt brick with frog mark shear cracking strength and ultimate strength decreases.



Figure 4.11 Failure pattern of shear test
Specimen C-3/4



Figure 4.12 Failure pattern of shear test specimen
C1-3/4

4.4.3 Machine Made Brick with Mortar Thickness 1/2"

The cracks were marked by permanent black pen and the corresponding loadings were note. The first crack initiated in the specimen M-1/2 when the applied load was 41.9 kN (Stress 1.55 Mpa) and in the specimen M1-1/2 when the applied load was 44.7 kN (Stress 1.67 Mpa). Then with the progress of loading the first crack was propagated. The ultimate capacity of the specimen M-1/2 and M1-1/2 are 59.7 kN (Stress 2.21 Mpa) and 54.3 kN (Stress 2.03 Mpa) respectively. The crack pattern of shear test specimen M-1/2 and M1-1/2 have shown in figure 4.13 and 4.14.



Figure 4.13 Failure Pattern of Shear Test

Specimen M-1/2



Figure 4.14 Failure Pattern of Shear Test

Specimen M1-1/2

4.4.4 Machine Made Brick with Mortar Thickness 3/4"

The cracks were marked by permanent black pen and the corresponding loadings were note. The first crack initiated in the specimen M-3/4 when the applied load was 39.3 kN (Stress 1.46 Mpa) and in the specimen M1-3/4 when the applied load was 36.5 kN (Stress 1.3 Mpa). Then with the progress of loading the first crack was propagated. The ultimate capacity of the specimen M-3/4 and M1-3/4 are 51.5 kN (Stress 1.92 Mpa) and 47.5 kN (Stress 1.69 Mpa) respectively. The crack pattern of shear test specimen M-3/4 and M1-3/4 have shown in figure 4.15 and 4.16. It is observed that, with the increasing mortar thickness in machine made brick without frog mark shear cracking strength and ultimate strength decreases.



Figure 4.15 Failure Pattern of Shear Test Specimen M-3/4



Figure 4.16 Failure Pattern of Shear Test Specimen M1-3/4

4.5 Shear Strength

The value of shear strength are shown in Table 4.5

Table: 4.5 Shear Strength Value

Type	Cracking Pressure (kg/cm ²)	Cracking Load, kN (Ton)	Ultimate Pressure (kg/cm ²)	Ultimate Load, kN (Ton)	Cracking Stress, Mpa, (psi)	Ultimate Stress, Mpa (psi)
C-1/2	470	63.87 (6.51)	580	78.91 (8.04)	2.23 (323)	2.75 (399)
C1-1/2	450	61.13 (6.23)	550	74.81 (7.63)	2.29 (332)	2.80 (406)
C-3/4	340	46.09 (4.70)	440	59.76 (6.09)	1.73 (251)	2.24 (325)
C1-3/4	320	43.35 (4.42)	460	62.50 (6.37)	1.62 (235)	2.33 (338)
M-1/2	310	41.98 (4.28)	440	59.76 (6.09)	1.55 (225)	2.21 (320)
M1-1/2	330	44.72 (4.56)	400	54.29 (5.53)	1.67 (242)	2.03 (294)
M-3/4	290	39.25 (4.00)	380	51.55 (5.26)	1.46 (212)	1.92 (278)
M1-3/4	270	36.52 (3.72)	350	47.46 (4.84)	1.30 (188)	1.69 (245)

4.6 Failure Modes of wall Stiffness

4.6.1 Crack Patterns of Specimen wall C-1/2

The black marked cracks, represented the cracking that appeared during the loading and unloading from leftward and rightward, as shown in figure 4.17 to figure 4.19. The flexural cracking seemed to be more widespread. The test of specimen C-1/2 was associated with its first crack at slab wall joint at negative (Rightward) 1st cycle loading with 2.0 ton load and corresponded to a horizontal displacement of 0.54 mm. The second crack of wall at negative 2nd cyclic loading with 3.0 ton load at right side to a corresponding horizontal displacement of 3.10 mm. The wall was failed at negative 4th cycle loading at right side with 5.0 ton load to a corresponding horizontal displacement of 14.38 mm. The failure pattern of the clay burnt brick wall (C-1/2) with mortar thickness 1/2" was flexure type.



Figure 4.17 Initial Crack (Flexure) Pattern of Specimen C-1/2



Figure 4.18 2nd Crack (Shear) Pattern of Specimen C-1/2

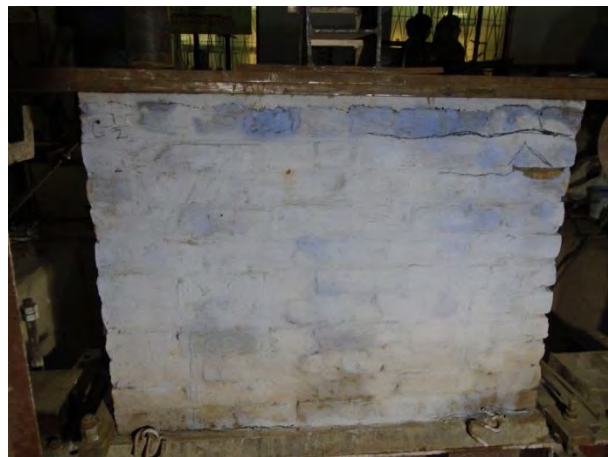


Figure 4.19 Final Crack Pattern of Specimen Wall C-1/2

4.6.2 Crack Patterns of Specimen wall C1-1/2

The black marked cracks, represented the cracking that appeared during the loading and unloading from leftward and rightward, as shown in figure 4.20 to figure 4.23. The shear cracking seemed to be more widespread. The test of specimen C1-1/2 was associated with its first crack at slab wall joint at negative (Rightward) 2nd cycle loading with 2.5 ton load and corresponded to a horizontal displacement of 1.87 mm. The second crack of wall at positive 3rd cyclic loading with 3.5 ton load at left side to a corresponding horizontal displacement of 1.66 mm. Third crack of the wall at positive 4th cyclic loading with 5.0 ton load at left side to a corresponding horizontal displacement of 2.53 mm. The wall was failed at positive 5th cycle loading at left side with 6.0 ton load to a corresponding horizontal displacement of 15.68 mm. The failure pattern of the clay burnt brick wall (C1-1/2) with mortar thickness 1/2" was shear type.



Figure 4.20 Initial Crack (Flexure) Pattern of Specimen C1-1/2



Figure 4.21 2nd Crack (Shear) Pattern of Specimen C1-1/2



Figure 4.22 3rd Crack (Shear) Pattern of Specimen C1-1/2



Figure 4.23 Final Crack Pattern of Specimen C1-1/2

4.6.3 Crack Patterns of Specimen wall C-3/4

The black marked cracks, represented the cracking that appeared during the loading and unloading from leftward and rightward, as shown in figure 4.24 to figure 4.27. The flexural cracking seemed to be more widespread. The test of specimen C-3/4 was associated with its first crack at slab wall joint at negative (Rightward) 2nd cycle loading with 3.0 ton load and corresponded to a horizontal displacement of 1.74 mm. The second crack of the wall at positive 3rd cyclic loading with 4.0 ton load at left side to a corresponding horizontal displacement of 1.02 mm. Third crack of the wall at negative 5th cyclic loading with 6.0 ton load at right side to a corresponding horizontal displacement of 5.49 mm. The wall was failed at negative 6th cycle loading at right side with 9.0 ton load to a corresponding horizontal displacement of 13.11 mm. The failure pattern of the clay burnt brick wall (C-3/4) with mortar thickness 3/4" was flexure type.



Figure 4.24 Initial Crack (Flexure) Patterns at
Base of Specimen C-3/4



Figure 4.25 2nd Cracks (Shear) Patterns of
Specimen C-3/4



Figure 4.26 3rd Cracks (Shear) Patterns of
Specimen C-3/4



Figure 4.27 Final Crack Pattern of Specimen
C-3/4

4.6.4 Crack Patterns of Specimen wall C1-3/4

The black marked cracks, represented the cracking that appeared during the loading and unloading from leftward and rightward, as shown in figure 4.28 to figure 4.30. The flexural cracking seemed to be more widespread. The test of specimen C1-3/4 was associated with its first crack at slab wall joint at negative (Rightward) 2nd cycle loading with 2.5 ton load and corresponded to a horizontal displacement of 0.38 mm and second crack of wall at positive 4th cyclic loading with 5.0 ton load at left side to a corresponding horizontal displacement of 0.73

mm. The wall was failed at positive 6th cycle loading at left side with 10.0 ton load to a corresponding horizontal displacement of 15.8 mm. The failure pattern of the clay burnt brick wall (C1-3/4) with mortar thickness 3/4" was flexure type.



Figure 4.28 Initial Crack (Flexure) Patterns at Specimen C1-3/4



Figure 4.29 2nd Cracks (Shear) Patterns of Specimen C1-3/4



Figure 4.30 Final Crack Pattern of Specimen C1-3/4

4.6.5 Crack Patterns of Specimen wall M-1/2

The black marked cracks, represented the cracking that appeared during the loading and unloading from leftward and rightward, as shown in figure 4.31 to figure 4.33. The flexural cracking seemed to be more widespread. The test of specimen M-1/2 was associated with its first crack at slab wall joint at negative (Rightward) 2nd cycle loading with 2.5 ton load and

corresponded to a horizontal displacement of 0.51 mm and second crack of wall at positive 3rd cyclic loading with 4.0 ton load at left side to a corresponding horizontal displacement of 1.08 mm. Third crack of the wall at positive 4th cyclic loading with 4.5 ton load at left side to a corresponding horizontal displacement of 2.34 mm. The wall was failed at positive 5th cycle loading at left side with 6.0 ton load to a corresponding horizontal displacement of 15.4 mm. The failure pattern of the machine made brick wall (M-1/2) with mortar thickness 1/2" was flexure type.



Figure 4.31 Initial Crack (Flexure) Patterns at Specimen M-1/2



Figure 4.32 2nd and 3rd Cracks Patterns of Specimen M-1/2



Figure 4.33 Final Crack Pattern of Specimen M-1/2

4.6.6 Crack Patterns of Specimen wall M1-1/2

The black marked cracks, represented the cracking that appeared during the loading and unloading from leftward and rightward, as shown in figure 4.34 to figure 4.36. The flexural cracking seemed to be more widespread. The test of specimen M1-1/2 was associated with its first crack at slab wall joint at positive (Leftward) 2nd cycle loading with 2.5 ton load and corresponded to a horizontal displacement of 1.35 mm and second crack of wall at positive 2nd cyclic loading with 3.0 ton load at left side to a corresponding horizontal displacement of 1.82 mm. Third crack of the wall at negative 3rd cyclic loading with 4.0 ton load at right side to a corresponding horizontal displacement of 3.37 mm. The wall was failed at positive 5th cycle loading at right side with 6.0 ton load to a corresponding horizontal displacement of 13.47 mm. The failure pattern of the machine made brick wall (M1-1/2) with mortar thickness 1/2" was flexure type.



Figure 4.34 Initial Crack (Flexure) Patterns at Specimen M1-1/2



Figure 4.35 2nd and 3rd Cracks Patterns of Specimen M1-1/2



Figure 4.36 Final Crack Pattern of Specimen M1-1/2

4.6.7 Crack Patterns of Specimen wall M-3/4

The black marked cracks, represented the cracking that appeared during the loading and unloading from leftward and rightward, as shown in figure 4.37 to figure 4.39. The flexural cracking seemed to be more widespread. The test of specimen M-3/4 was associated with its first crack at slab wall joint at negative (rightward) 1st cycle loading with 2.0 ton load and corresponded to a horizontal displacement of 0.7 mm and second crack of wall at positive 2nd cyclic loading with 2.5 ton load at left side to a corresponding horizontal displacement of 1.07 mm. The wall was failed at positive 5th cycle loading at left side with 6.0 ton load to a corresponding horizontal displacement of 20.89 mm. The failure pattern of the machine made brick wall (M-3/4) with mortar thickness 3/4" was flexure type.



Figure 4.37 Initial Crack (Flexure) Patterns at Specimen M-3/4



Figure 4.38 2nd Cracks Patterns of Specimen M-3/4



Figure 4.39 Final Crack Pattern of Specimen M-3/4

4.7 Load – Deformation Response

Load-deformation responses of all seven specimens were monitored by dial gauges throughout each test specimen. Dial gauges were placed at the top of the wall to record the lateral displacement. Testing was terminated when the specimen was failed. Figures 4.40 to figure 4.46 provide the load-deformation responses of each specimen. [The responses from dial gauges are available in the Appendices A].

With a view to the load-deformation curve it can be found that all gave almost smooth curve.

From figures it can be observed that, specimen made of clay burnt brick with mortar thickness 3/4" (Type C-3/4 and C1-3/4) gave almost same highest loading which is done by 6 ton vertical loads and clay burnt brick with mortar thickness 1/2" (type C-1/2 and C1-1/2) was performed by 3 tons vertical loads. Type M-1/2, M1-1/2 and M-3/4 specimens gave no same highest loading. This represents the more ductile quality of clay burnt brick wall. Nevertheless, type C-3/4 and C1-3/4 specimen undergoes larger deformations without rupture before failure than type C-1/2 and C1-1/2 specimen. Also type C-1/2 and C1-1/2 specimen undergoes larger deformations without rupture before failure than type M-1/2 and M1-1/2 specimen. The maximum load of (type C-3/4 and C1-3/4) sample was 9 to 10 ton, where for (type C-1/2 and C1-1/2) sample it was 5 to 6 ton, for (type M-1/2 and M1-1/2) sample it was 6 ton and type M-3/4 sample it was also 6 ton. Maximum displacement of type C-1/2 and C1-1/2 sample under loading were 14.38 and 15.68mm respectively. Where for type C-3/4 and C1-3/4 sample maximum displacement were 13.11 mm and 15.80mm. For type M-1/2 and M1-1/2 sample maximum displacement were 15.4 mm and 13.47mm. And for type M-3/4 sample maximum displacement was 20.89mm. From the hysteresis loop of type M1-1/2 specimen it is shown abnormal result. So that we use the result of machine made brick with mortar thickness 1/2" only type M-1/2 and reject the results of type M1-1/2 specimen results.

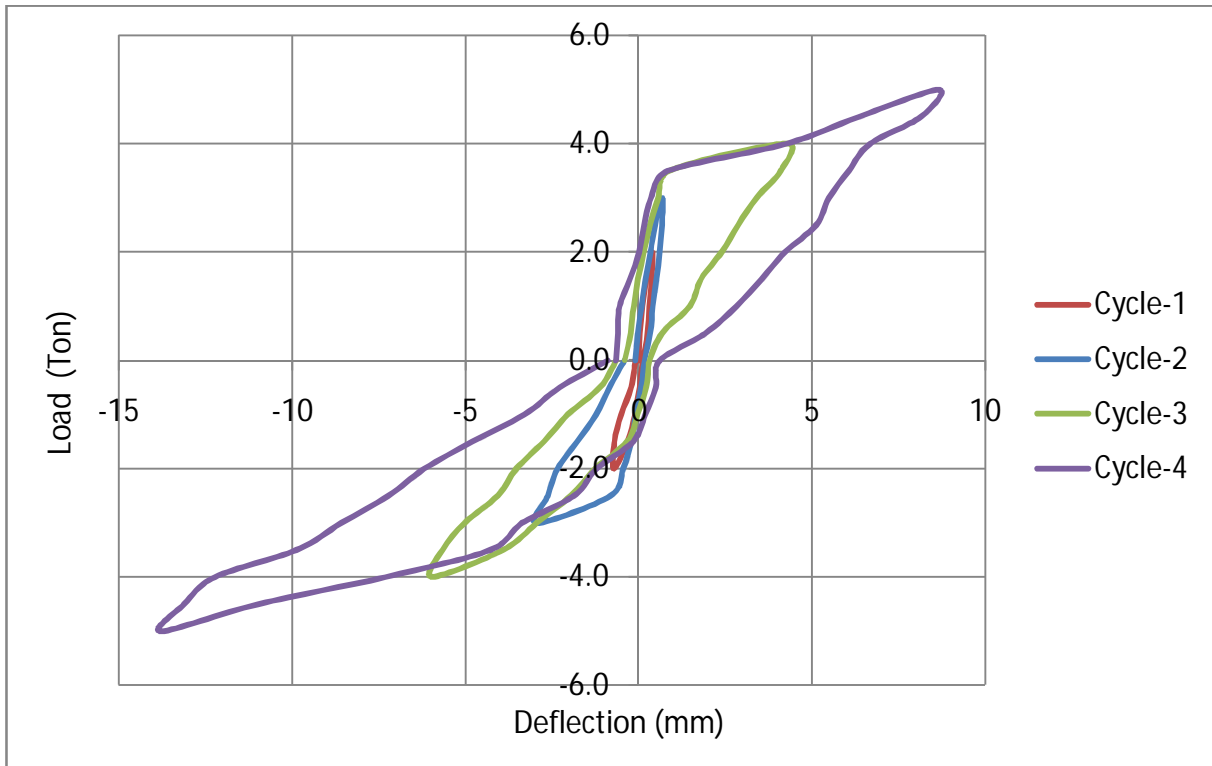


Figure 4.40 Load- Deformation Response of Specimen wall C-1/2

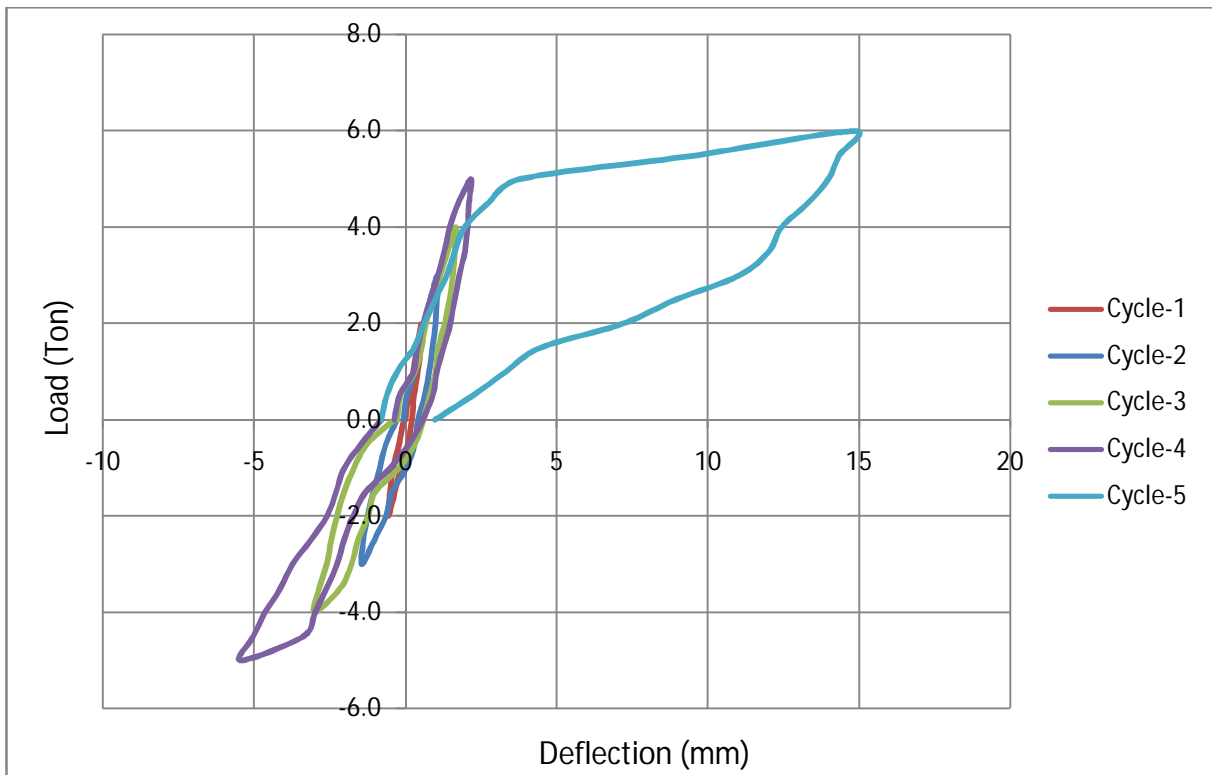


Figure 4.41 Load- Deformation Response of Specimen wall C1-1/2

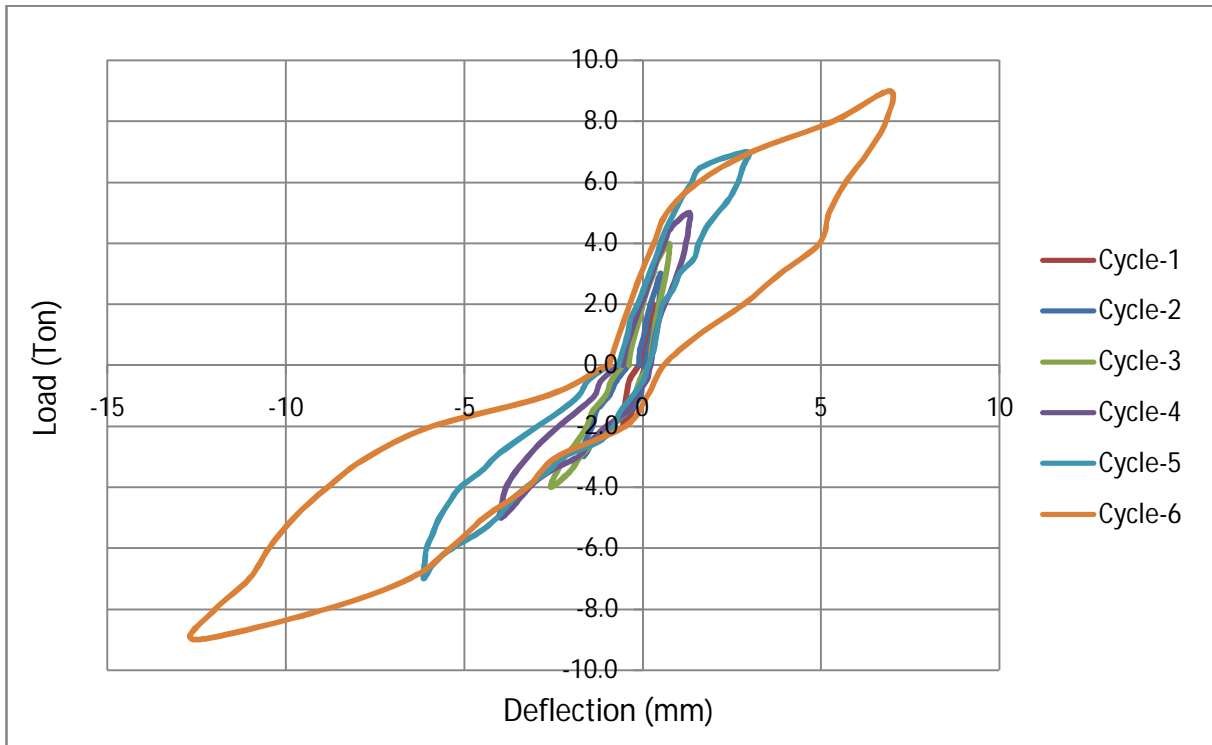


Figure 4.42 Load- Deformation Response of Specimen wall C-3/4

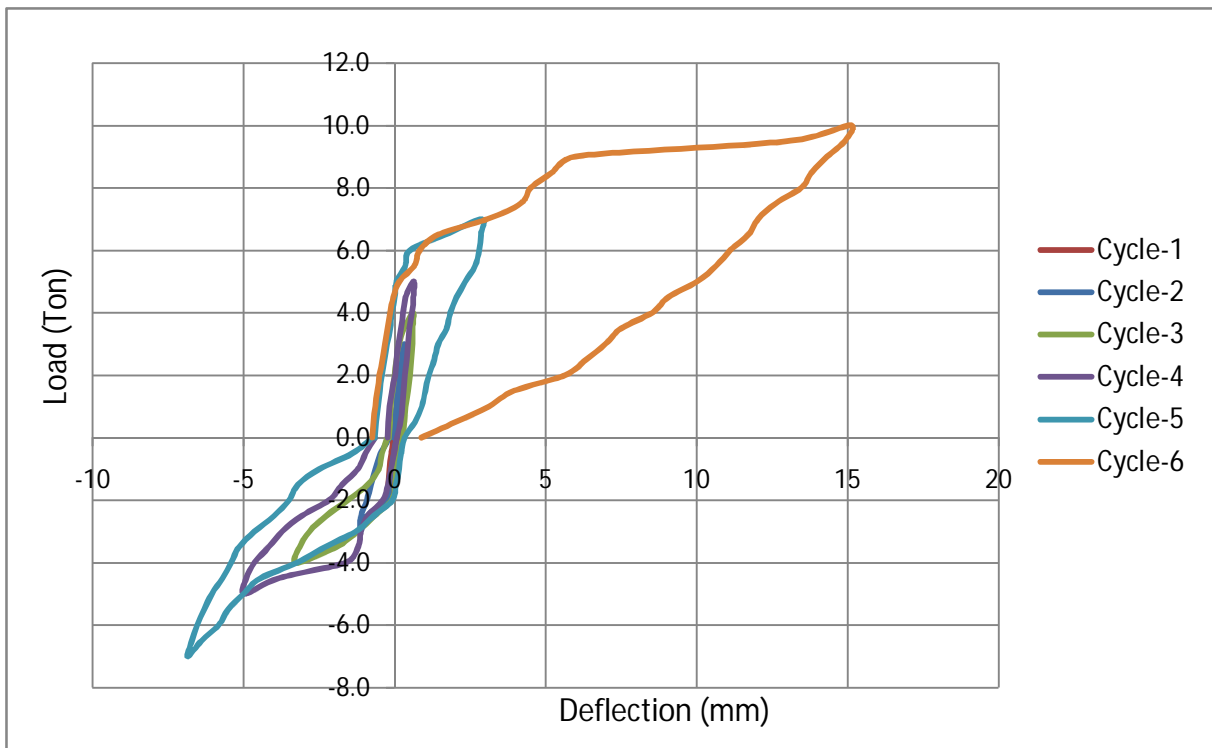


Figure 4.43 Load- Deformation Response of Specimen wall C1-3/4

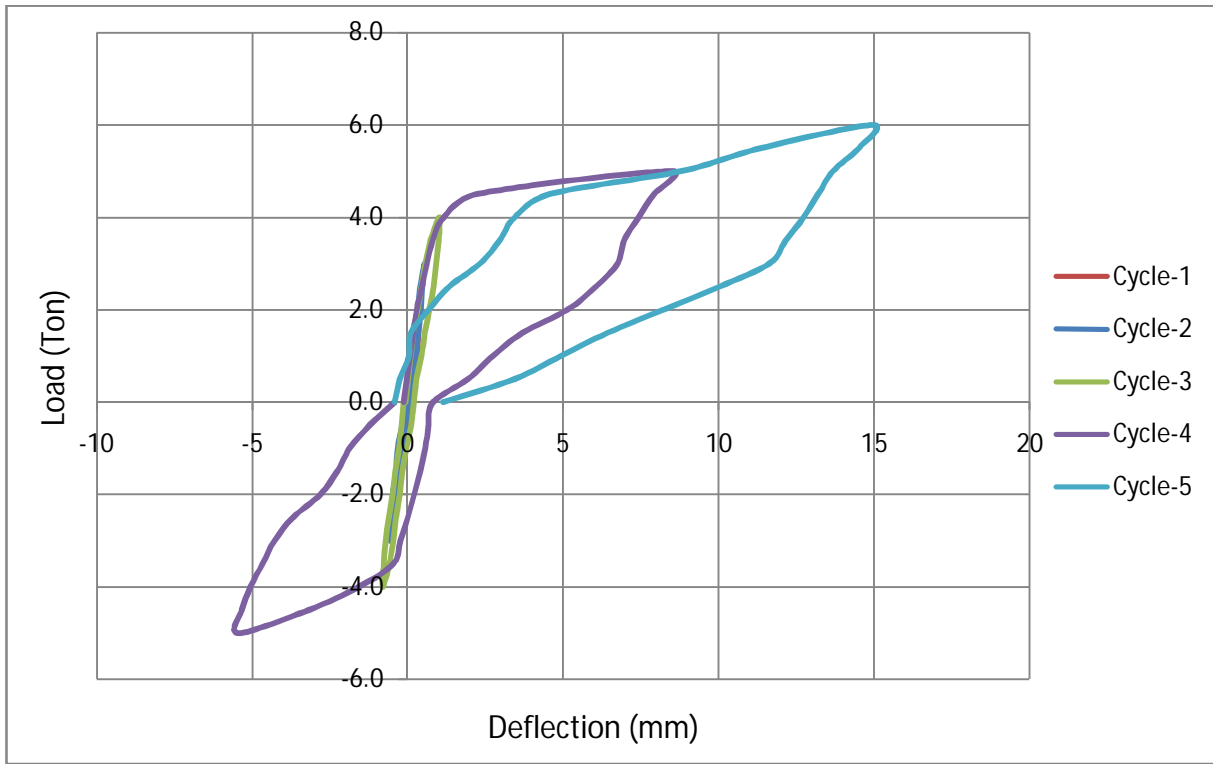


Figure 4.44 Load- Deformation Response of Specimen wall M-1/2

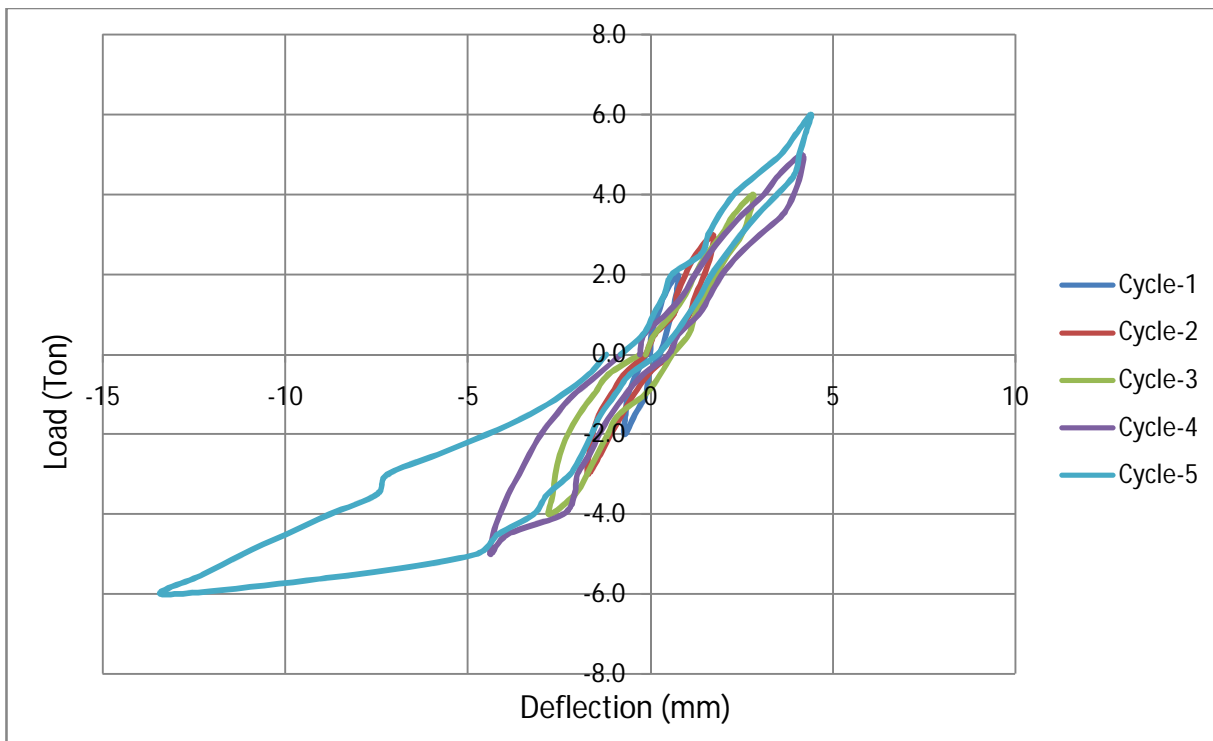


Figure 4.45 Load- Deformation Response of Specimen wall M1-1/2

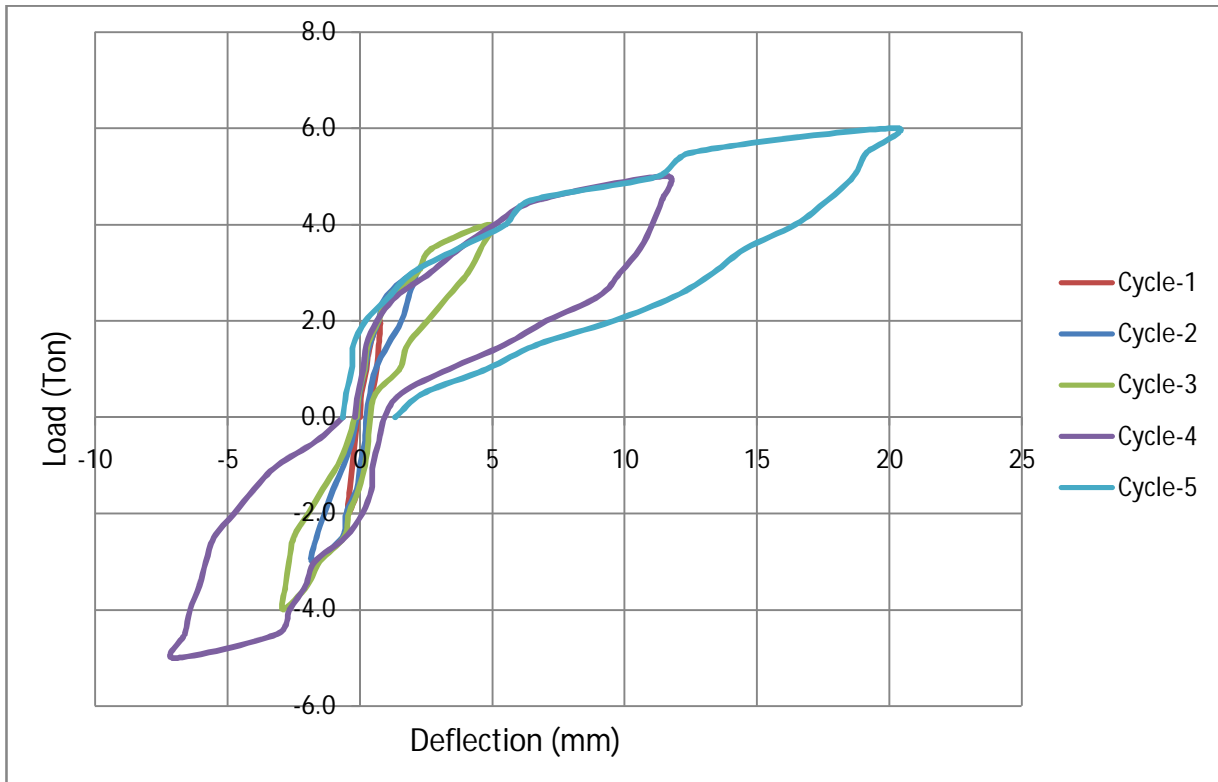


Figure 4.46 Load- Deformation Response of Specimen wall M-3/4

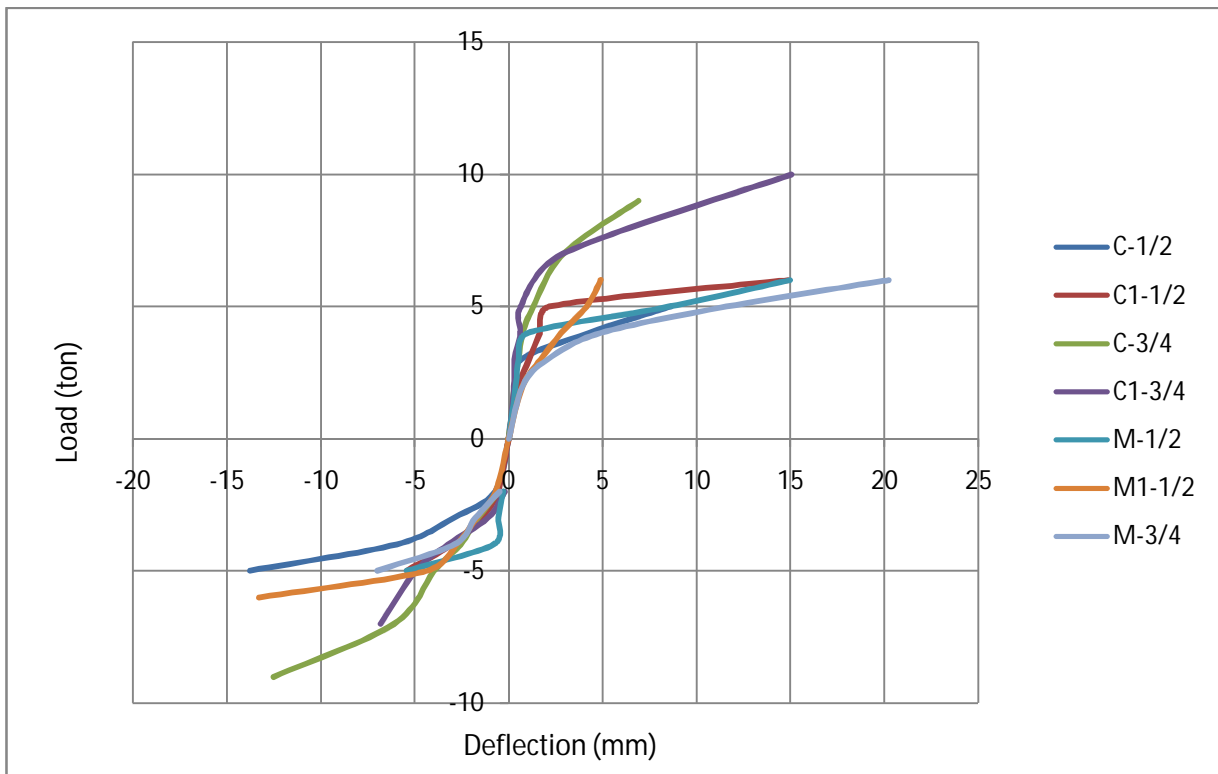


Figure 4.47: Hysteresis Loop Envelopes of all types of Specimens

The hysteresis loop envelopes of seven samples are shown in Figure 4.47. At every point of the hysteresis loop curves type C-3/4 and C1-3/4 specimen showed more loading value and less displacement value than type C-1/2 and C1-1/2 specimen. Also at every point of the hysteresis loop curves type C-1/2 and C1-1/2 specimen showed more loading value and less displacement value than type M-1/2 and M1-1/2. And at every point of the hysteresis loop curves type M-1/2 and M1-1/2 specimen showed more loading value and less displacement value than M-3/4. This is obviously the sign of comparative better performance. Hence Type C-3/4 and C1-3/4 specimen is more ductile, stiffer and stronger than type C-1/2 and C1-1/2 specimen, where type C-1/2 and C1-1/2 specimen is more ductile, stiffer and stronger than type M-1/2 specimen. And type M-1/2 specimen is more ductile, stiffer and stronger than type M-3/4 specimen.

4.8 Summary of Test Results of Seven Specimens

Table 4.6 Test Results of Seven Specimens

Name of the Specimen	Maximum Load (Ton)	Maximum Displacement (mm)
C-1/2	5.0	13.77
C1-1/2	6.0	14.89
C-3/4	9.0	12.52
C1-3/4	10.0	15.06
M-1/2	6.0	14.98
M1-1/2	6.0	13.29
M-3/4	6.0	20.25

Table 4.7 Secant Stiffness (average of L/D) of Seven Specimens at Each Cycle

Cycle	C-1/2	C1-1/2	C-3/4	C1-3/4	M-1/2	M1-1/2	M-3/4
1st	3.57	3.64	4.88	5.56	6.06	2.78	3.33
2nd	1.66	2.38	2.78	4.00	5.45	1.75	1.56
3rd	0.78	1.71	2.41	2.07	4.40	1.43	1.03
4th	0.45	1.32	1.89	1.79	0.72	1.17	0.54
5th		0.40	1.55	1.44	0.40	0.68	0.30
6th			0.93	0.66			

Table 4.8: Characteristics of First Crack of Seven Specimens

Type	1st Crack Cycle	1st Crack Side	1st Crack Load (ton)	1st Crack Displacement (mm)
C-1/2	1 st	Right	2.0	0.72
C1-1/2	2 nd	Right	2.5	1.03
C-3/4	2 nd	Right	3.0	1.65
C1-3/4	2 nd	Right	2.5	0.91
M-1/2	2 nd	Right	2.5	0.46
M1-1/2	2 nd	Left	2.5	1.24
M-3/4	1 st	Right	2.0	0.67

4.9 Characteristics of First Crack Formation

For specimens C-1/2 and C1-1/2 first crack occurred at 2.0 ton and 2.5 ton when displacements were 0.72 mm and 1.03 mm respectively. For specimens C-3/4 and C1-3/4 first crack occurred at 3.0 ton and 2.5 ton with displacements of 1.65mm and 0.91 mm respectively. For specimen M-1/2 and M1-1/2 the first crack occurred at 2.5 ton and 2.5 ton with the displacement of 0.46 mm and 1.24 mm respectively. For specimen M-3/4 the first crack load was 2.0 ton with the displacement of 0.67 mm at 1st cycle. Load at first crack formation of all seven samples are expressed in Figure 4.48.

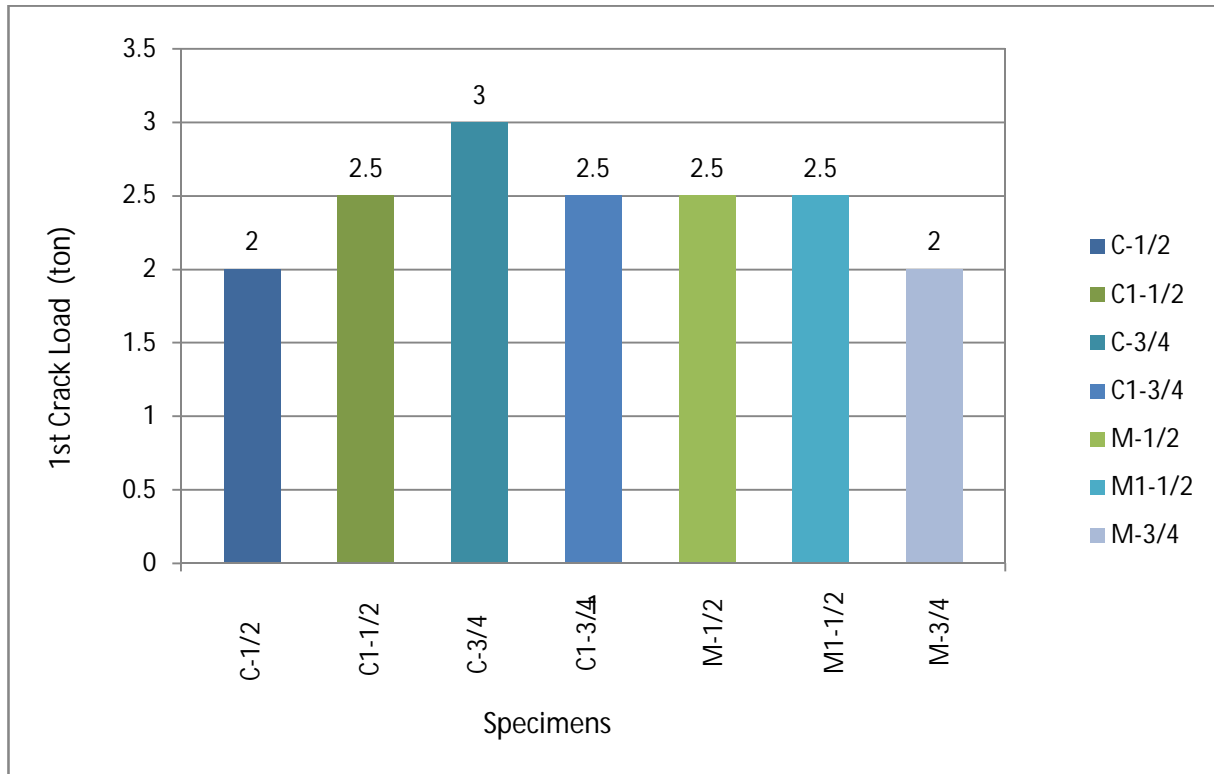


Figure 4.48 Load at First Crack Formation of Seven Specimens

4.10 Stiffness of Specimens

The average stiffness obtained for the two half cycles in a hysteretic loop therefore gave the approximate stiffness for that particular cycle. In other words, the secant stiffness was formulated with standard mathematical formula,

$$\text{Secant Stiffness} = \text{Shear Force} / \text{Displacement} (k = F/\Delta).$$

The values of the secant stiffness obtained for each cycle are plotted for all the specimens. The degradation of the secant stiffness is plotted, the ultimate stiffness versus corresponding cycle number for each specimen tested. Figure 4.49 shows secant stiffness of each cycle. Figure 4.50 shows degradation of stiffness of each cycle. It can be noted that as the number of cycles increases, stiffness decreases. Here the value of stiffness of clay burnt brick with mortar thickness 3/4" (C-3/4 and C1-3/4) is stiffer than clay burnt brick with mortar thickness 1/2" (type C-1/2 and C1-1/2) because clay burnt brick wall with mortar thickness 1/2" was tested with 3 ton vertical loads and clay burnt brick with mortar thickness 3/4" was tested with 6 ton vertical loads. The value of stiffness of machine made brick with mortar thickness 1/2" (type M-1/2 and M1-1/2) is stiffer than machine made brick with mortar thickness 3/4" (type M-3/4). The result

of type M1-1/2 specimen was rejected because of abnormal result. Stiffness after first cycle and final cycle are shown in Figure 4.51 and 4.52.

The increase in stiffness between different categories at first cycle and final cycle are shown in Figure 4.50 and 4.52. For type C-1/2 and C1-1/2 stiffness varies from 3.57 to 0.45 and 3.64 to 0.40 where for type C-3/4 and C1-3/4 it varies from 4.88 to 0.93 and 5.56 to 0.66. Again, for type M-1/2 stiffness varies from 6.06 to 0.40 where for type M-3/4 it varies from 3.33 to 0.30.

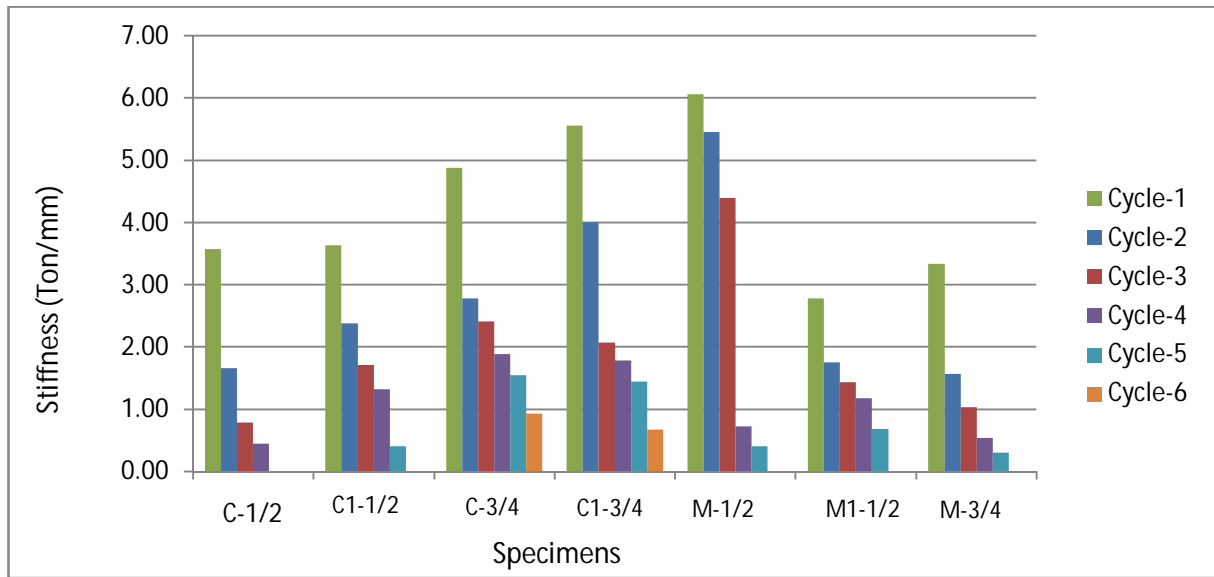


Figure 4.49 Secant Stiffness of Each Cycle for Seven Samples

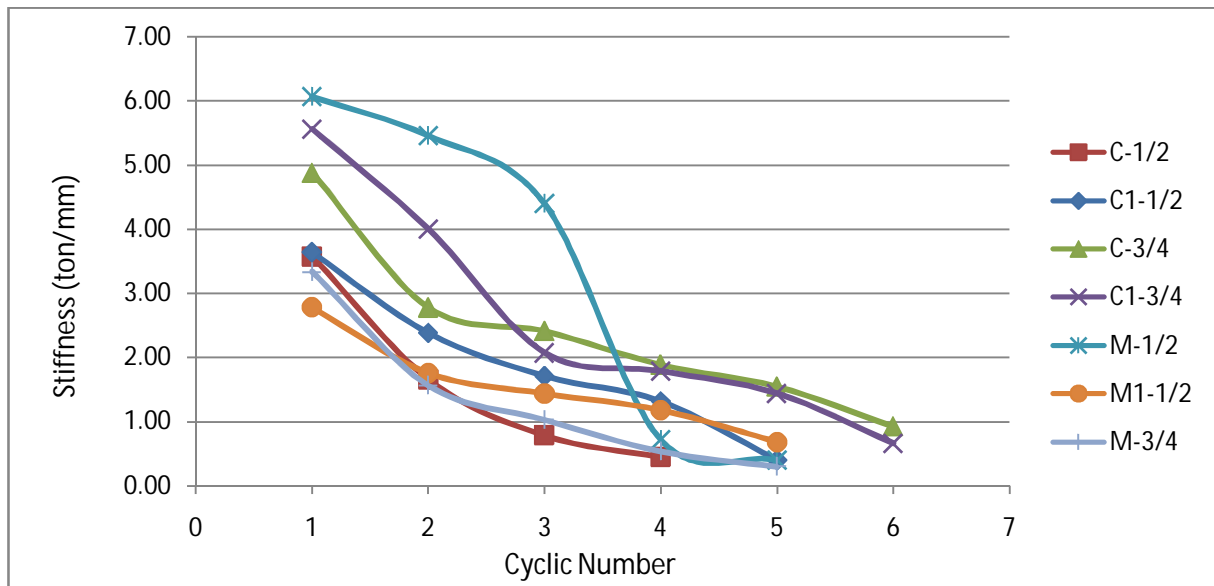


Figure 4.50: Degradation of Stiffness of Each Cycle for Seven Specimens

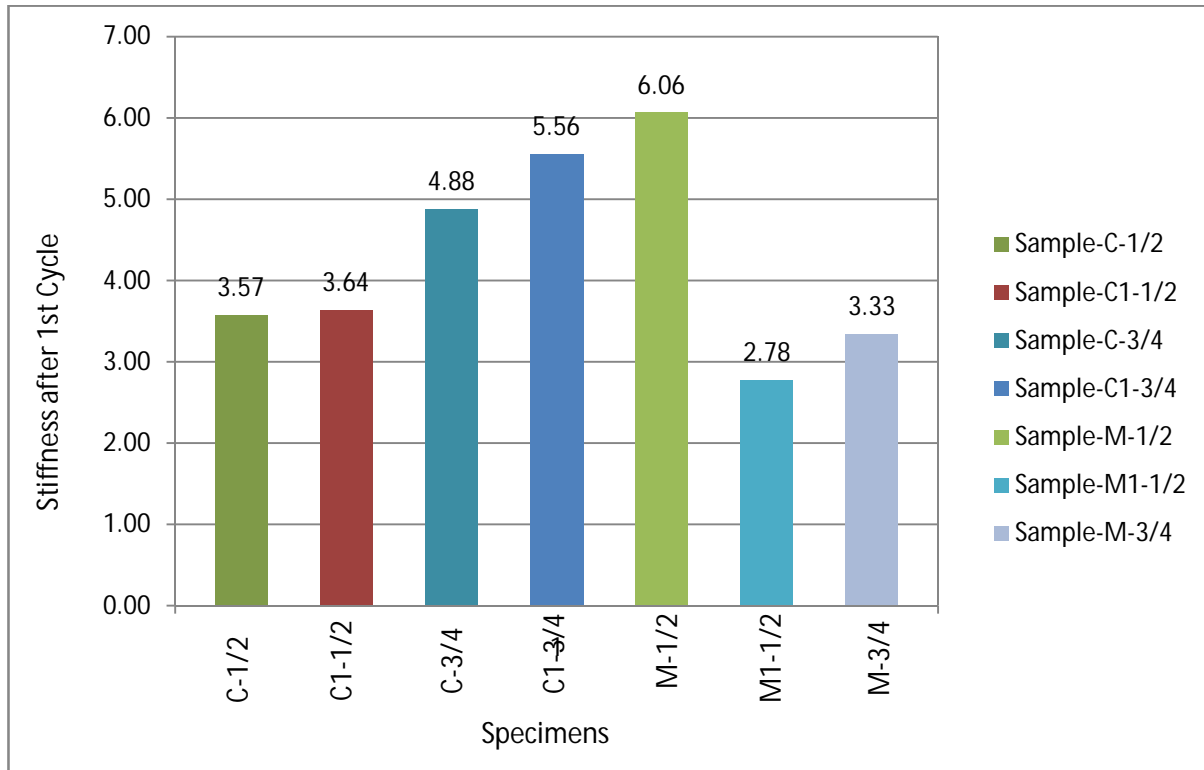


Figure 4.51: Stiffness after 1st Cycle of Seven Samples

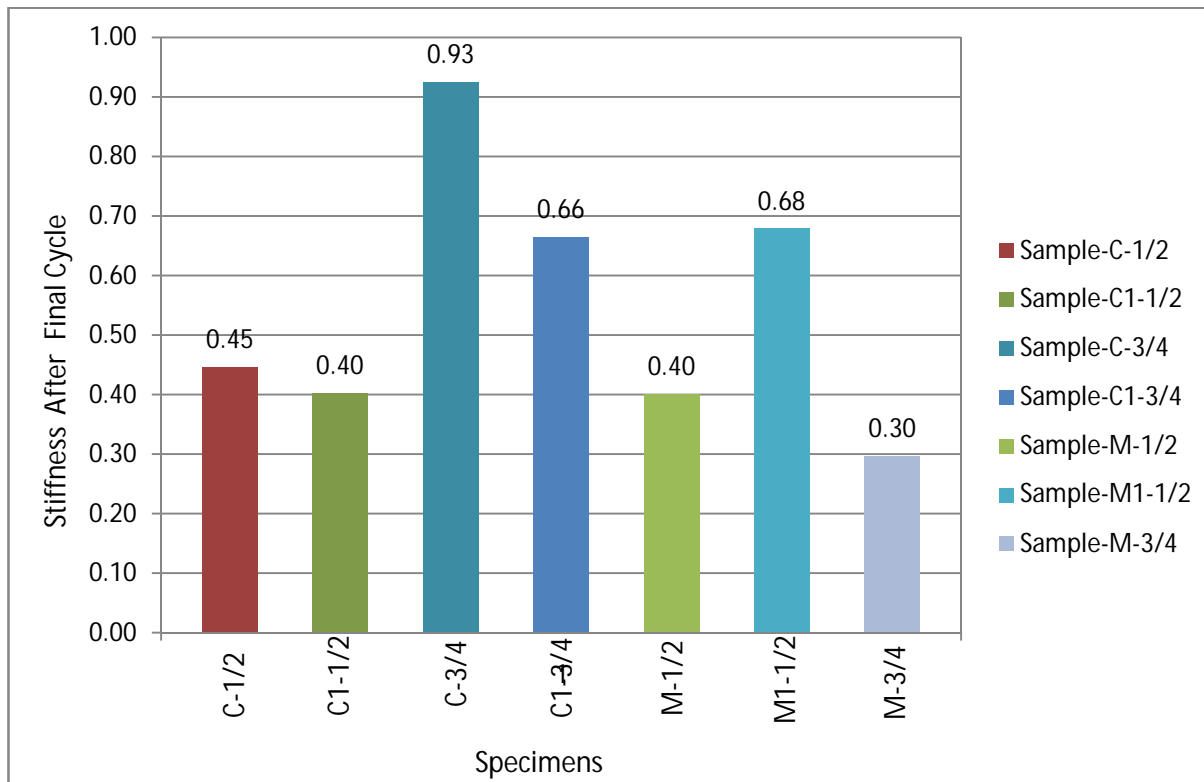


Figure 4.52: Stiffness after Final Cycle of Seven Samples

4.11 Load Characteristics

Machine made brick wall with mortar thickness 1/2" is more strength than machine made brick wall with mortar thickness 3/4". Figure 4.53 represents the load of the specimens at every cycle. Figure 4.54 express the maximum load of all seven specimens. This can be observed from Figure 4.53. Maximum load increased from 5 ton to 6 ton for specimen C-1/2 and C1-1/2. In case of type C-3/4 and C1-3/4 it increased from 9 ton to 10 ton. For Type M-1/2, M1-1/2 and M-3/4 maximum load increased 6 ton.

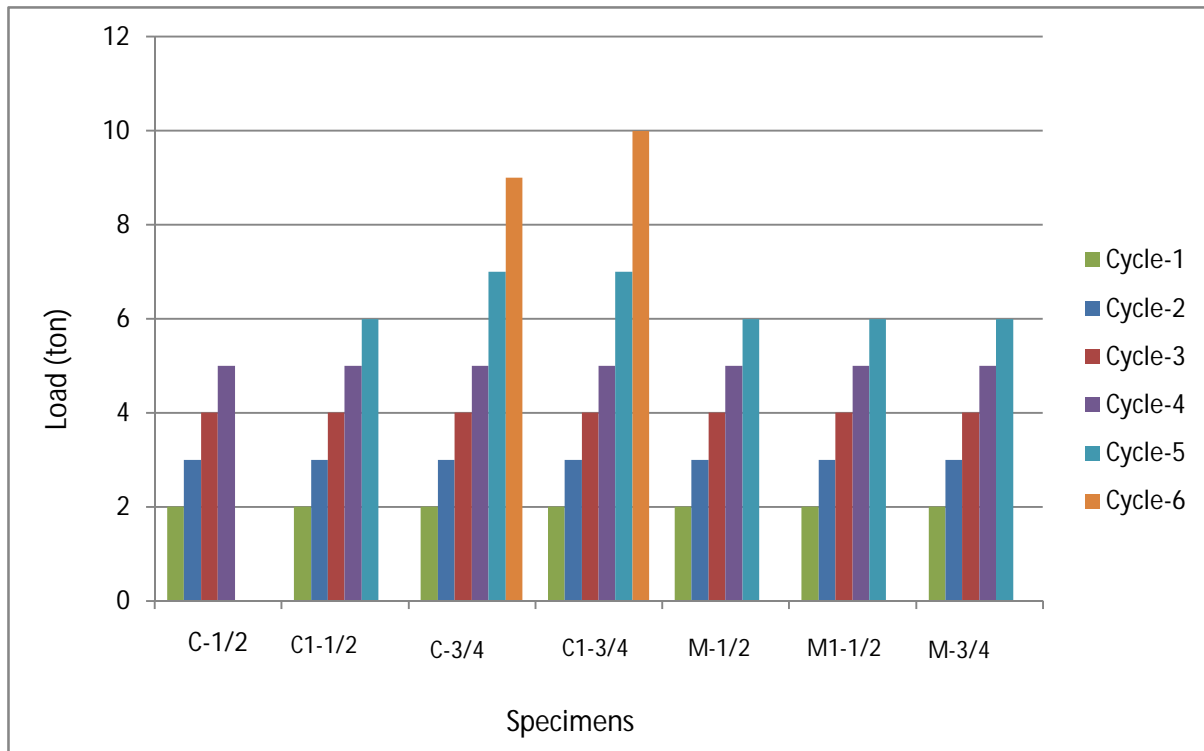


Figure 4.53 The Load of the Specimens at Every Cycle

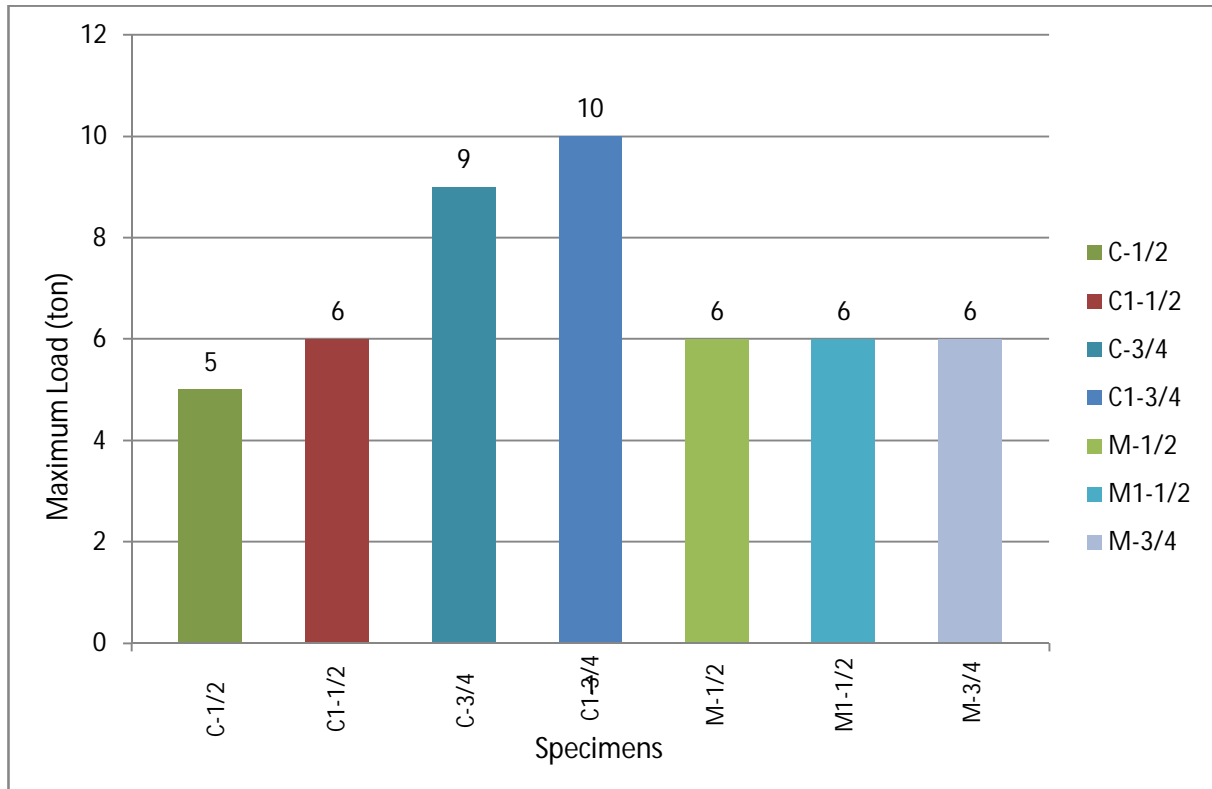


Figure 4.54 Maximum load of seven Specimens

4.12 Maximum Displacement

Table 4.9: Maximum Displacement of Each Specimen during Test

Specimens	Maximum Displacements (mm)
C-1/2	13.77
C1-1/2	14.89
C-3/4	12.52
C1-3/4	15.06
M-1/2	13.58
M1-1/2	13.29
M-3/4	20.25

Table 4.9 summarized the maximum displacements of every specimens of different type during loading and unloading. It was found that the maximum displacements were increases with the increasing mortar thickness. Figure 4.55 represents the maximum displacement of all seven specimens.

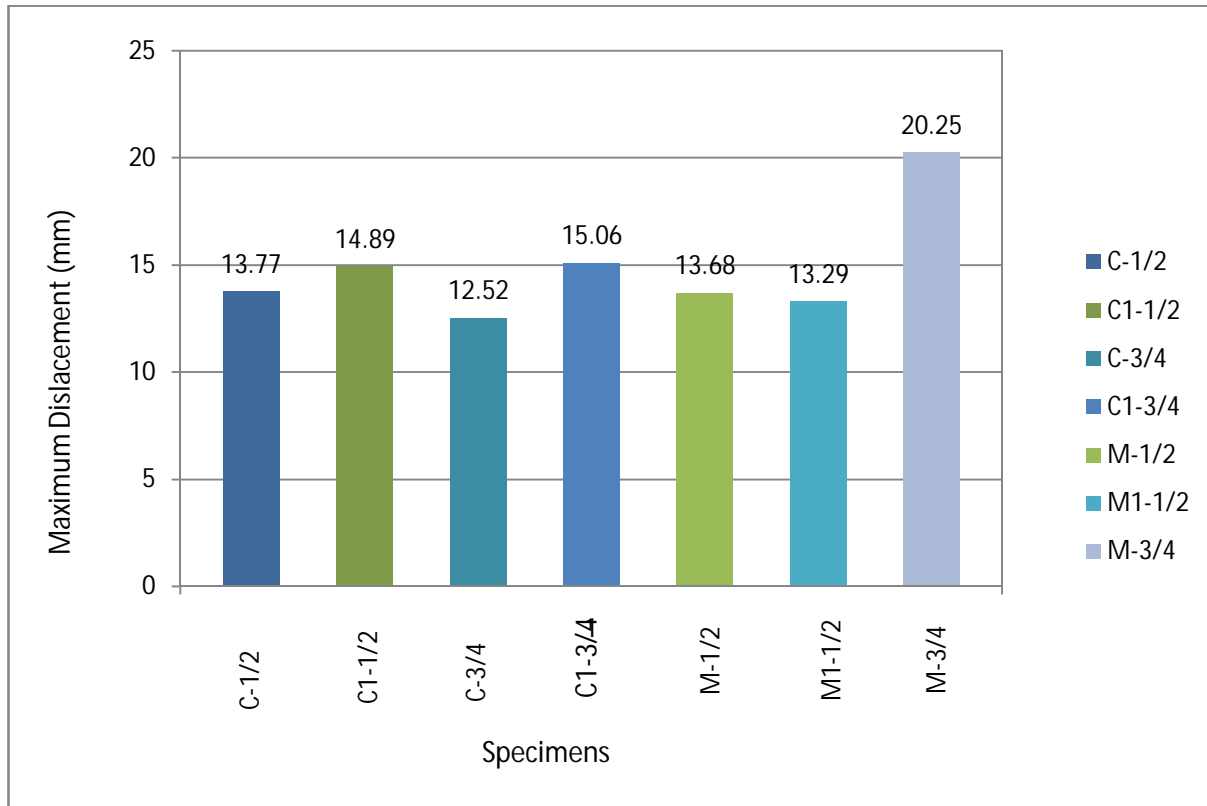


Figure 4.55 Maximum Displacement of seven Specimens

4.13 Residual Displacement

Table 4.10: Residual Displacement of Each Specimen during Test

Specimens	Residual Displacements (mm)
C-1/2	0.89
C1-1/2	0.99
C-3/4	1.07
C1-3/4	1.02
M-1/2	1.14
M1-1/2	1.21
M-3/4	1.33

Table 4.10 summarized the residual displacements of every specimens of different type after total removal of loading. It was found that the residual displacements were decreasing with the increasing mortar thickness. Figure 5.56 represents the residual displacement of all seven specimens.

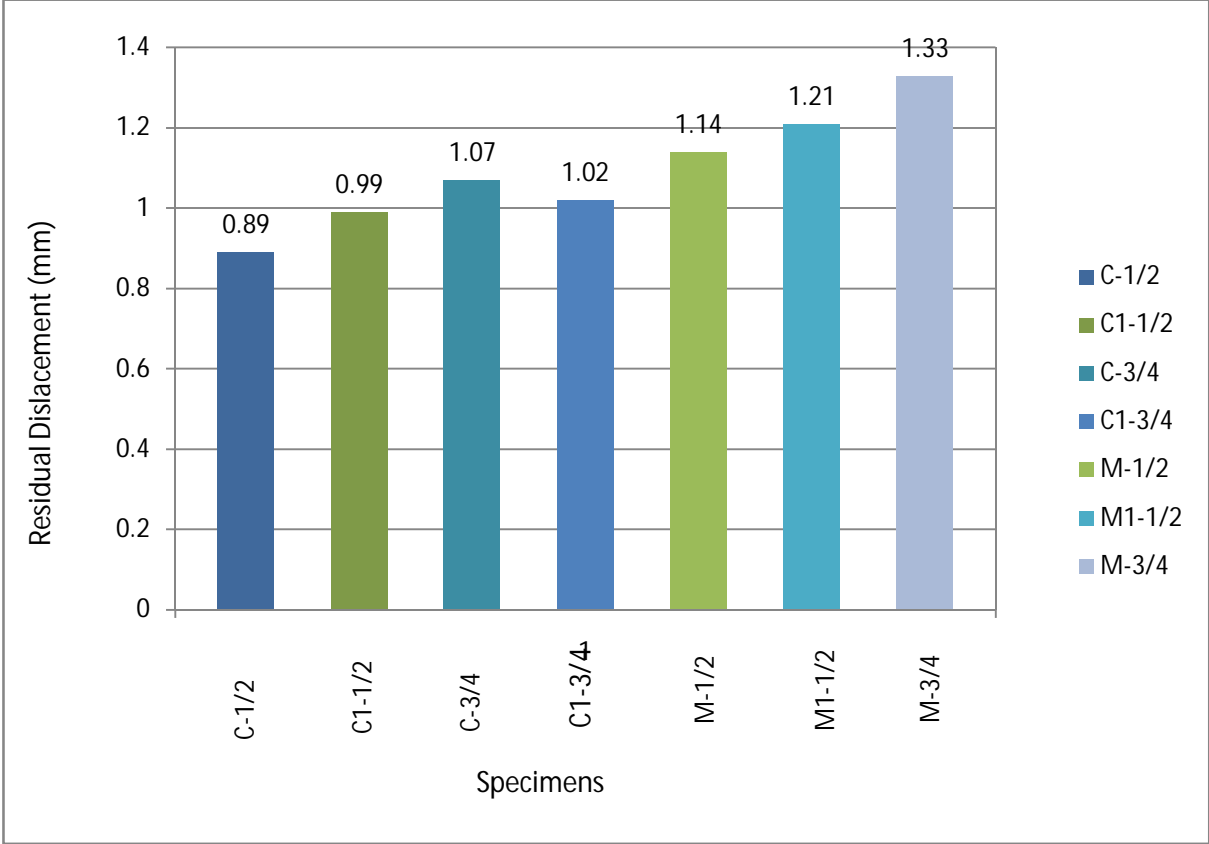


Figure 4.56 Residual Displacement of seven Specimens

4.14 Ductility of the specimen wall

Drift is calculated as the ratio between the lateral displacements experienced at each loading level divided by the effective height of the test unit. Displacement ductility μ_{Δ} is a commonly used parameter to determine overall structural lateral response. It is obtained experimentally from the idealized bilinear approximation to the monotonic spine or cyclic peak envelope of the load-displacement curve shown in Fig. 4.40 to 4.46. Displacement ductility is defined as the ratio of deformation at a given response level to the deformation at ideal yield (Priestley et al. 1996).

$$\mu_{\Delta} = \Delta / \Delta_y$$

Ductility is a measure of how much strain a given stress produces. Highly ductile metals can exhibit significant strain before fracturing, whereas brittle materials frequently display very little strain. An overly simplistic way of viewing ductility is the degree to which a material is forgiving of local deformation without the occurrence of fracture. Ductility measures the amount of plastic deformation that a material goes through by the time it breaks.

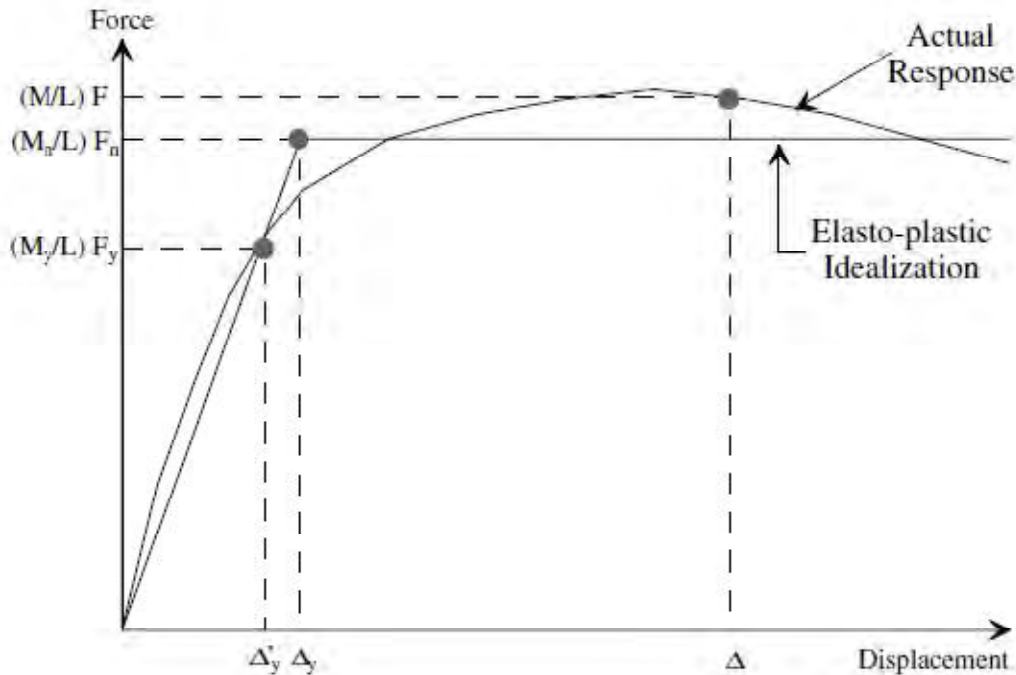


Figure 4.57 Bilinear approximation for displacement ductility parameter

From the figure 4.40 and 4.41 it is observed that, the specimen made of clay burnt brick with mortar thickness 1/2" (Specimens-C-1/2 and C1-1/2), the inelastic deformations are 13.77mm and 14.89mm and proportional deformations are 1.08mm and 1.40mm respectively.

For Specimen C-1/2, Ductility $\mu = \Delta_{\max}/\Delta_y = 13.77/0.88 = 15.68$

For Specimen C1-1/2, Ductility $\mu = \Delta_{\max}/\Delta_y = 14.89/1.08 = 13.89$

From the figure 4.42 and 4.43 it is observed that, the specimen made of clay burnt brick with mortar thickness 3/4" (Specimens-C-3/4 and C1-3/4), the inelastic deformations are 12.52mm and 15.06mm and proportional deformations are 1.29mm and 1.66mm respectively.

For Specimen C-3/4, Ductility $\mu = \Delta_{\max}/\Delta_y = 12.52/1.29 = 9.71$

For Specimen C1-3/4, Ductility $\mu = \Delta_{\max}/\Delta_y = 15.06/1.66 = 9.07$

From the figure 4.44 and 4.45 it is observed that, the specimen made of machine made brick with mortar thickness 1/2" (Specimen- M-1/2), the inelastic deformation and proportional deformation are 14.98mm and 1.01mm respectively. Due to abnormal result type M1-1/2 was rejected.

For Specimen M-1/2, Ductility $\mu = \Delta_{\max}/\Delta_y = 14.98/1.01 = 14.83$

From the figure 4.46 it is observed that, the specimen made of machine made brick with mortar thickness 3/4" (Specimen-M-3/4), the inelastic deformation and proportional deformation are 20.25mm and 2.06mm respectively.

For Specimen M-3/4, Ductility $\mu = \Delta_{\max}/\Delta_y = 20.25/2.06 = 9.83$

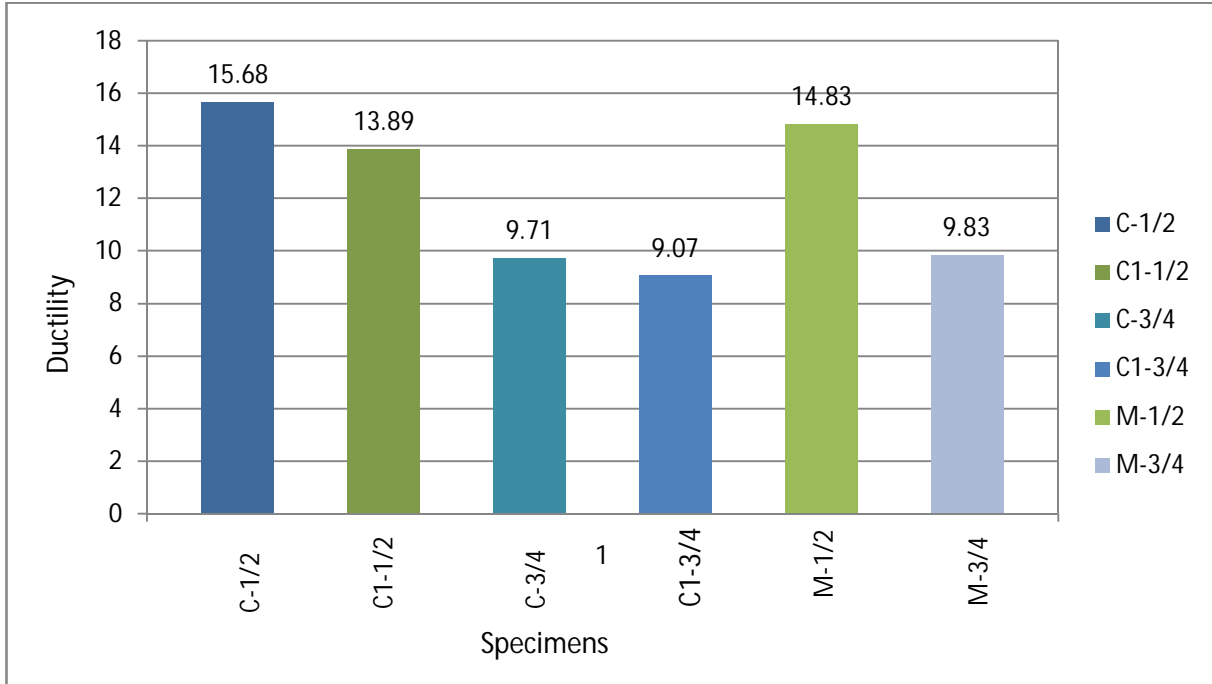


Figure 4.58 Ductility of the Specimens

4.15 Stiffness degradation Calculation

Stiffness degradation has been calculated by measuring slope of each cycle. Slope is calculated by positive and negative pick points of each loop. Stiffness degradation calculations are as follows:

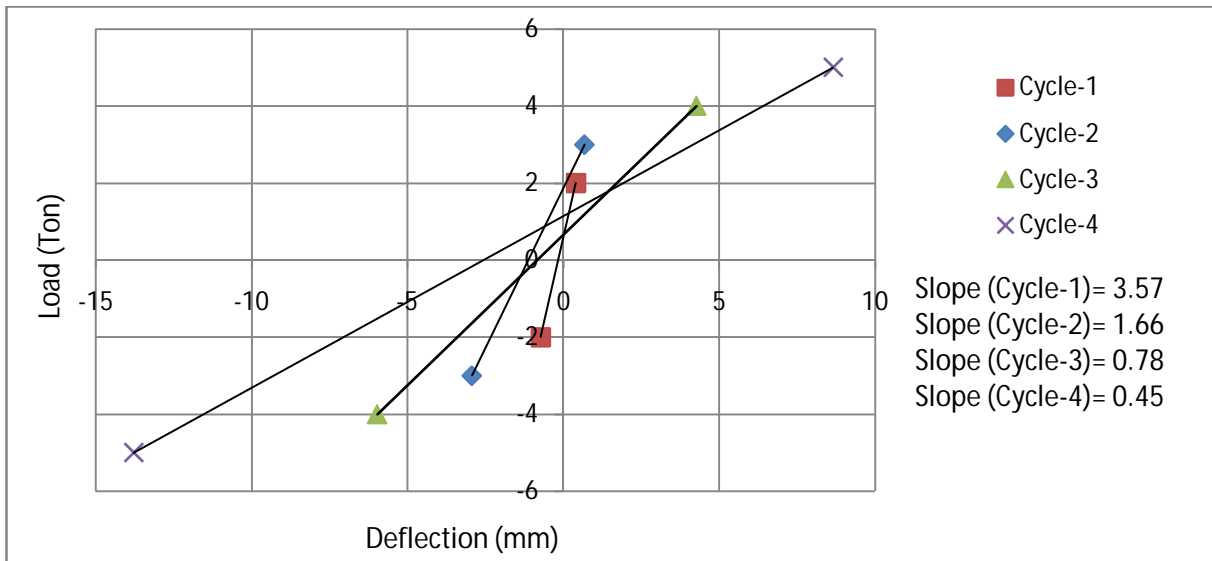


Figure 4.59 Stiffness degradation of Specimen C-1/2

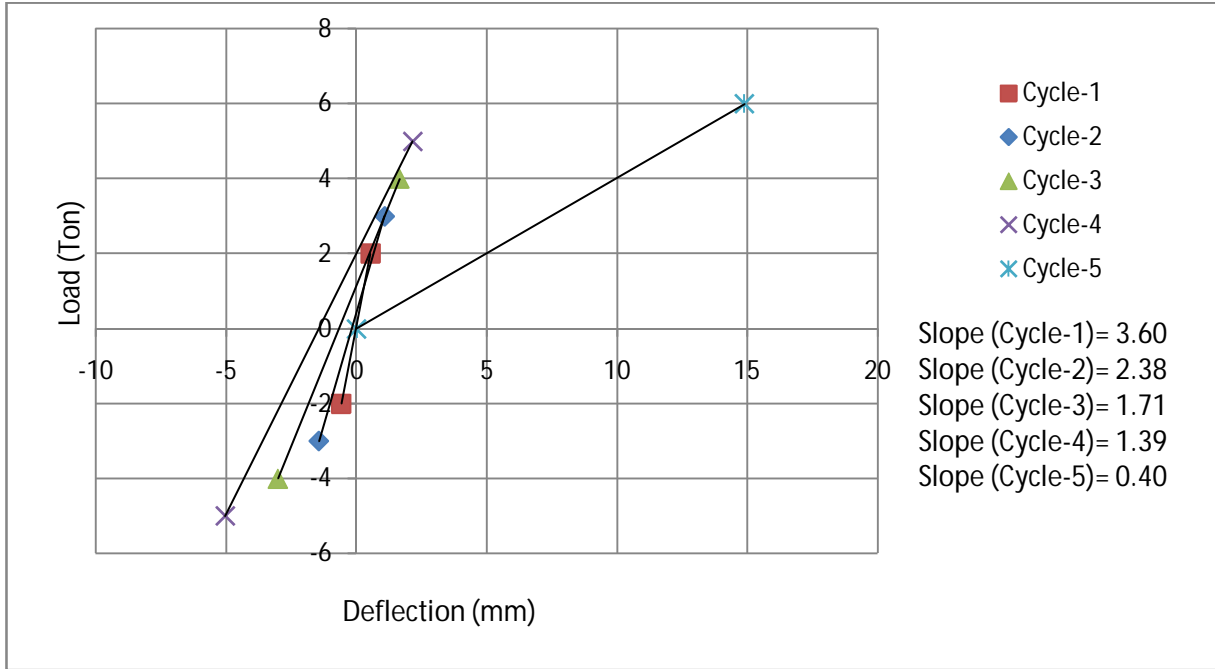
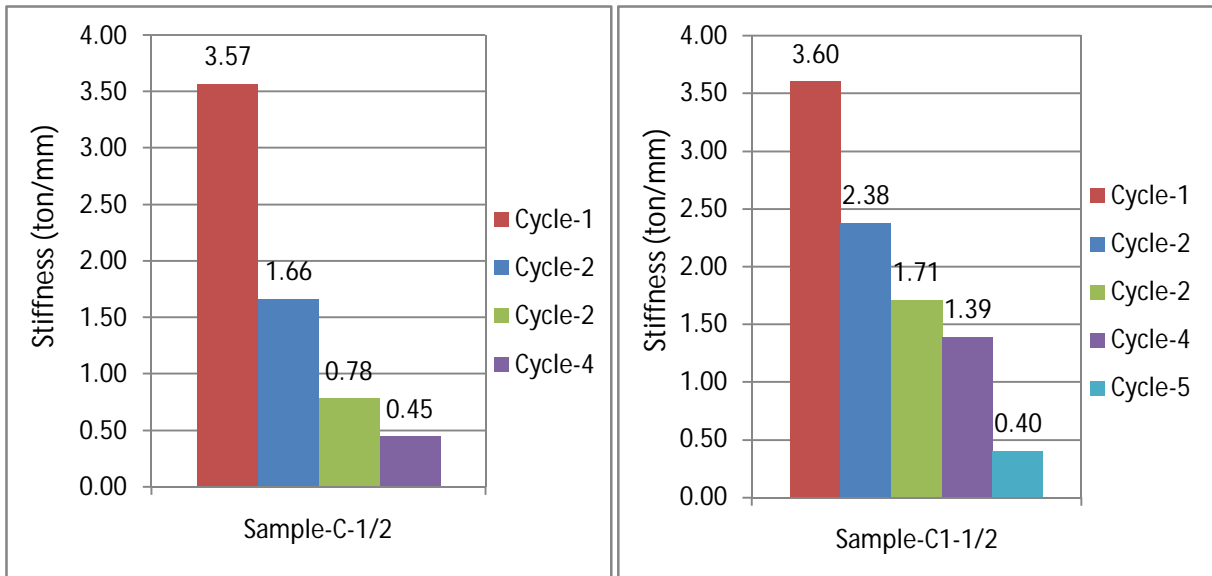


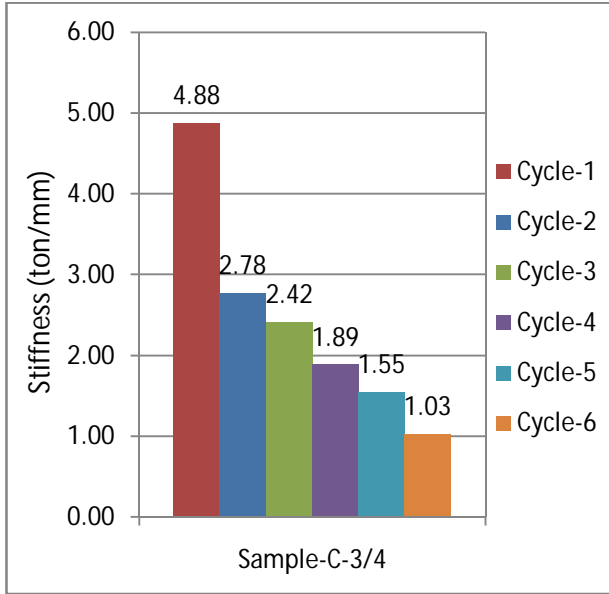
Figure 4.60 Stiffness degradation of Specimen C1-1/2

Bar chart shows the stiffness degradation of each specimen

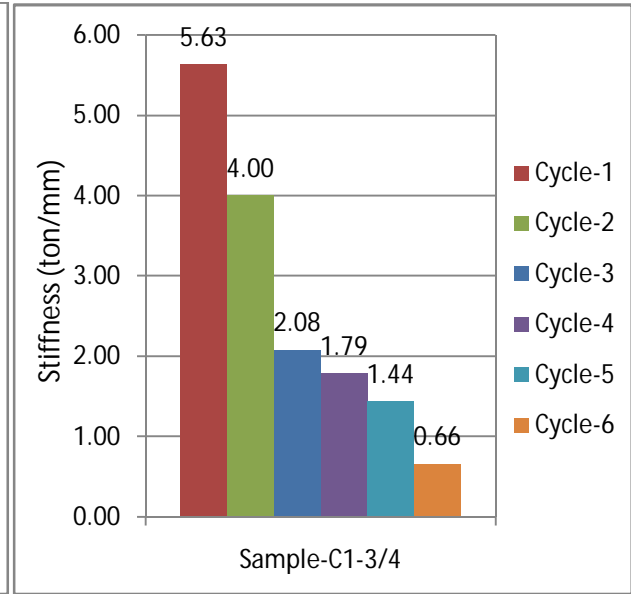


a. Stiffness degradation of clay burnt brick wall (C-1/2) with mortar thickness 1/2"

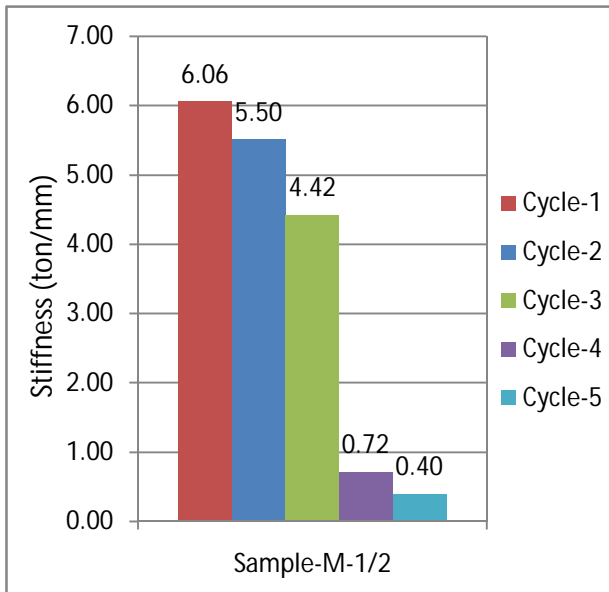
b. Stiffness degradation of clay burnt brick (C1-1/2) with mortar thickness 1/2"



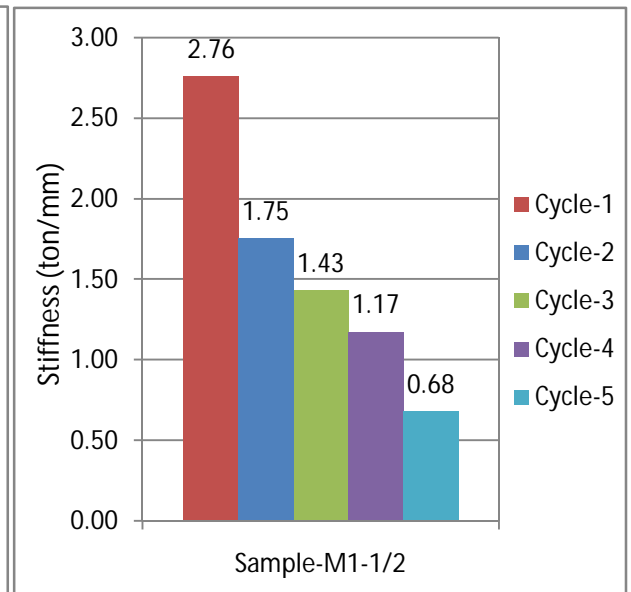
c. Stiffness degradation of clay burnt brick wall (C-3/4) with mortar thickness 3/4"



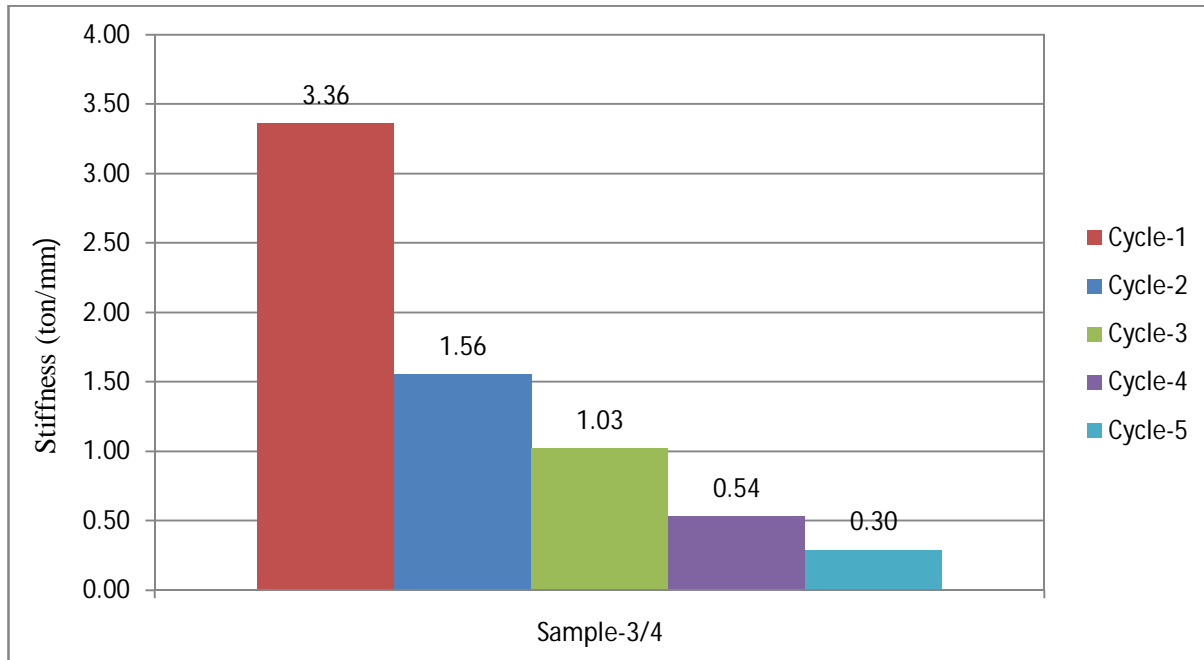
d. Stiffness degradation of clay burnt brick wall (C1-3/4) with mortar thickness 3/4"



e. Stiffness degradation of machine made brick wall (M-1/2) with mortar thickness 1/2"



f. Stiffness degradation of machine made brick wall (M1-1/2) with mortar thickness 1/2"



g. Stiffness degradation of machine made brick wall (M-3/4) with mortar thickness 3/4"

Figure 4.61: Stiffness Degradation of Different Types Of Walls

From figures 4.61a and 4.61b showing stiffness degradation it can be observed that, for specimen made of clay burnt brick with mortar thickness 1/2"(specimens- C-1/2 and C1-1/2), the average slope degradation of the 2nd cycle is 56.3% of the 1st cycle and the average slope degradation of the 3rd cycle is 61.8% of the 2nd cycle. Also the average slope degradation of the 4th cycle is 73.6% of the 3rd cycle and the average slope degradation of the 5th cycle is 43.5% of the 4th cycle for C1-1/2 sample. The average slope degradation of clay burnt brick with mortar thickness 1/2" is 20.0% per cycle.

From figures 4.61c and 4.61d showing stiffness degradation it can be observed that, for specimen made of clay burnt brick with mortar thickness 3/4"(specimens- C-3/4 and C1-3/4), the average slope degradation of the 2nd cycle is 64.5% of the 1st cycle and the average slope degradation of the 3rd cycle is 66.4% of the 2nd cycle. Also the average slope degradation of the 4th cycle is 81.7% of the 3rd cycle and the average slope degradation of the 5th cycle is 81.5% of the 4th cycle. The average slope degradation of the 6th cycle is 56.6% of the 5th cycle. The average slope degradation of clay burnt brick with mortar thickness 3/4" is 13.93% per cycle.

From figures 4.61e showing stiffness degradation it can be observed that, for specimen made of machine made brick with mortar thickness 1/2"(specimens- M-1/2), the slope degradation of the 2nd cycle is 90.7% of the 1st cycle and the slope degradation of the 3rd cycle is 80.3% of the 2nd cycle. Also the slope degradation of the 4th cycle is 16.3% of the 3rd cycle and the slope degradation of the 5th cycle is 55.5% of the 4th cycle. The average slope degradation of machine made brick with mortar thickness 1/2" is 18.68% per cycle.

From figures 4.61g showing stiffness degradation it can be observed that, for specimen made of machine made brick with mortar thickness 3/4"(specimens- M-3/4), the slope degradation of the 2nd cycle is 46.4% of the 1st cycle and the slope degradation of the 3rd cycle is 66.0% of the 2nd cycle. Also the slope degradation of the 4th cycle is 52.4% of the 3rd cycle and the slope degradation of the 5th cycle is 55.5% of the 4th cycle. The average slope degradation of machine made brick with mortar thickness 3/4" is 18.21% per cycle.

4.16 Energy dissipation Calculation

Energy dissipation has been calculated by measuring energy i.e area of each cycle. Energy has been calculated by AUTO CAD. Energy dissipation calculations are as follows:

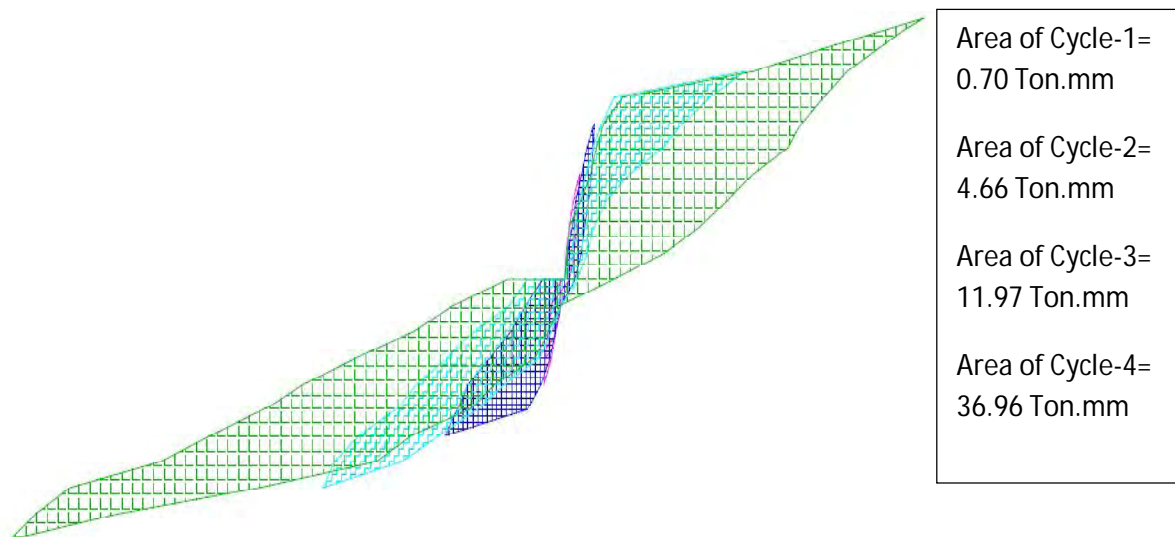


Figure 4.62 Energy Dissipation Calculation Sample Specimen (C-1/2)

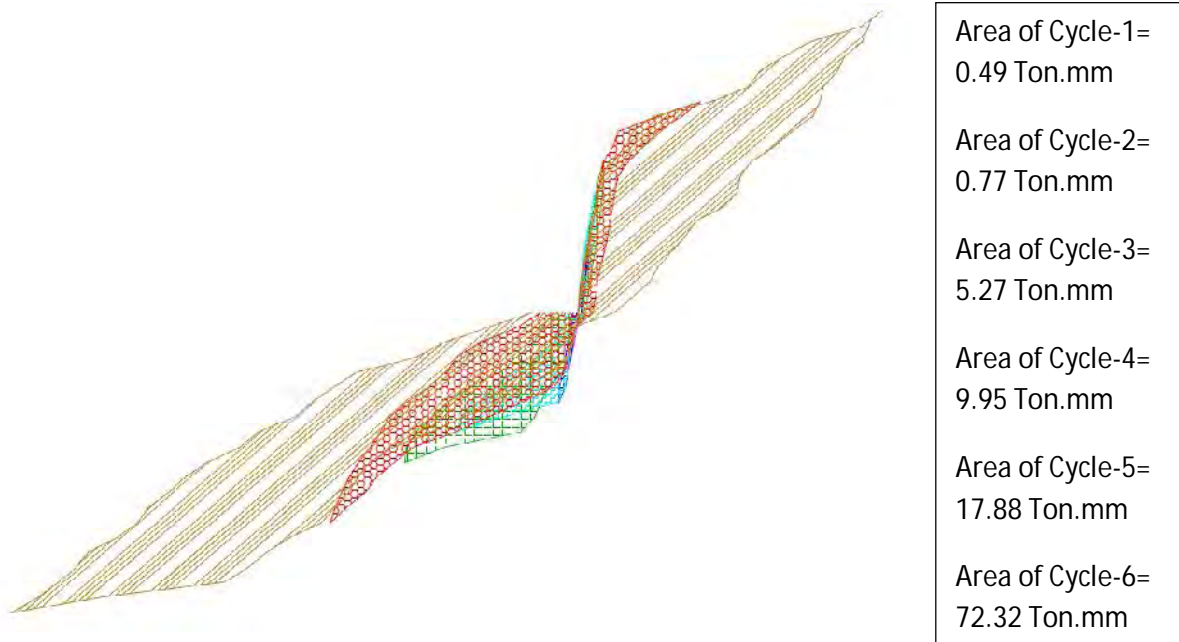
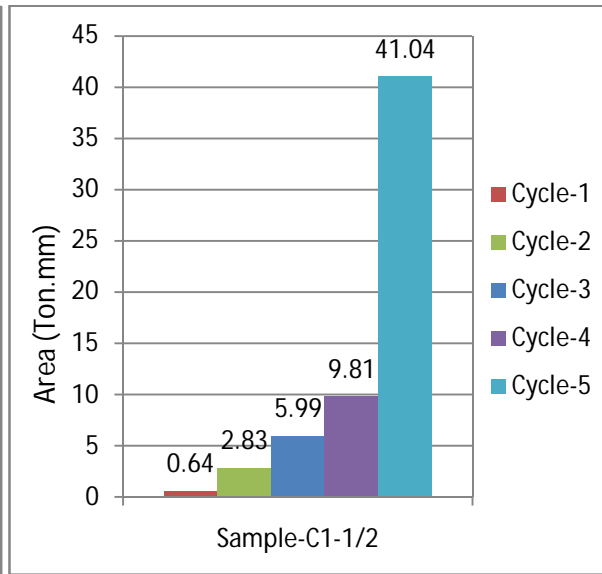
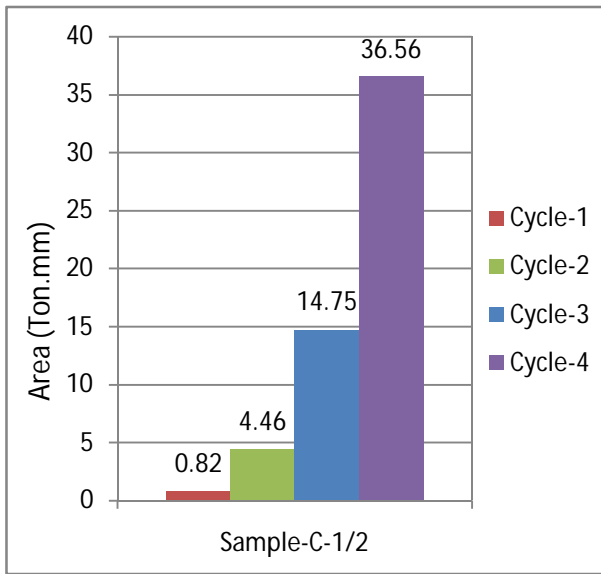
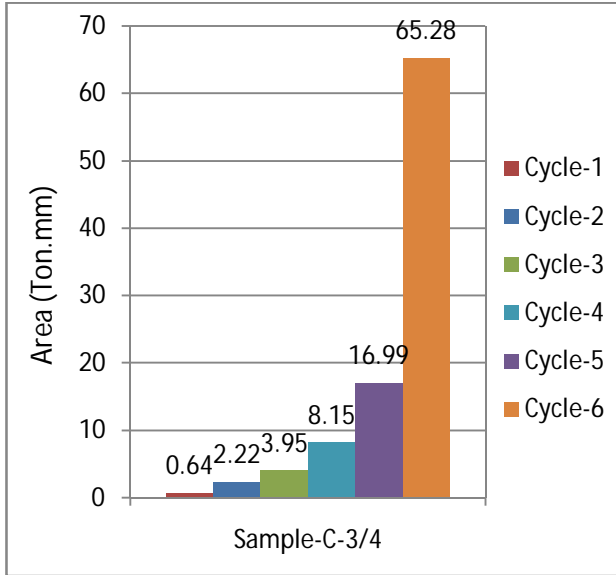


Figure 4.63 Energy Dissipation Calculation Sample Specimen (C-3/4)

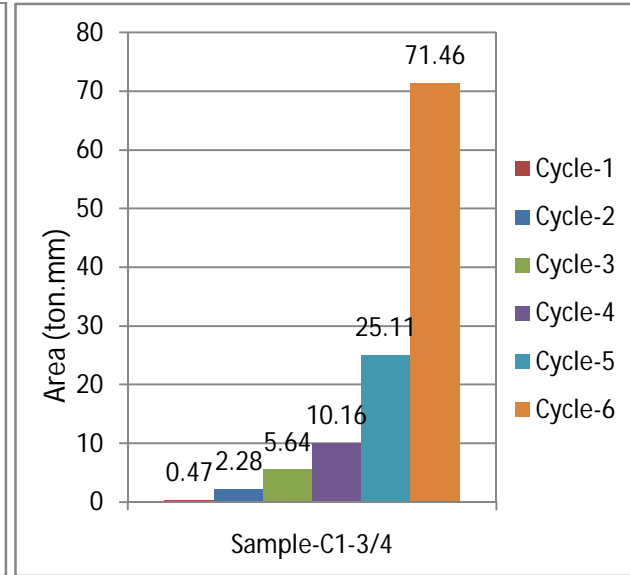


a. Energy dissipation of clay burnt brick wall (C-1/2) with mortar thickness 1/2"

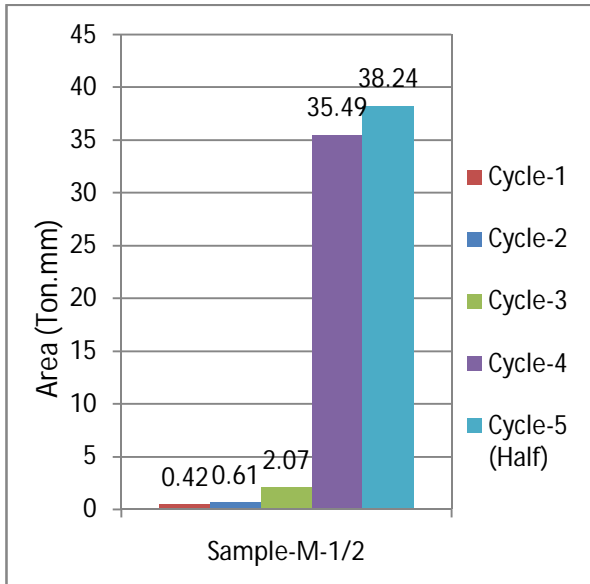
b. Energy dissipation of clay burnt brick wall (C1-1/2) with mortar thickness 1/2"



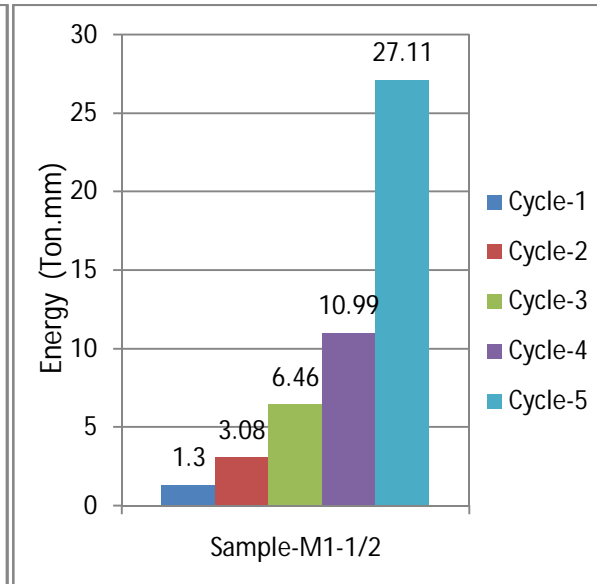
c. Energy dissipation of clay burnt brick wall (C-3/4) with mortar thickness 3/4"



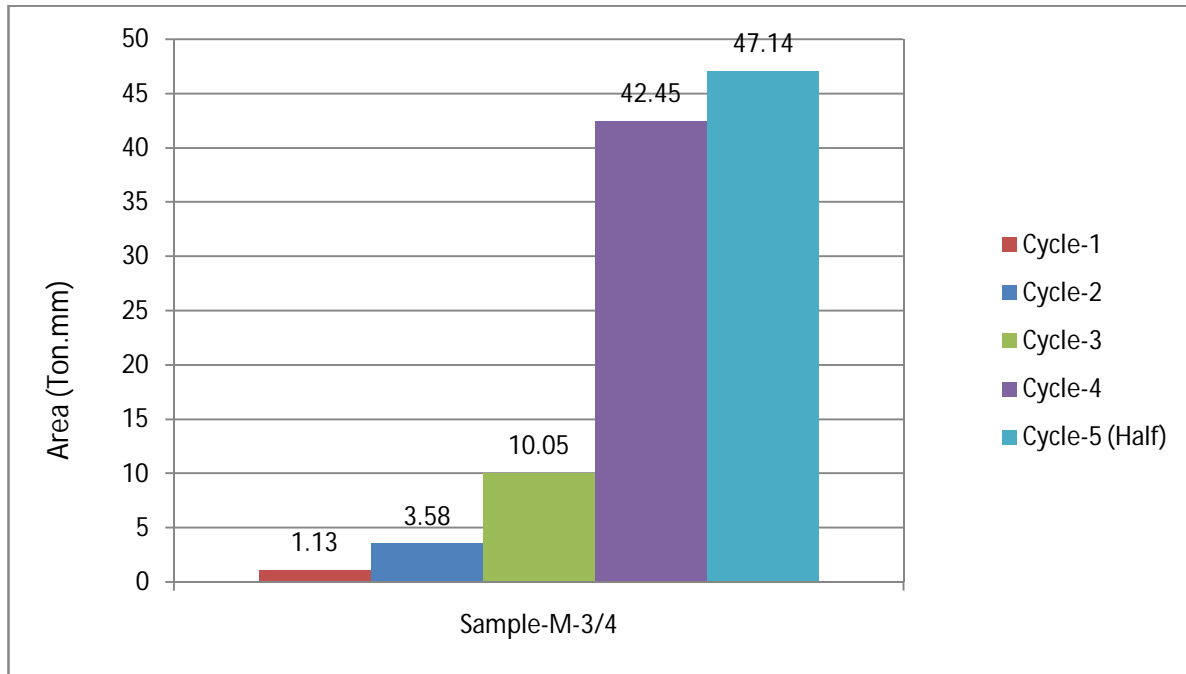
d. Energy dissipation of clay burnt brick wall (C1-3/4) with mortar thickness 3/4"



e. Energy dissipation of machine made brick wall (M-1/2) with mortar thickness 1/2"



f. Energy dissipation of machine made brick wall (M1-1/2) with mortar thickness 1/2"



g. Energy dissipation of machine made brick wall (M-3/4) with mortar thickness 3/4"

Figure 4.64: Energy Dissipation of Different Types of Walls

From figures 4.64 showing energy dissipation, it can be observed that, the specimen made of clay burnt bricks with mortar thickness 1/2" (specimens C-1/2 and C1-1/2), the absorbed total average energy 58.48 ton.mm. The specimen made of clay burnt brick with mortar thickness 3/4" (Specimens C-3/4 and C1-3/4), the absorbed total average energy 106.2 ton.mm. The energy absorbed by clay burnt brick wall with mortar thickness 1/2" is 55.1% of allowable total energy absorbed by clay burnt brick wall with mortar thickness 3/4". The specimen made of machine made brick with mortar thickness 1/2" (Specimens M-1/2), the absorbed total energy 76.83ton.mm and the specimen made of machine made brick with mortar thickness 3/4" (Specimens M-3/4), the absorbed total energy 104.35ton.mm. Hence energy absorbed by machine made brick wall with mortar thickness 1/2" is 73.6% of total energy absorbed by machine made brick wall with mortar thickness 3/4". It seems that, with the increasing mortar thickness energy dissipation is increases.

4.17 Hysteresis Damping

The quantitative parameter that can be evaluated at each performance level is the equivalent viscous damping ratio, ξ_{eq} , which describes the equivalent viscous hysteretic damping. It is based on an equal area approach that represents the same amount of energy loss per cycle as seen in the real experiment (Priestley et al. 1996). The calculation of ξ_{eq} for cases with symmetric hysteresis loops is shown in Fig. 4.65. The area within the inelastic force-displacement response curve, E_d in the figure, is a measure of the hysteretic damping or energy-dissipating capacity of the structure. The hatched region in Fig. 4.65 depicts the elastic strain energy stored in an equivalent linear elastic system, E_s . The equivalent viscous damping ratio, ξ_{eq} is represented by Equation (Hose and Seible, 1999).

$$\xi_{eq} = 1/4\pi(E_d/E_s)$$

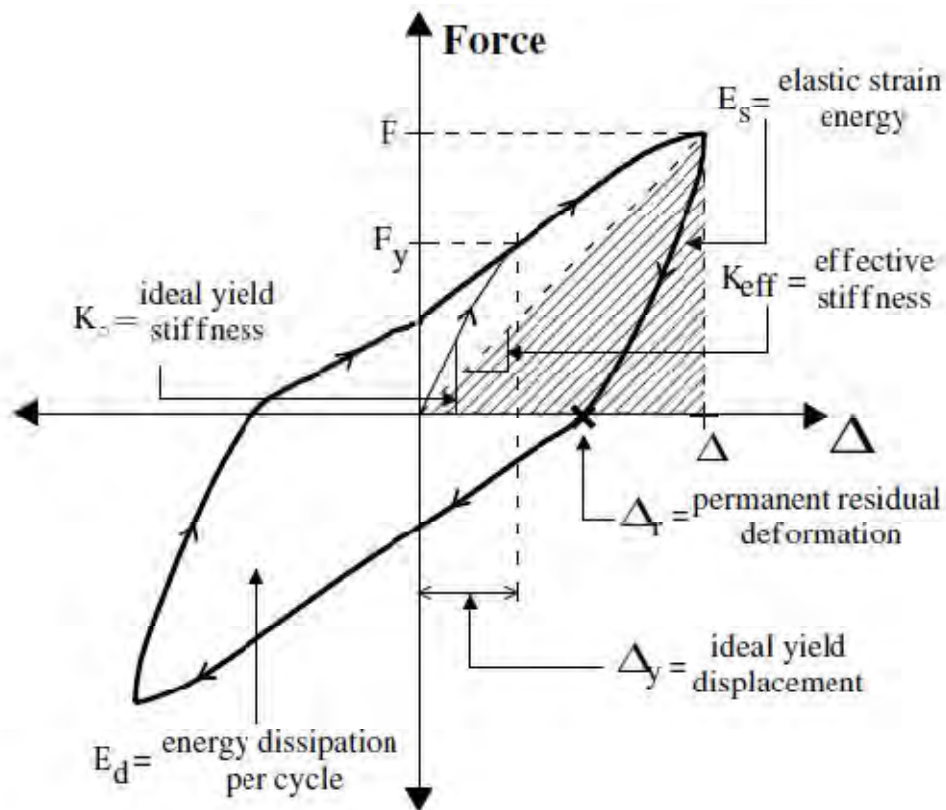


Figure 4.65 Equivalent viscous damping ratio for symmetric hysteresis loops

The equivalent viscous damping ratio for the full asymmetric cycle at a specific force level is derived in following equation and further defined in Fig. 4.66. The energy input or damping

energy loss for the push half cycle of the idealized force-displacement loop is represented by area E_{d1} in Fig. 4.66. Similarly, the energy loss for the pull half cycle is depicted as area E_{d2} . The hatched regions in Fig. 4.66 define E_{s1} and E_{s2} , which represent the elastic strain energy stored in an equivalent linear elastic system for the push and pull half cycles respectively.

$$\xi_{eq} = \frac{\xi_{eq1} + \xi_{eq2}}{2} = \frac{1}{4\pi} (E_{d1}/E_{s1} + E_{d2}/E_{s2})$$

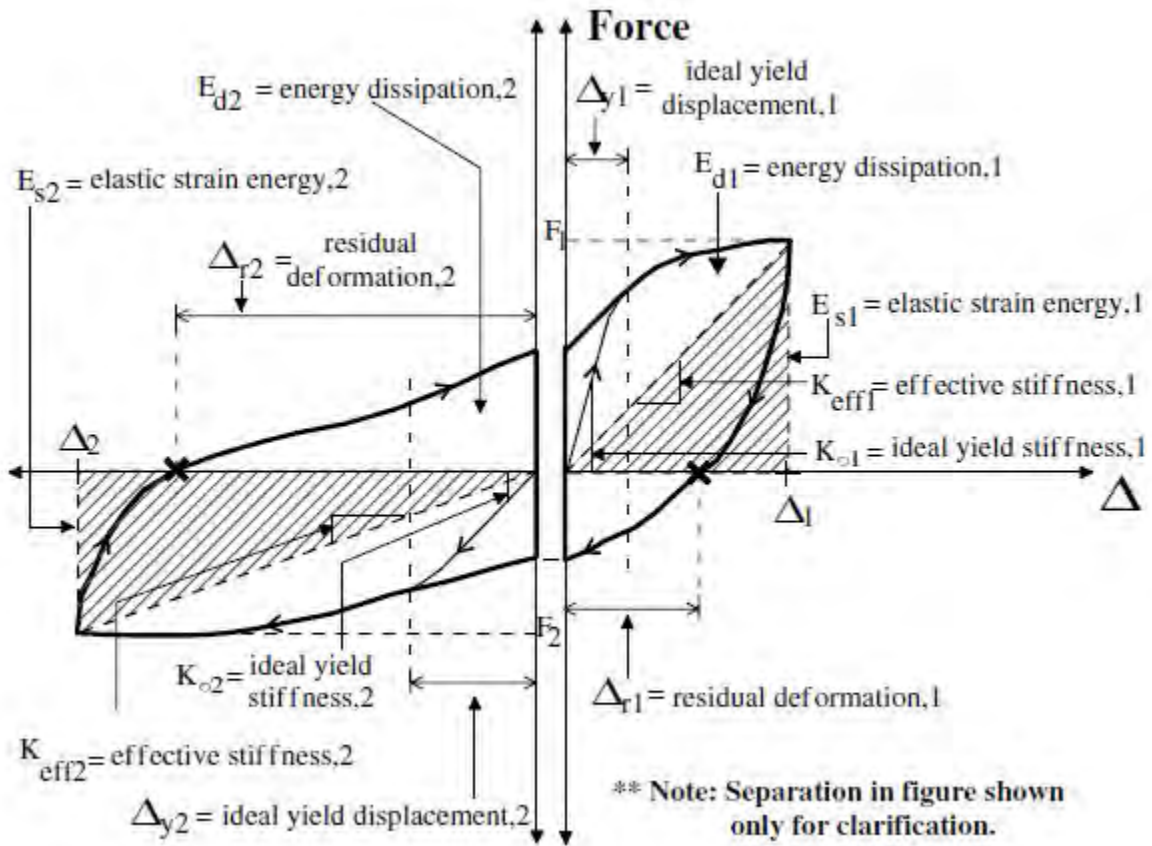


Figure 4.66 Equivalent viscous damping ratio for asymmetric hysteresis loops

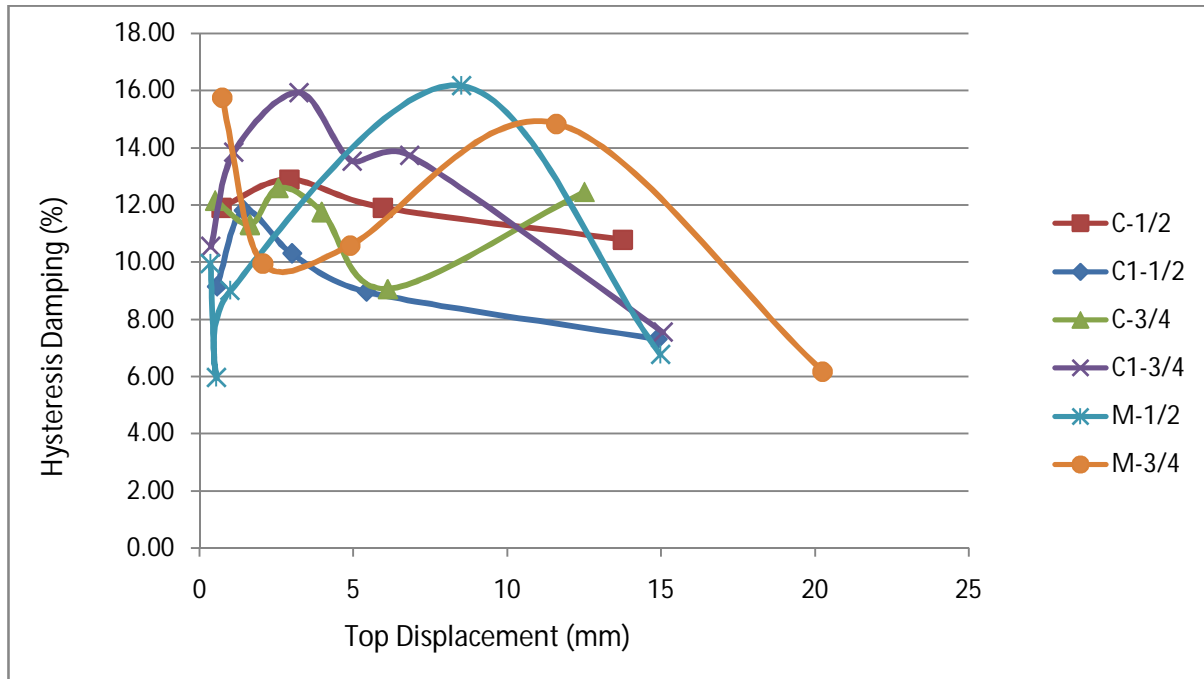


Figure 4.67 Hysteresis Damping Percentages for Wall Assemblies

The hysteresis damping was plotted against lateral top displacement for wall shown in figure 4.67. The specimens made of clay burnt brick with mortar thickness 1/2" (Specimens-C-1/2 and C1-1/2), the average hysteresis damping ranges from 9% to 13% and the specimens made of clay burnt brick with mortar thickness 3/4" (Specimens-C-3/4 and C1-3/4), the average hysteresis damping ranges from 9% to 16%. The specimen made of machine made brick with mortar thickness 1/2" (Specimens-M-1/2), the average hysteresis damping ranges from 6% to 16% and the specimen made of machine made brick with mortar thickness 3/4" (Specimens-M-3/4), the average hysteresis damping ranges from 6% to 16%.

4.18 Relationship between Prism Strength and Shear Strength

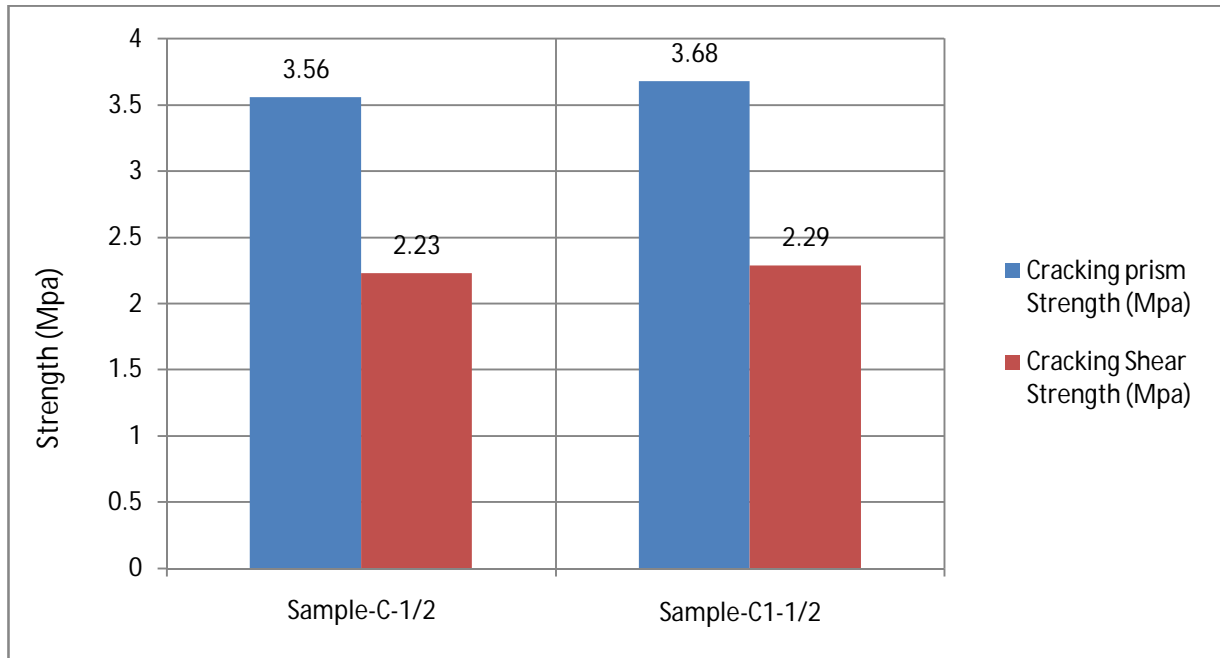
From the prism test of clay burnt brick and machine made brick, prism cracking strength and ultimate strength increases with increasing mortar thickness and prism compressive strength is more than shear strength in both types of bricks. On the other hand, from the shear test of clay burnt brick and machine made brick, cracking shear strength and ultimate shear strength decreases with increasing mortar thickness and shear strength is less than prism compressive strength in both types of bricks.

From the figure 4.68 it is observed that, the specimen made of clay burnt brick with mortar thickness 1/2" (specimens-C-1/2 and C1-1/2), the average cracking shear strength is 62.6% of average cracking prism strength and average ultimate shear strength is 54.4% of average ultimate prism strength.

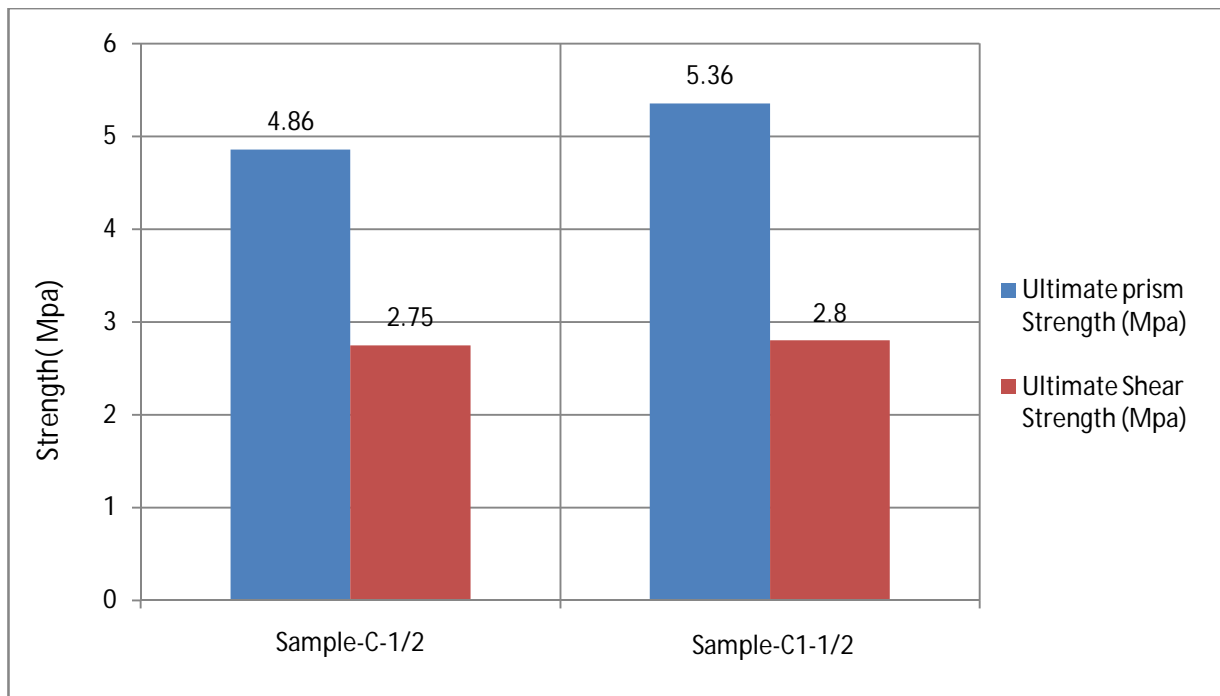
From the figure 4.69 it is observed that, the specimen made of clay burnt brick with mortar thickness 3/4" (specimens-C-3/4 and C1-3/4), the average cracking shear strength is 53.9% of average cracking prism strength and average ultimate shear strength is 31.0% of average ultimate prism strength.

From the figure 4.70 it is observed that, the specimen made of machine made brick with mortar thickness 1/2" (specimens-M-1/2 and M1-1/2), the average cracking shear strength is 72.7% of average cracking prism strength and average ultimate shear strength is 25.9% of average ultimate prism strength.

From the figure 4.71 it is observed that, the specimen made of machine made brick with mortar thickness 3/4" (specimens-M-3/4 and M1-3/4), the average cracking shear strength is 59.9% of average cracking prism strength and average ultimate shear strength is 20.7% of average ultimate prism strength.

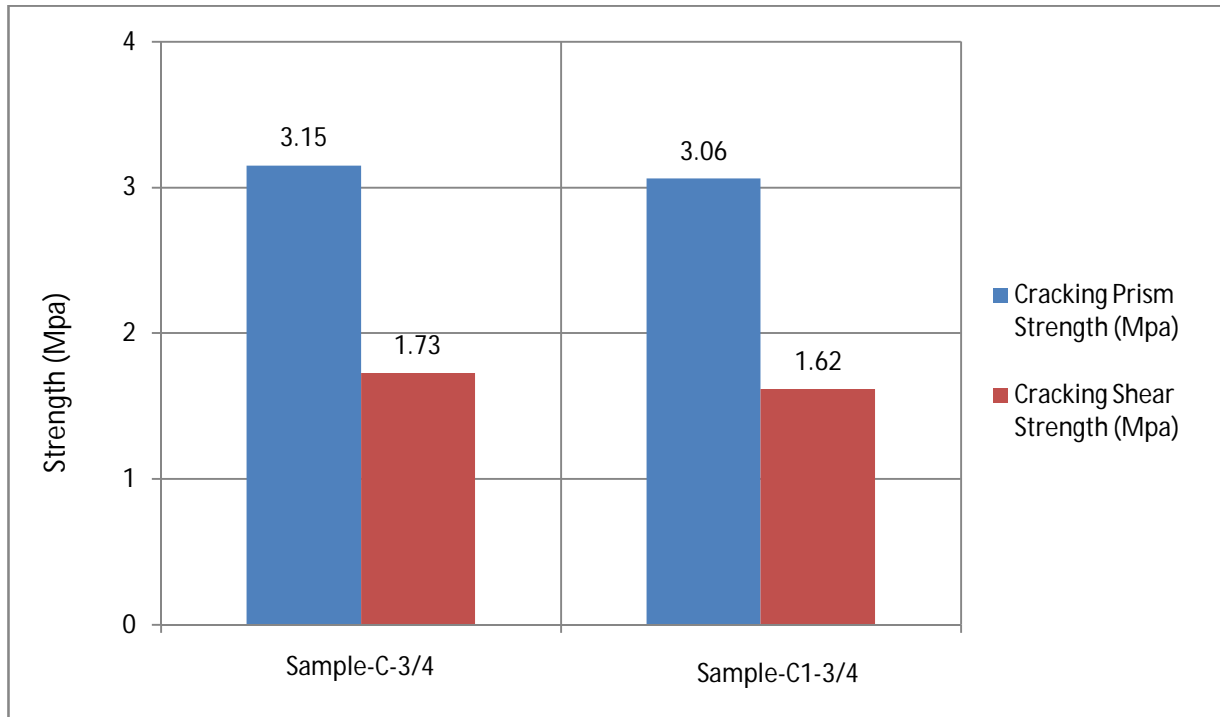


a. Cracking Strength

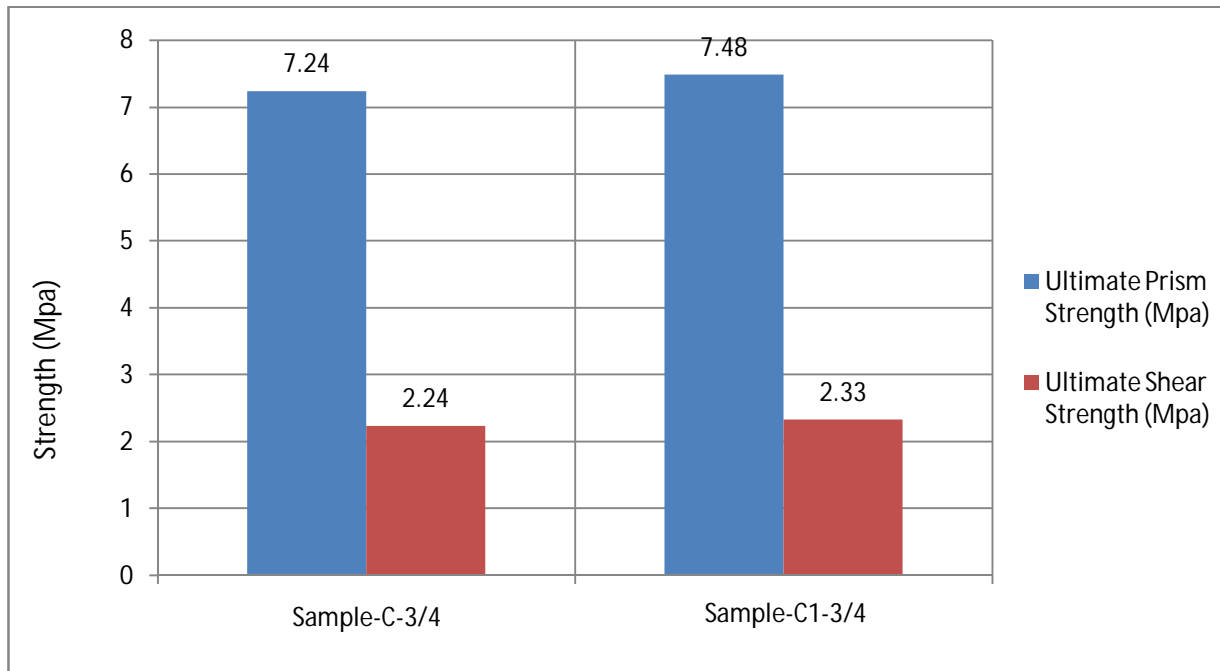


b. Ultimate Strength

Figure 4.68: Relationship between Shear Strength & Prism Compressive Strength of Clay Burnt Brick Wall With Mortar Thickness 1/2"

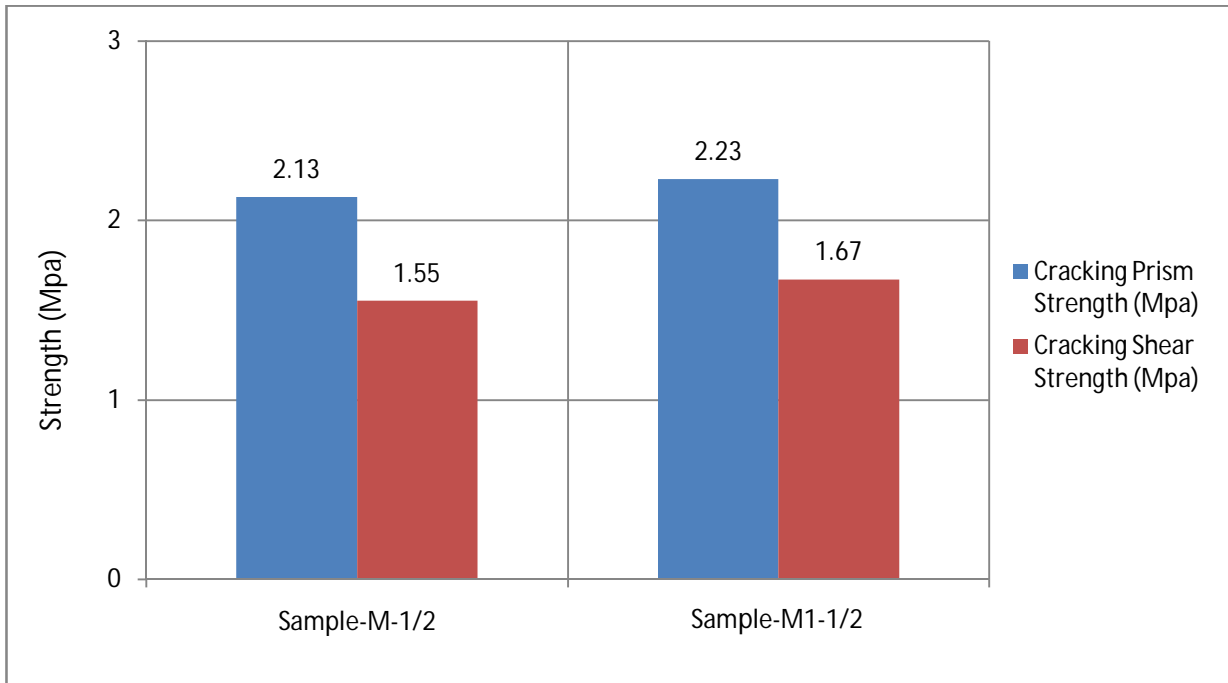


a. Cracking Strength

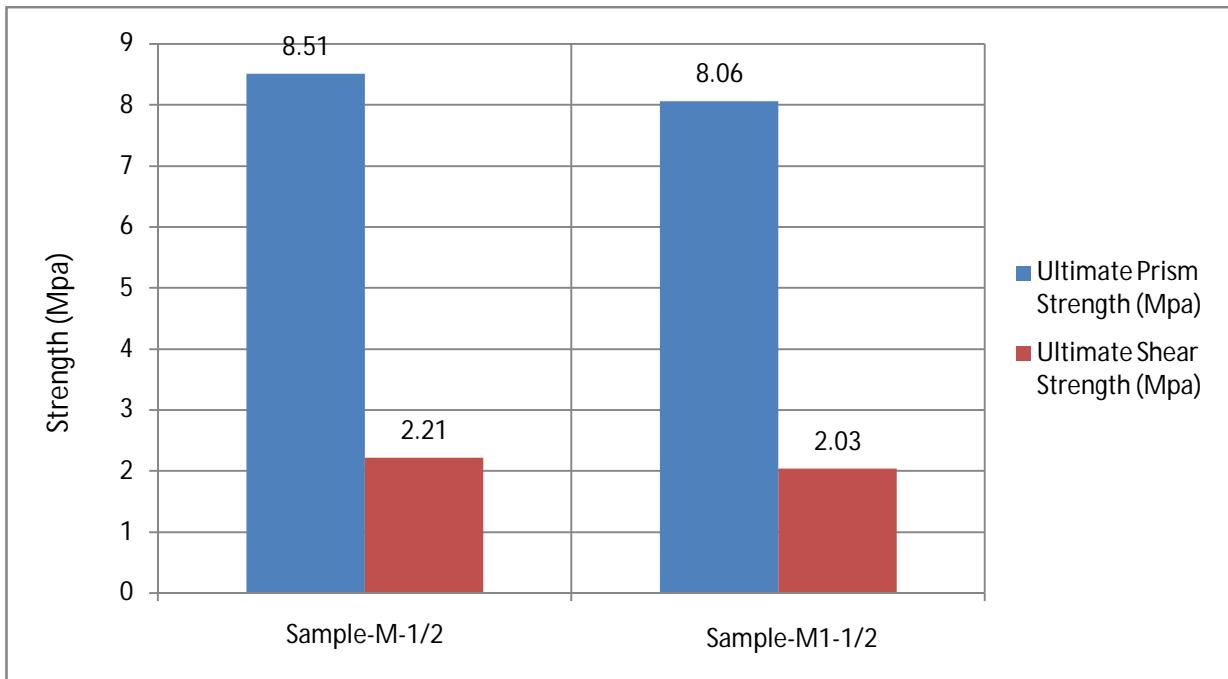


b. Ultimate Strength

Figure 4.69: Relationship between Shear Strength & Prism Compressive Strength of Clay Burnt Brick Wall With Mortar Thickness 3/4"

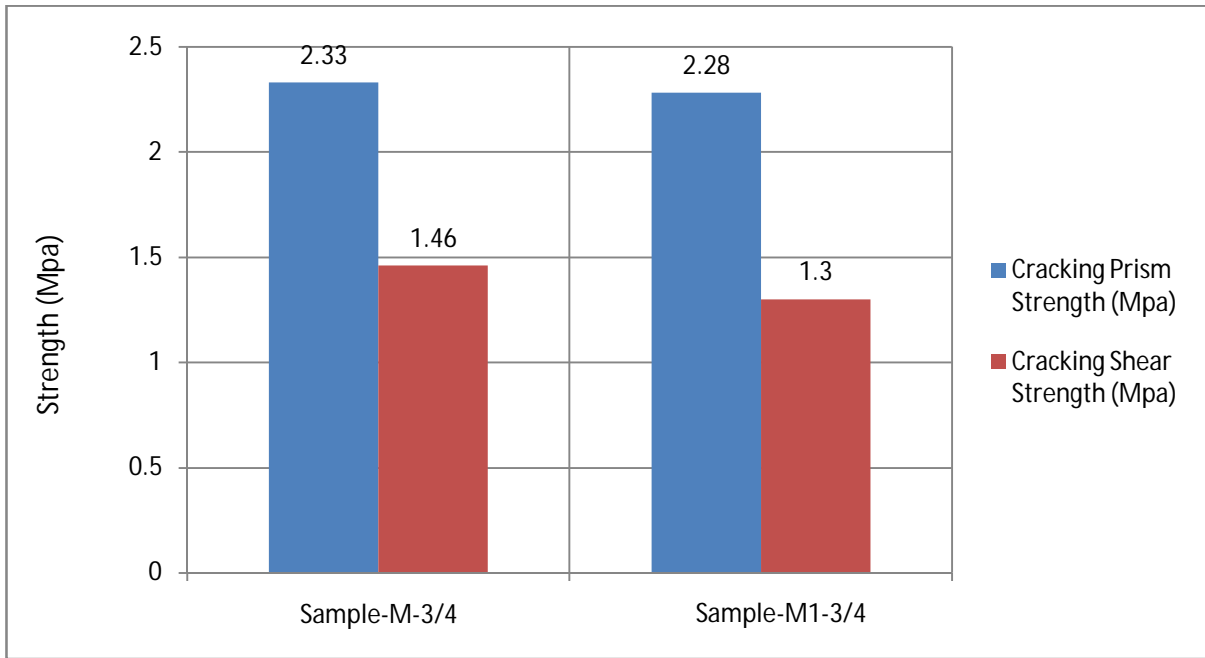


a. Cracking Strength

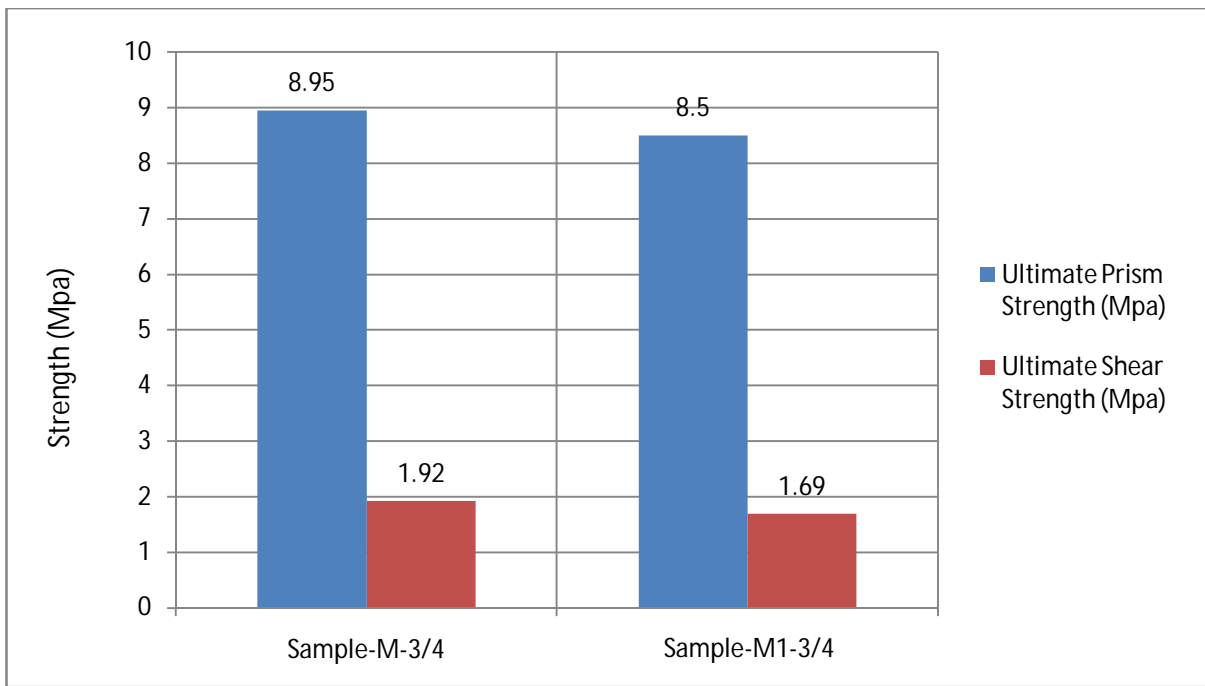


b. Ultimate Strength

Figure 4.70: Relationship between Shear Strength & Prism Compressive Strength of Machine Made Brick Wall With Mortar Thickness 1/2"



a. Cracking Strength



b. Ultimate Strength

Figure 4.71: Relationship between Shear Strength & Prism Compressive Strength of Machine Made Brick Wall with Mortar Thickness 3/4"

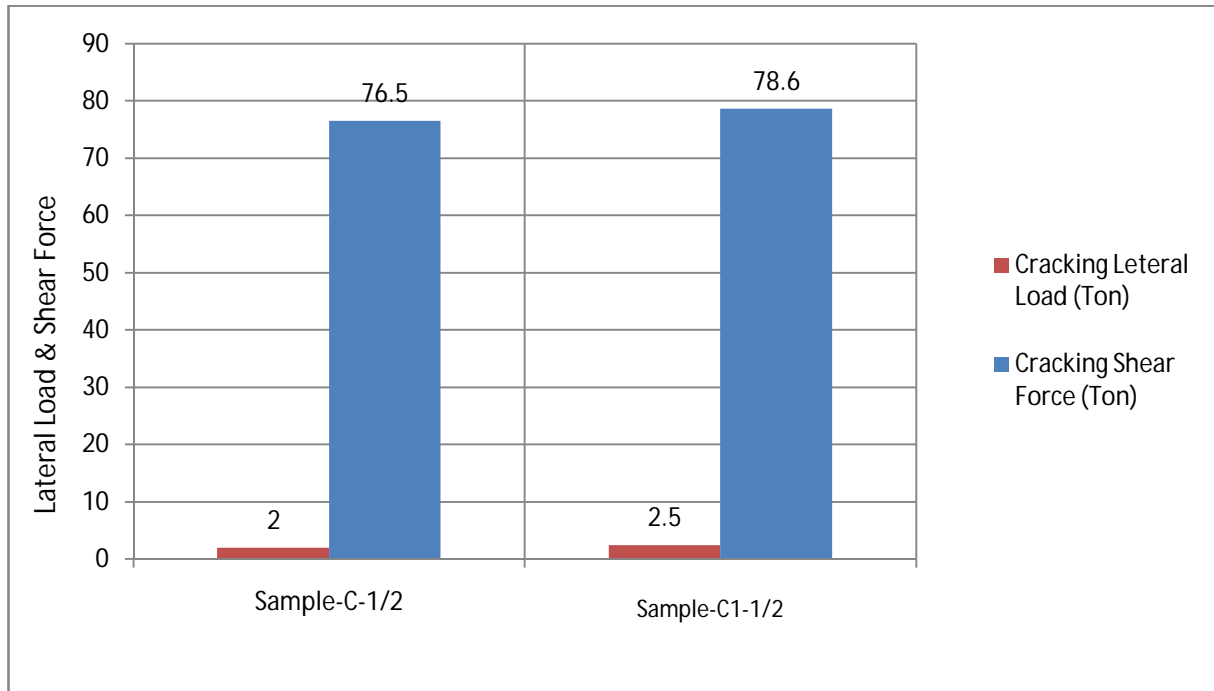
4.19 Relationship between Lateral Load vs Shear Force

From the figure 4.72a and 4.72b it is observed that, the average cracking and ultimate shear strength for (specimens-C-1/2 and C1-1/2) is 2.26 Mpa (327.7 psi) and 2.78Mpa (403.1 psi) respectively. The length of wall is 53 inch and the width of wall is 10 inch. So that the average cracking and ultimate shear force are 77.5 ton and 95.4 ton. The average cracking and ultimate lateral load are 2.25 ton and 5.5 ton. The average cracking lateral load is 2.90% of average cracking shear force and the average ultimate lateral load is 5.77% of average ultimate shear force.

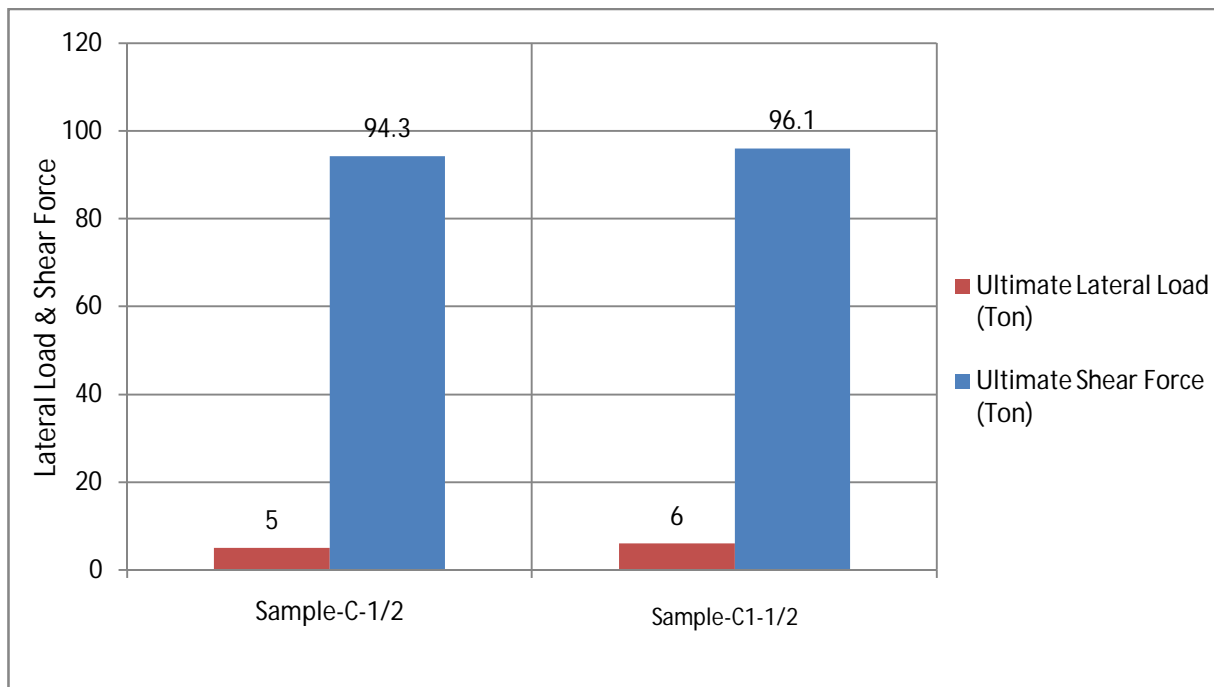
From the figure 4.73a and 4.73b it is observed that, the average cracking and ultimate shear strength for (specimens-C-3/4 and C1-3/4) is 1.68 Mpa (243.6 psi) and 2.29Mpa (332.1 psi) respectively. The length of wall is 53 inch and the width of wall is 10 inch. So that the average cracking and ultimate shear force are 57.6 ton and 78.6 ton. The average cracking and ultimate lateral load are 2.75 ton and 9.5 ton. The average cracking lateral load is 4.77% of average cracking shear force and the average ultimate lateral load is 12.09% of average ultimate shear force.

From the figure 4.74a and 4.74b it is observed that, the cracking and ultimate shear strength for (specimens-M-1/2) is 1.61 Mpa (233.5 psi) and 2.12Mpa (307.4 psi) respectively. The length of wall is 56 inch and the width of wall is 10 inch. So that the cracking and ultimate shear force are 58.4 ton and 76.9 ton. The cracking and ultimate lateral loads are 2.5 ton and 6.0 ton. The cracking lateral load is 4.28% of cracking shear force and the ultimate lateral load is 7.81% of ultimate shear force.

From the figure 4.75a and 4.75b it is observed that, the cracking and ultimate shear strength for (specimens-M-3/4) is 1.46 Mpa (211.7psi) and 1.92Mpa (278.4 psi) respectively. The length of wall is 56 inch and the width of wall is 10 inch. So that the cracking and ultimate shear force are 52.9 ton and 69.6 ton. The cracking and ultimate lateral loads are 2.0 ton and 6.0 ton. The cracking lateral load is 3.78% of cracking shear force and the ultimate lateral load is 8.62% of ultimate shear force.

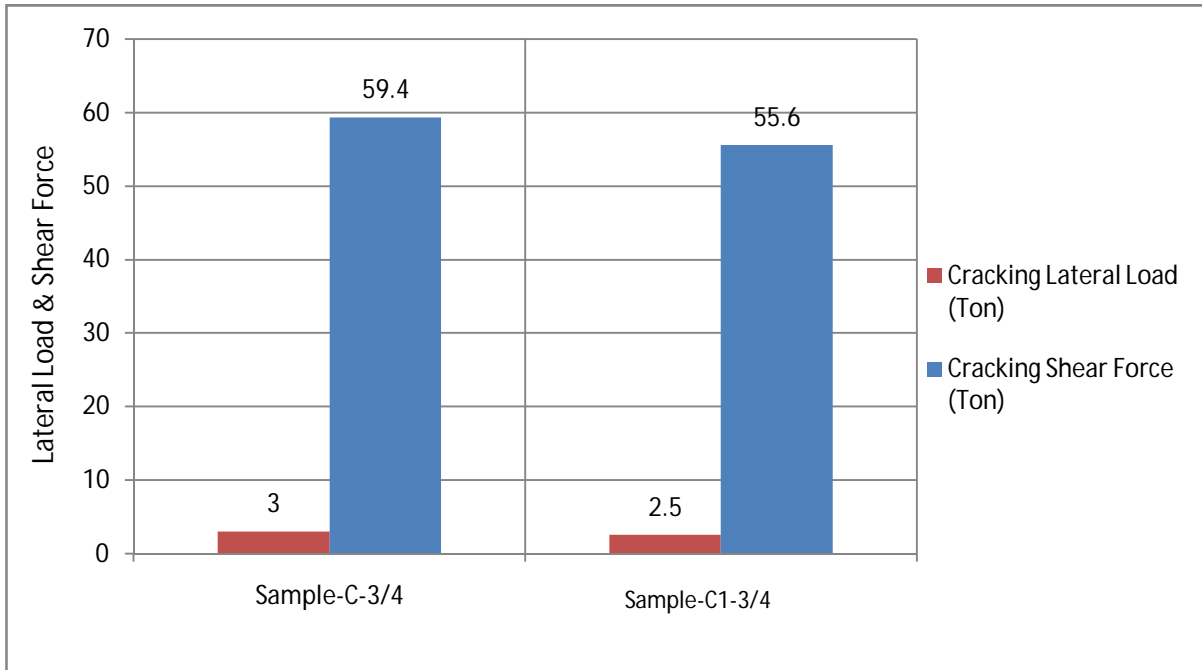


a. Cracking Force (Ton)

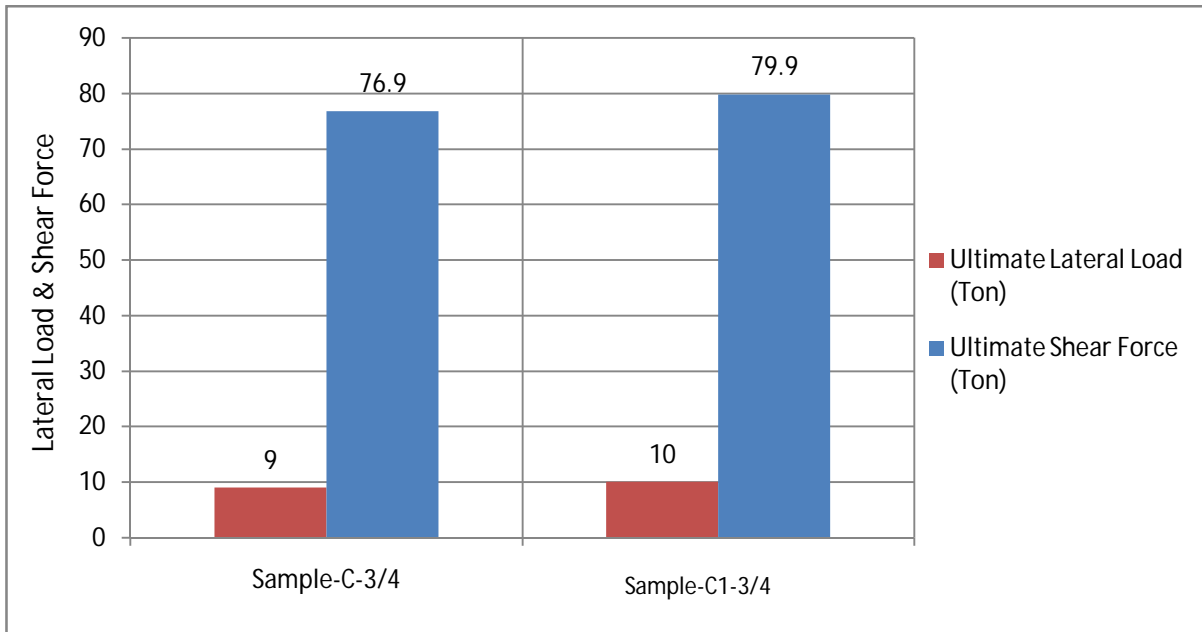


b. Ultimate Force (Ton)

Figure 4.72: Relationship between Lateral Load Vs Shear Force of Clay Burnt Brick Wall with Mortar Thickness 1/2"

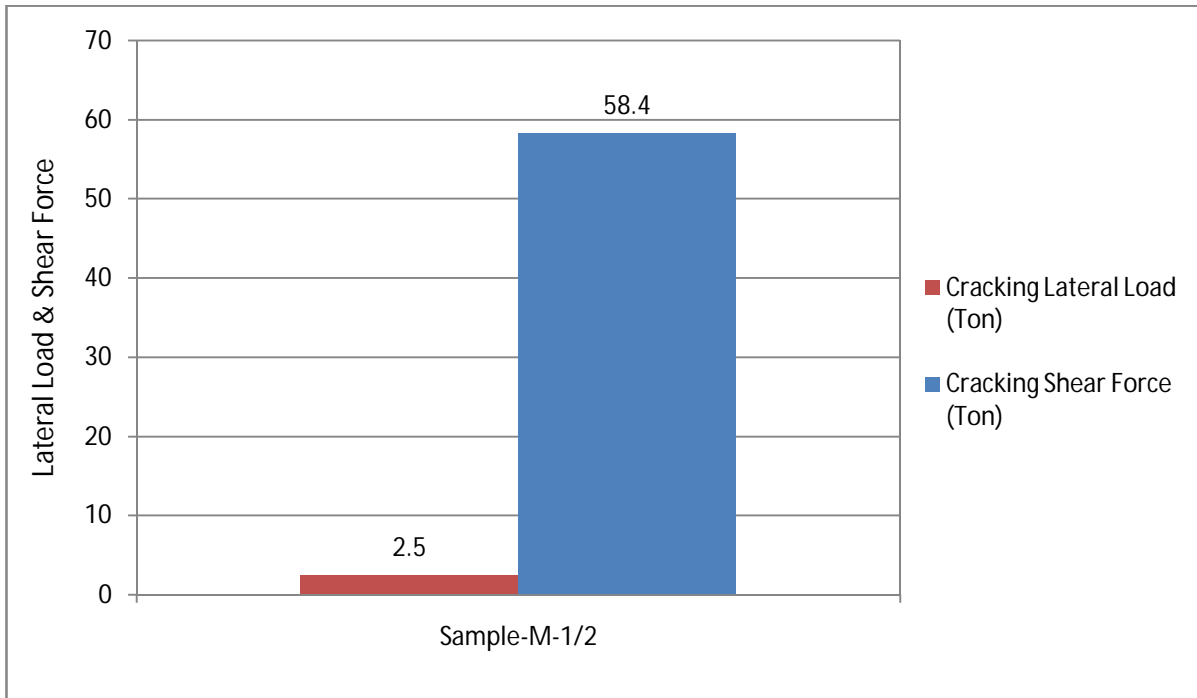


a. Cracking Force (Ton)

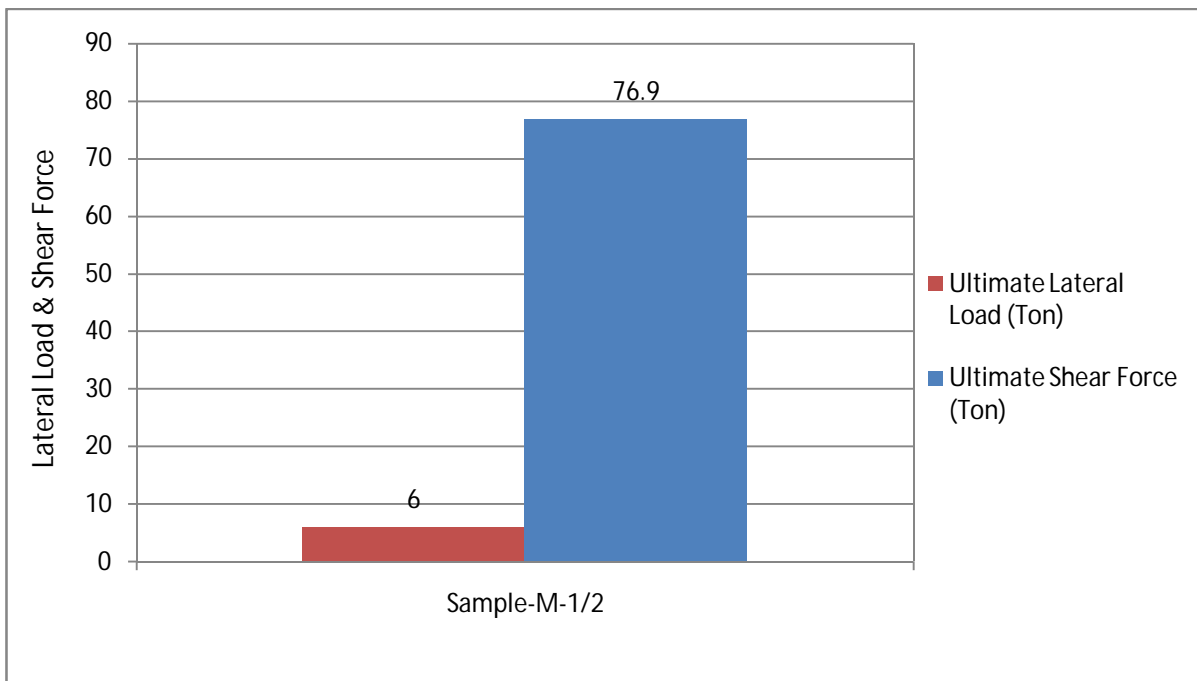


b. Ultimate Force (Ton)

Figure 4.73: Relationship between Lateral Load Vs Shear Force of Clay Burnt Brick Wall with Mortar Thickness 3/4"

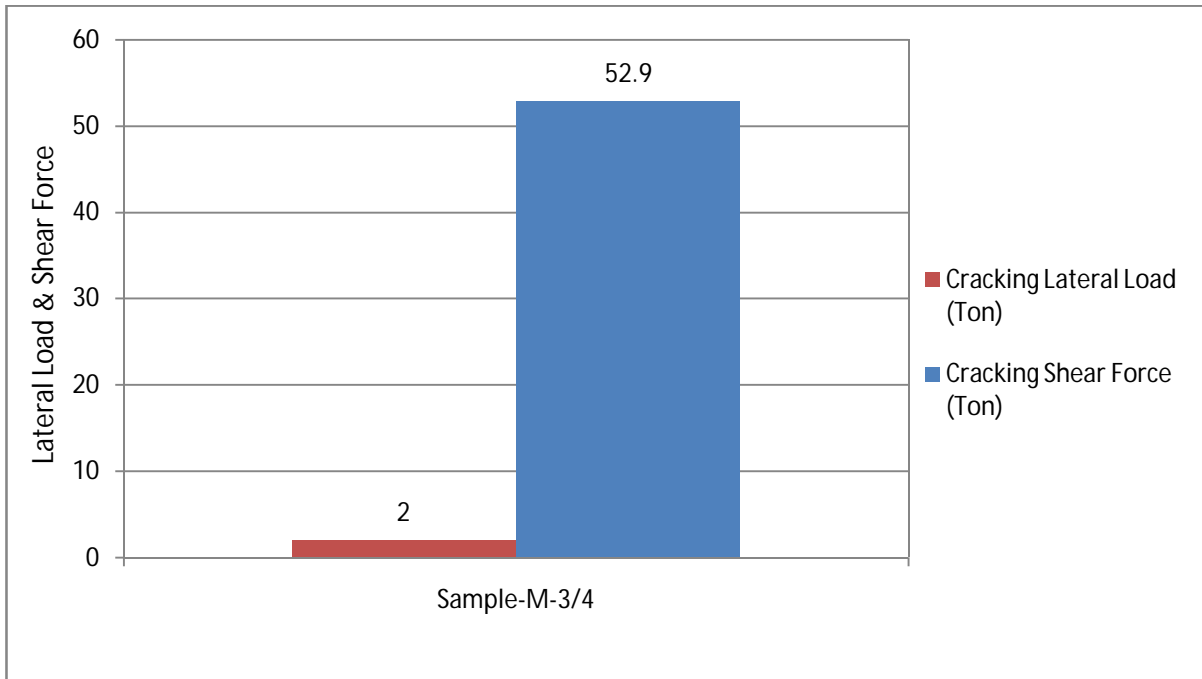


a. Cracking Force (Ton)

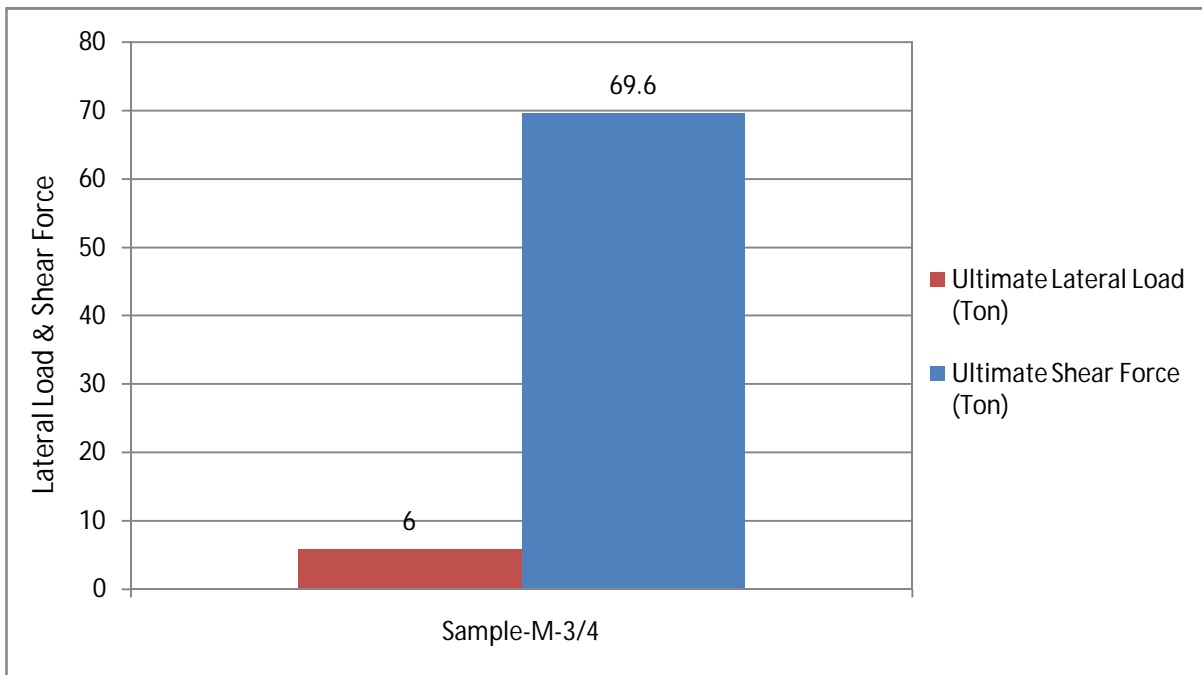


b. Ultimate Force (Ton)

Figure 4.74: Relationship between Lateral Load vs Shear Force of Machine made Brick wall with mortar thickness 1/2"



a. Cracking Force (Ton)



b. Ultimate Force (Ton)

Figure 4.75: Relationship between Lateral Load vs Shear Force of Machine made Brick wall with mortar thickness 3/4"

4.20 Relationship between Lateral Load vs Prism Strength

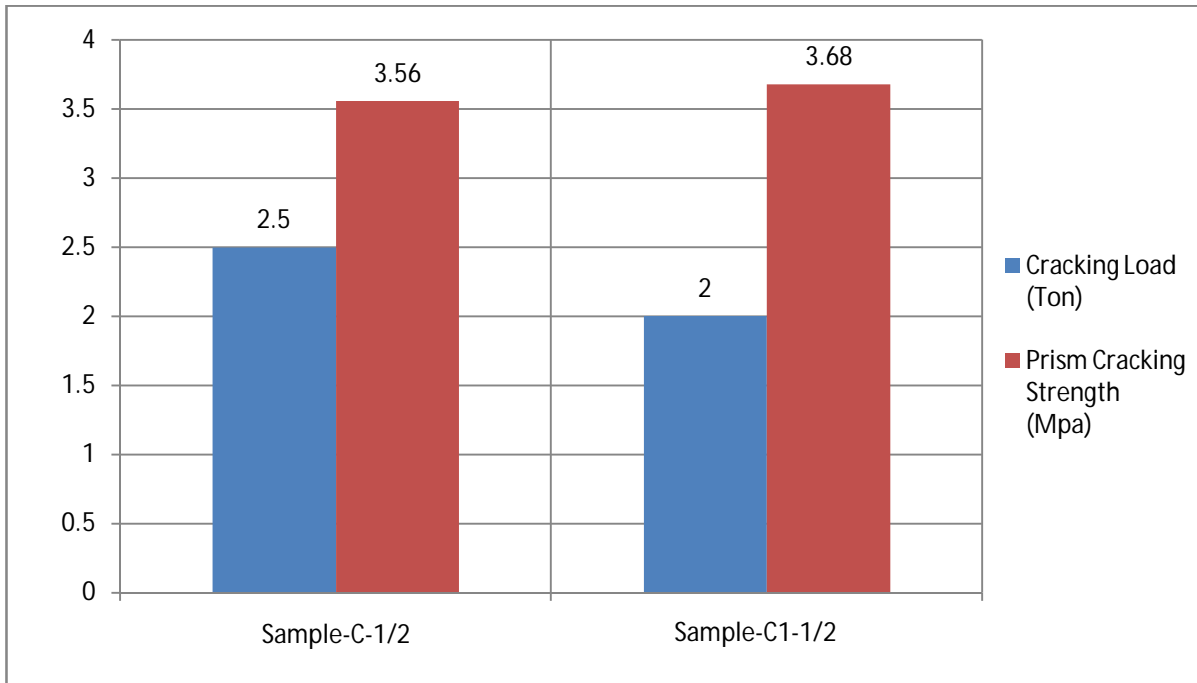
There is relationship developed between lateral capacities of the wall vs prism strength shown in figure 4.76.

From the figure 4.76a and 4.76b it is observed that, the specimen made of clay burnt brick with mortar thickness 1/2" (specimens-C-1/2 and C1-1/2), the average cracking horizontal load is 62% of average cracking prism strength and average ultimate prism strength is 93.3% of average ultimate horizontal load. The lateral capacity of the specimen wall made of clay burnt brick with mortar thickness 1/2" was performed by 3 ton vertical loads.

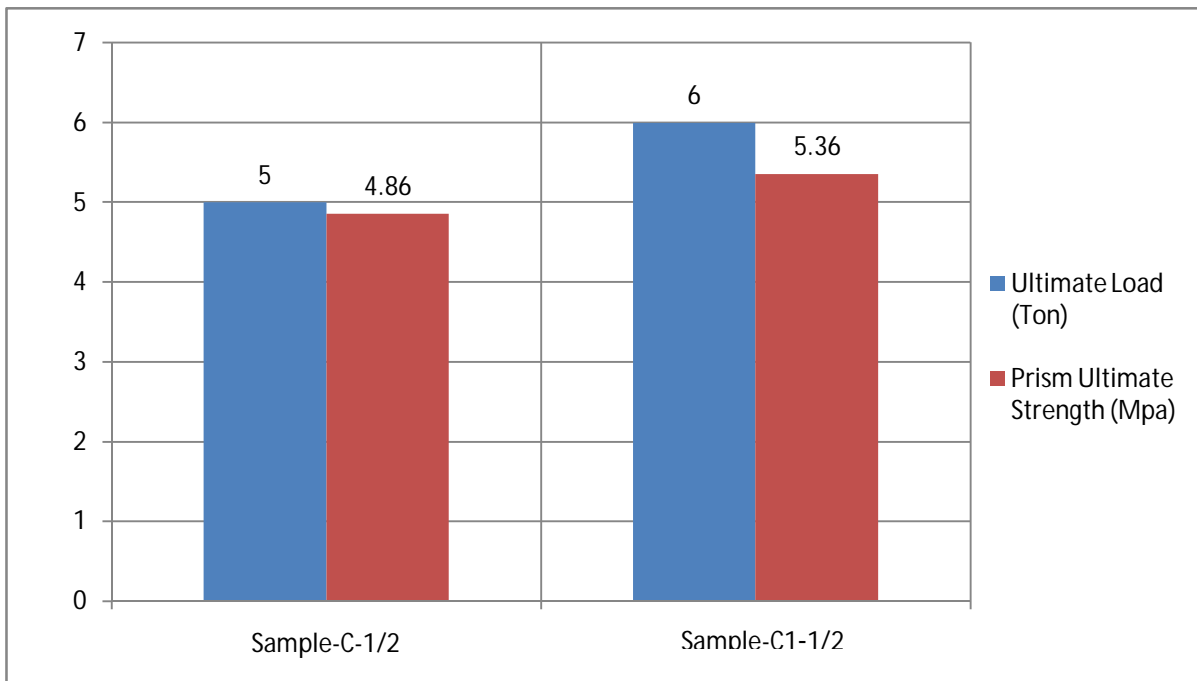
From the figure 4.76c and 4.76d it is observed that, the specimen made of clay burnt brick with mortar thickness 3/4" (specimens-C-3/4 and C1-3/4), the average cracking horizontal load is 88.5% of average cracking prism strength and average ultimate prism strength is 77.6% of average ultimate horizontal load. The lateral capacity of the specimen wall made of clay burnt brick with mortar thickness 3/4" was performed by 6 ton vertical loads.

From the figure 4.76e and 4.76f it is observed that, the specimen made of machine made brick with mortar thickness 1/2" (specimens-M-1/2 and M1-1/2), the cracking prism strength is 85.6% of average cracking horizontal load and ultimate horizontal load is 70.5% of average ultimate prism strength. The lateral capacity of the specimen wall made of machine made brick with mortar thickness 1/2" was performed by 6 ton vertical loads. The result of type M1-1/2 was rejected because of abnormal result. Machine made brick wall with mortar thickness 1/2" only type M-1/2 result is accepted.

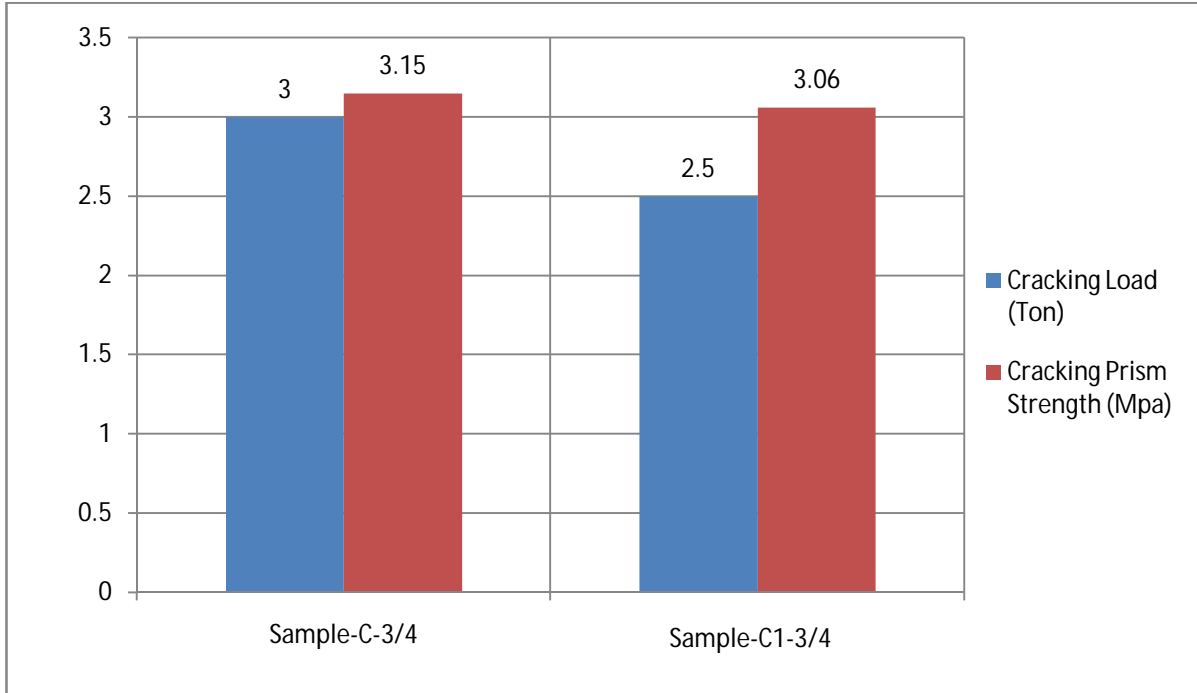
From the figure 4.76g and 4.76h it is observed that, the specimen made of machine made brick with mortar thickness 3/4" (specimens-M-3/4), the cracking horizontal load is 85.8% of cracking prism strength and ultimate horizontal load is 67.0% of ultimate prism strength. The lateral capacity of the specimen wall made of machine made brick with mortar thickness 3/4" was performed by 6 ton vertical loads.



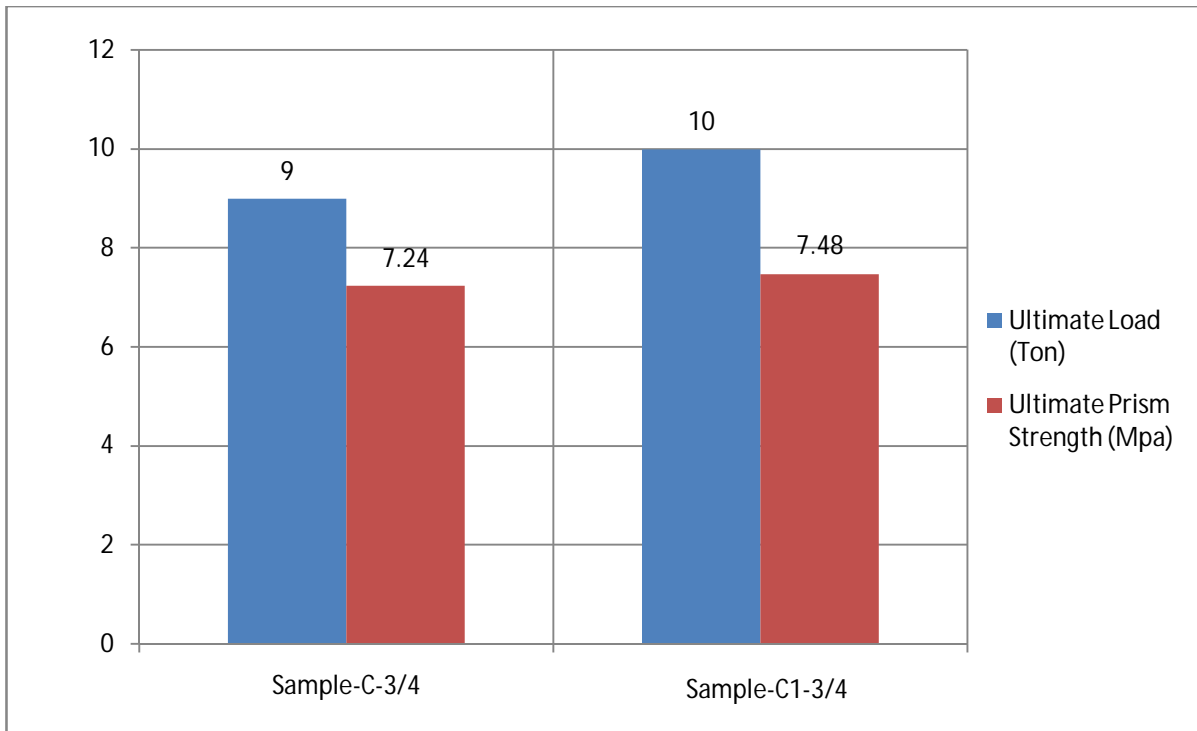
a. Cracking load vs cracking prism strength of clay burnt brick wall with mortar thickness 1/2"



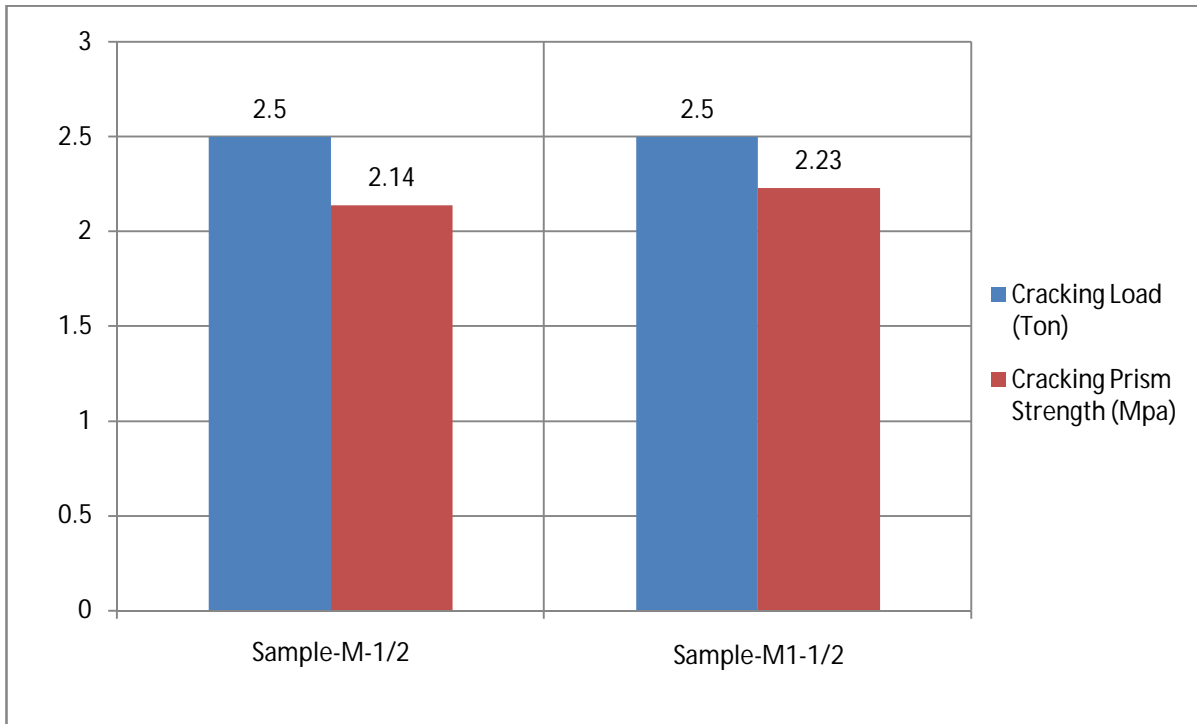
b. Ultimate load vs Ultimate prism strength of clay burnt brick wall with mortar thickness 1/2"



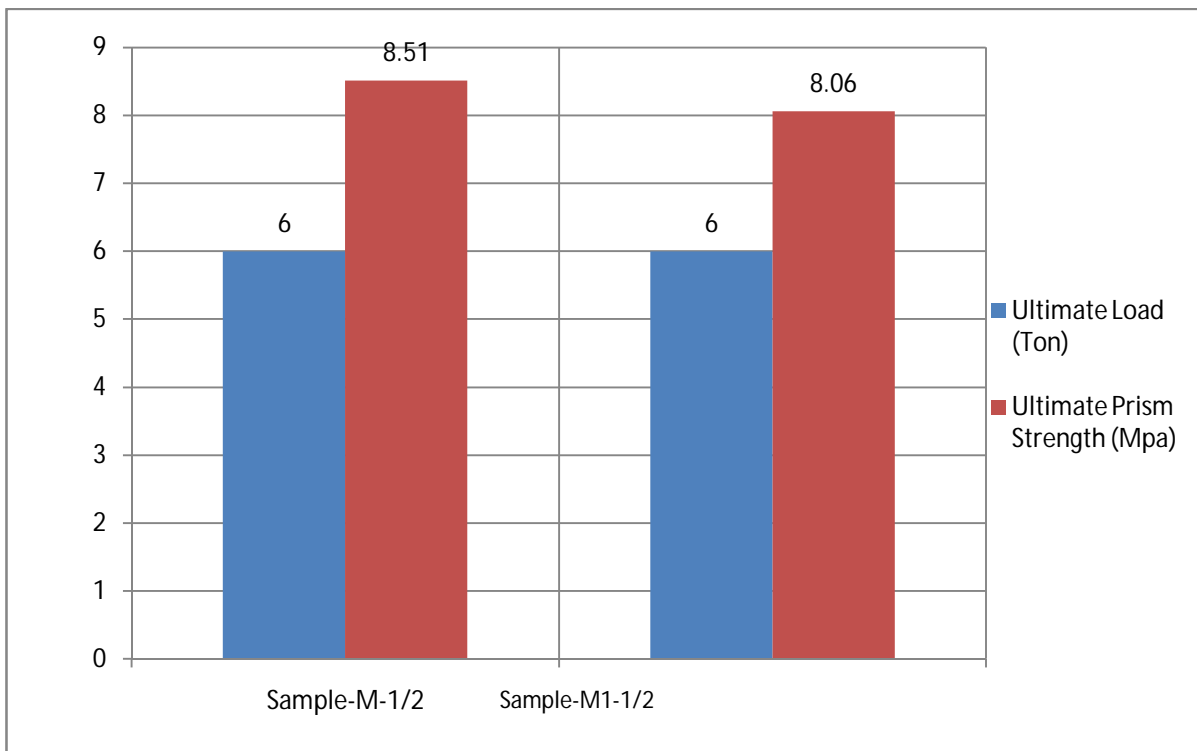
c. Cracking load vs cracking prism strength of clay burnt brick wall with mortar thickness 3/4"



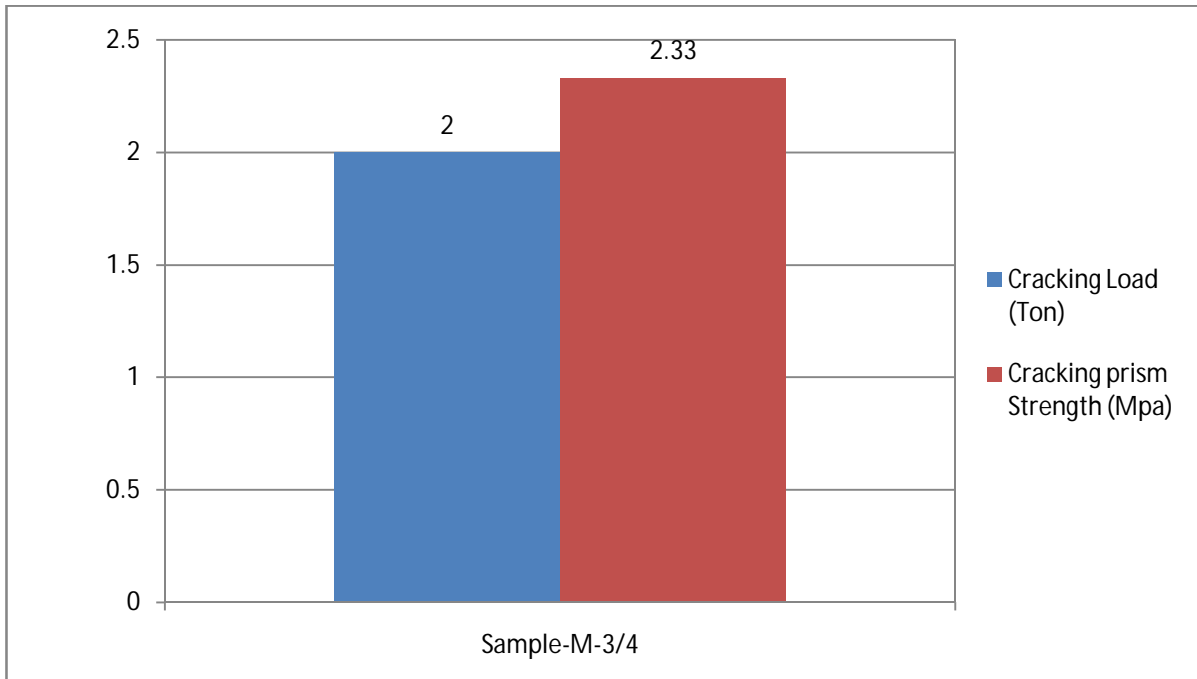
d. Ultimate load vs Ultimate prism strength of clay burnt brick wall with mortar thickness 3/4"



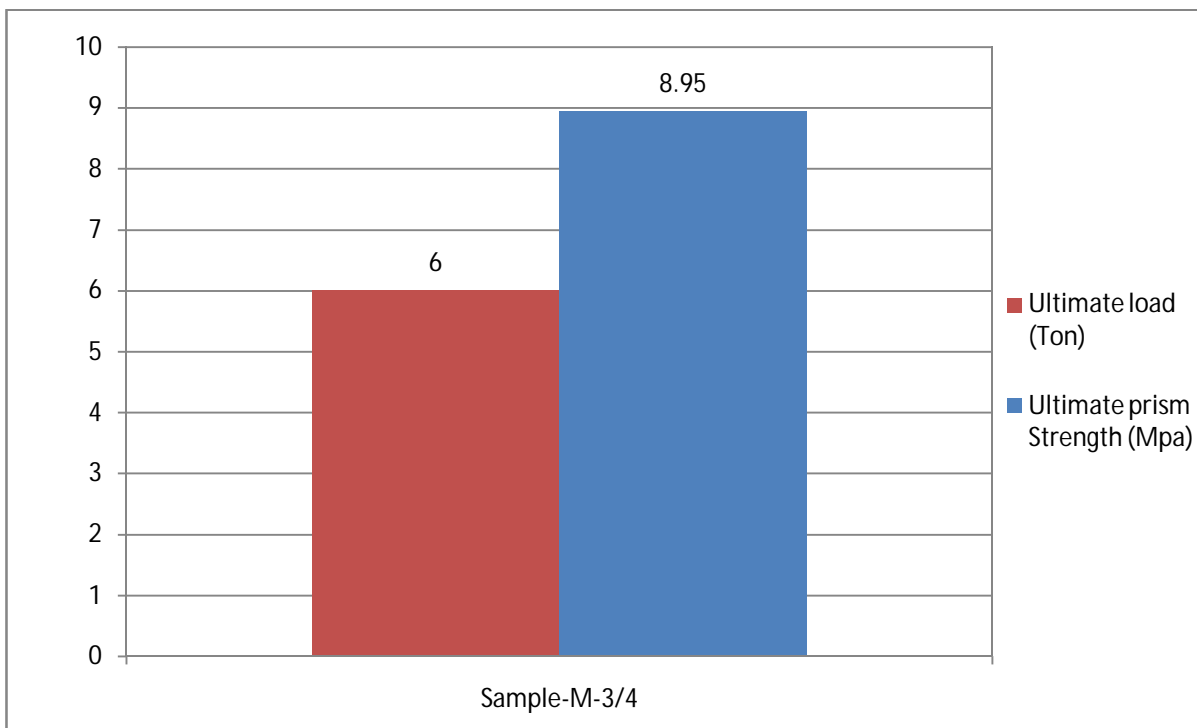
e. Cracking load vs cracking prism strength of machine brick wall with mortar thickness 1/2"



f. Ultimate load vs Ultimate prism strength of machine brick wall with mortar thickness 1/2"



g. Cracking load vs cracking prism strength of machine brick wall with mortar thickness 3/4"



h. Ultimate load vs Ultimate prism strength of machine brick wall with mortar thickness 3/4"

Figure 4.76: Relationship between horizontal load vs prism Strength of different types of wall

4.21 Relationship between Lateral Load vs Shear Strength

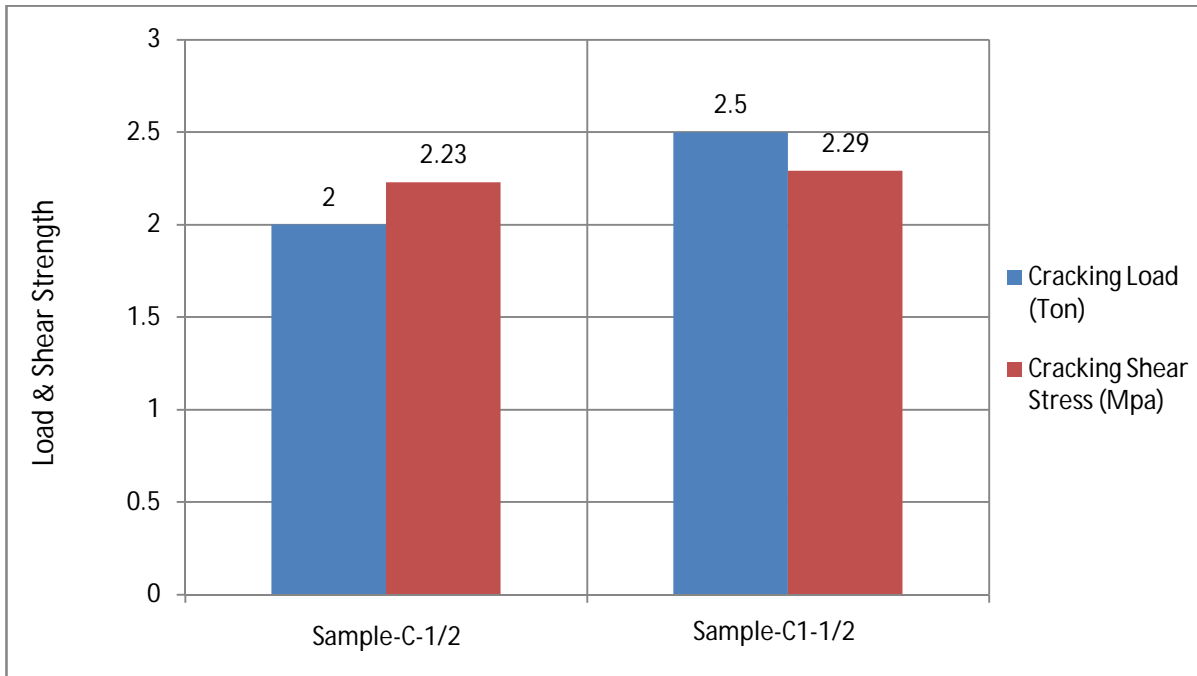
There is relationship developed between lateral capacities of the wall vs shear strength shown in figure 4.77.

From the figure 4.77a and 4.77b it is observed that, the specimen made of clay burnt brick with mortar thickness 1/2" (specimens C-1/2 and C1-1/2), the average cracking horizontal load is 99% of average cracking shear strength and average ultimate shear strength is 50.8% of average ultimate horizontal load. The lateral capacity of the specimen wall made of clay burnt brick with mortar thickness 1/2" was performed by 3 ton vertical loads.

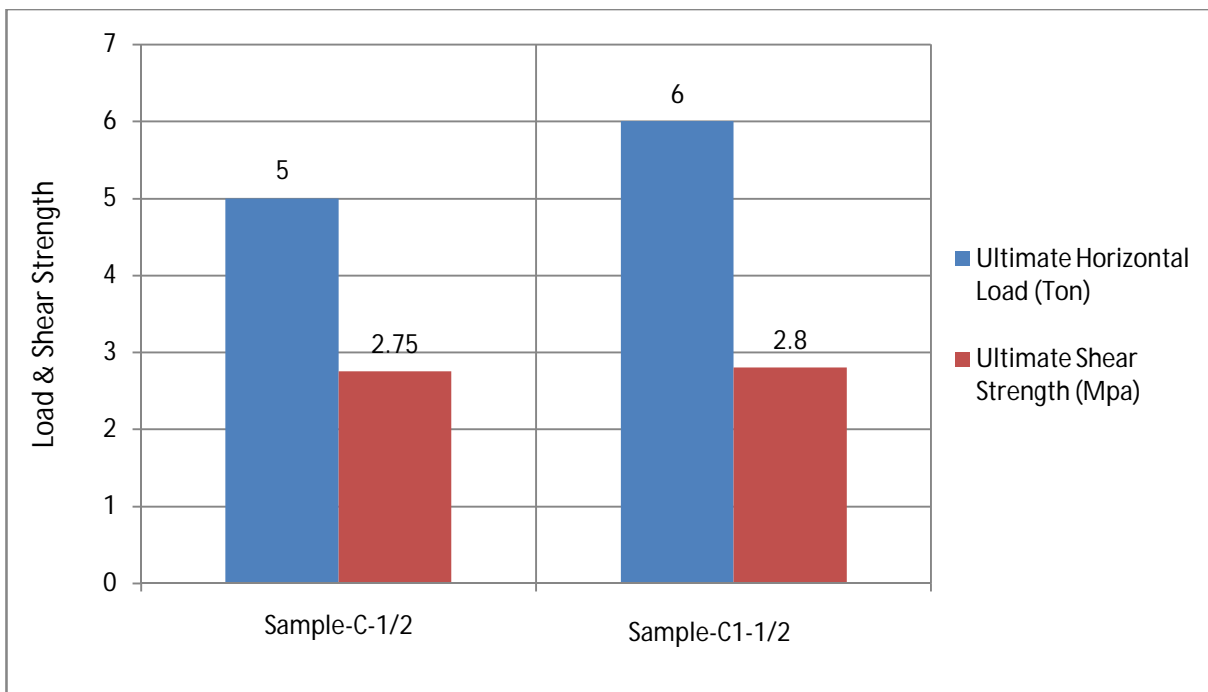
From the figure 4.77c and 4.77d it is observed that, the specimen made of clay burnt brick with mortar thickness 3/4" (specimens C-3/4 and C1-3/4), the average cracking shear strength is 61.3% of average horizontal load and average ultimate shear strength is 24.1% of average ultimate horizontal load. The lateral capacity of the specimen wall made of clay burnt brick with mortar thickness 3/4" was performed by 6 ton vertical loads.

From the figure 4.77e and 4.77f it is observed that, the specimen made of machine made brick with mortar thickness 1/2" (specimens M-1/2 and M1-1/2), the cracking shear strength is 66.8% of average cracking horizontal load and ultimate shear strength is 33.8% of average ultimate horizontal load. The lateral capacity of the specimen wall made of machine made brick with mortar thickness 1/2" was performed by 6 ton vertical loads. The result of type M1-1/2 was rejected because of abnormal result. Machine made brick wall with mortar thickness 1/2" only type M-1/2 result is accepted.

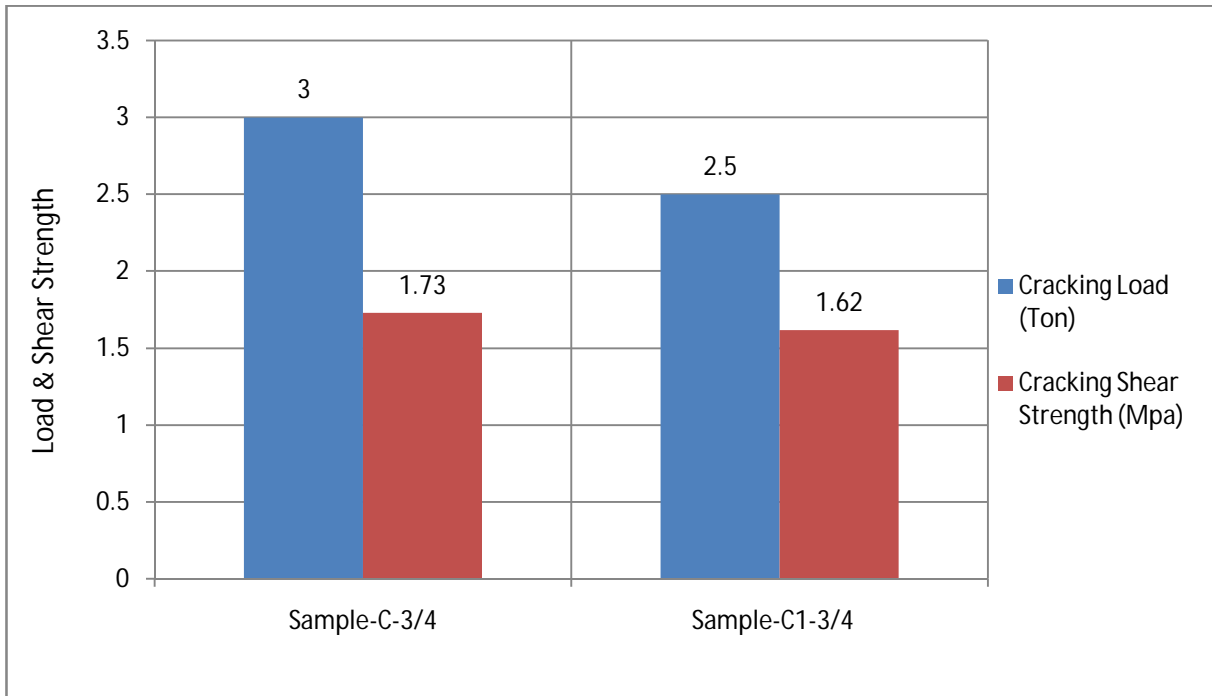
From the figure 4.77g and 4.77h it is observed that, the specimen made of machine made brick with mortar thickness 3/4" (specimens M-3/4), the cracking shear strength is 73.0% of cracking horizontal load and ultimate shear strength is 32.0% of ultimate horizontal load. The lateral capacity of the specimen wall made of machine made brick with mortar thickness 3/4" was performed by 6 ton vertical loads.



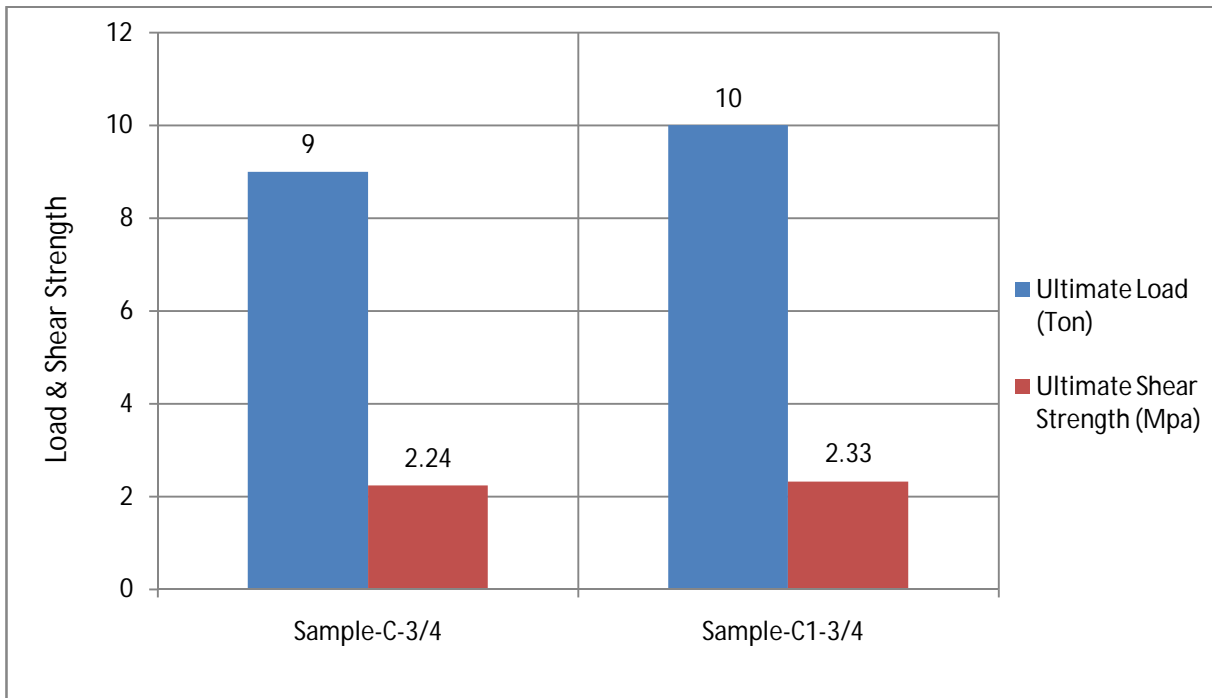
a. Cracking load vs cracking shear strength of clay burnt brick wall with mortar thickness 1/2"



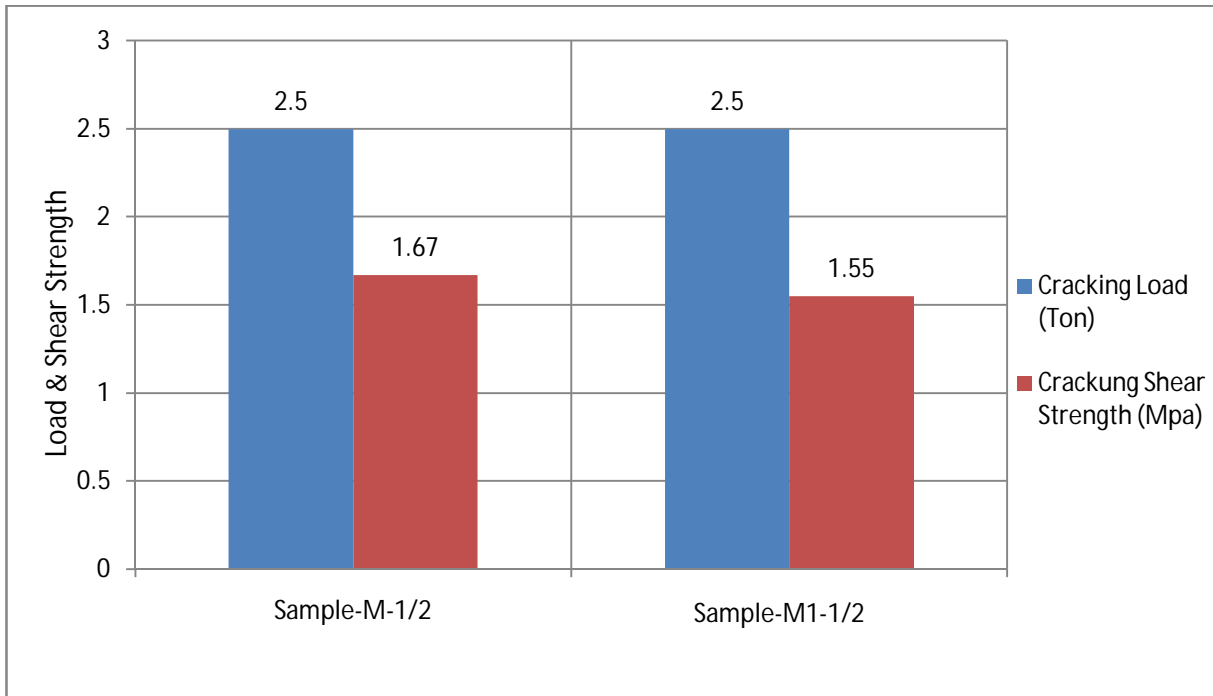
b. Ultimate load vs Ultimate shear strength of clay burnt brick wall with mortar thickness 1/2"



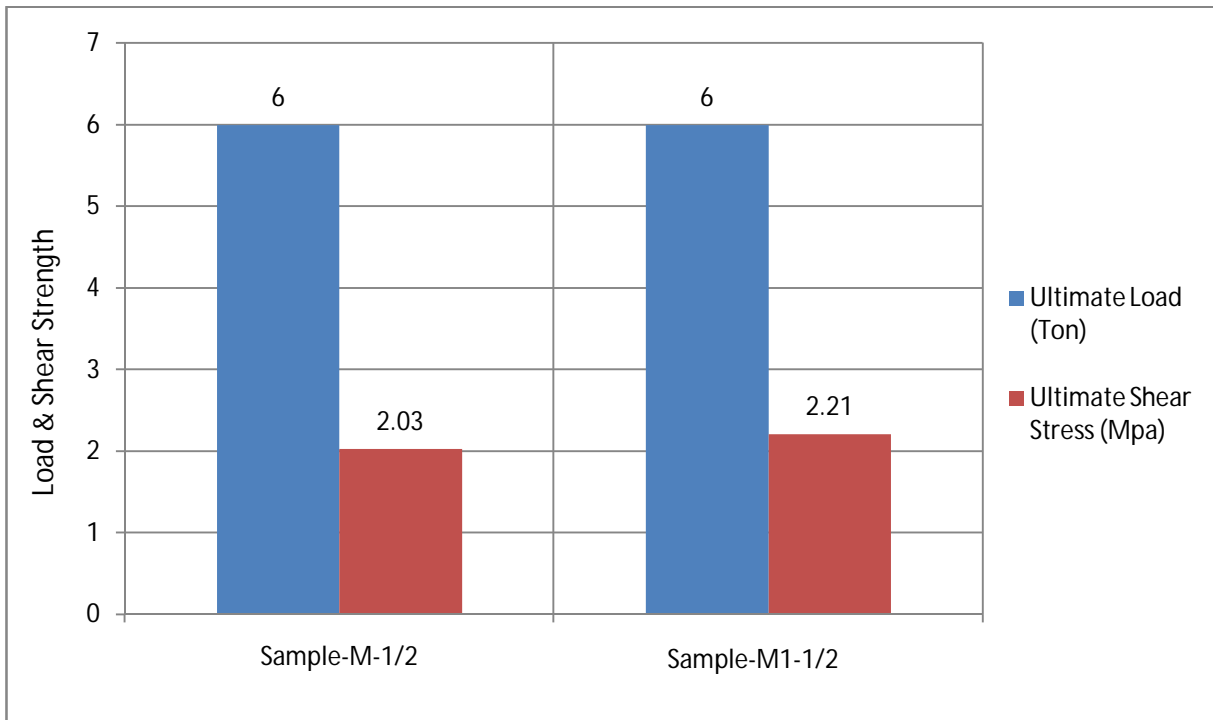
c. Cracking load vs cracking shear strength of clay burnt brick wall with mortar thickness 3/4"



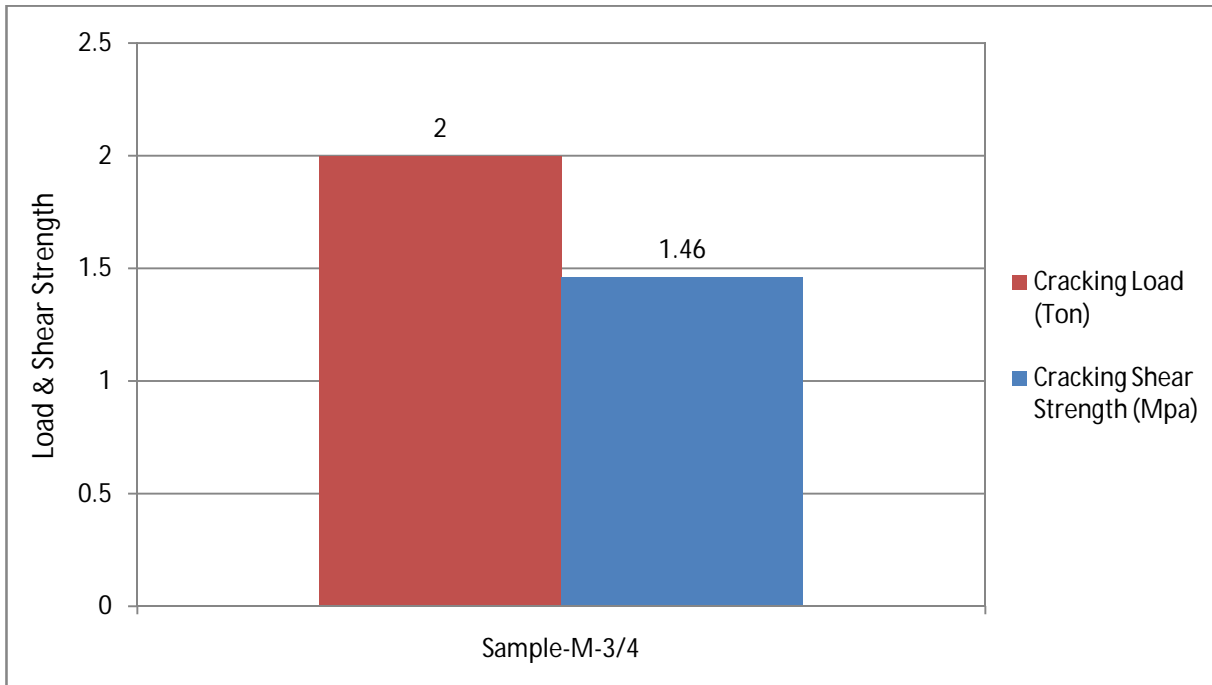
d. Ultimate load vs Ultimate shear strength of clay burnt brick wall with mortar thickness 3/4"



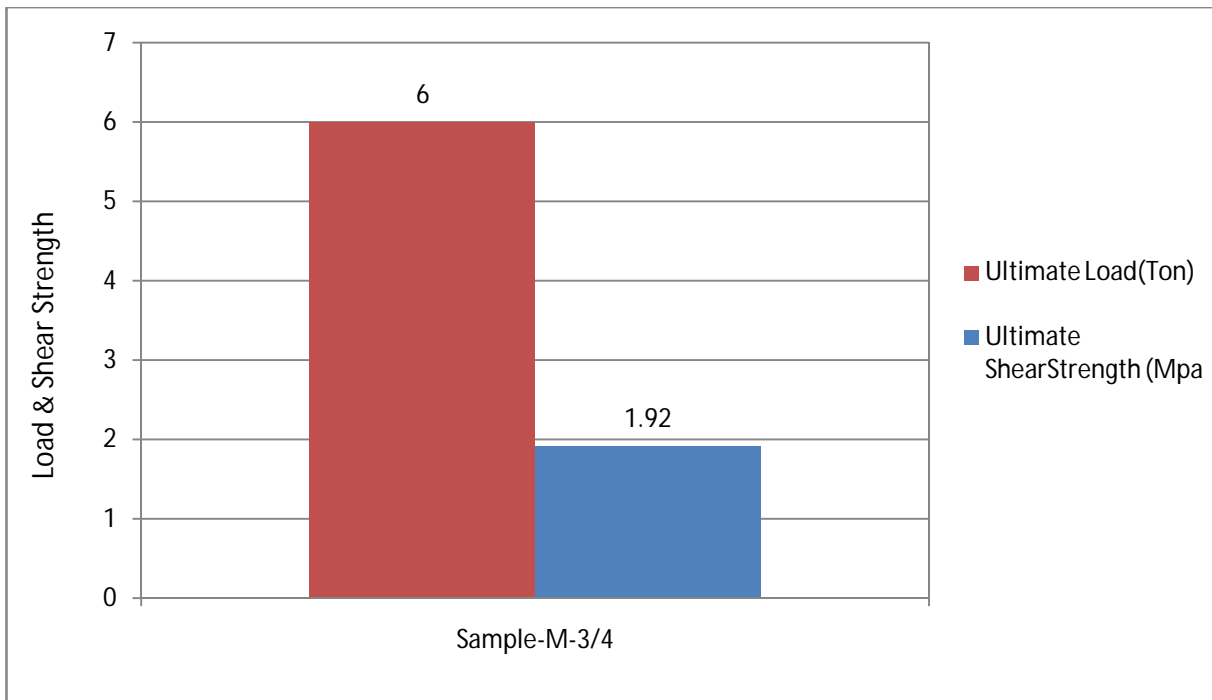
e. Cracking load vs cracking shear strength of machine brick wall with mortar thickness 1/2"



f. Ultimate load vs Ultimate shear strength of machine brick wall with mortar thickness 1/2"



g. Cracking load vs cracking shear strength of machine brick wall with mortar thickness 3/4"



h. Ultimate load vs Ultimate shear strength of machine brick wall with mortar thickness 3/4"

Figure 4.77: Relationship between Horizontal Load vs Shear Strength of Different Types of Wall

4.22 Relationship between Calculated Lateral Load vs Tested Lateral Load

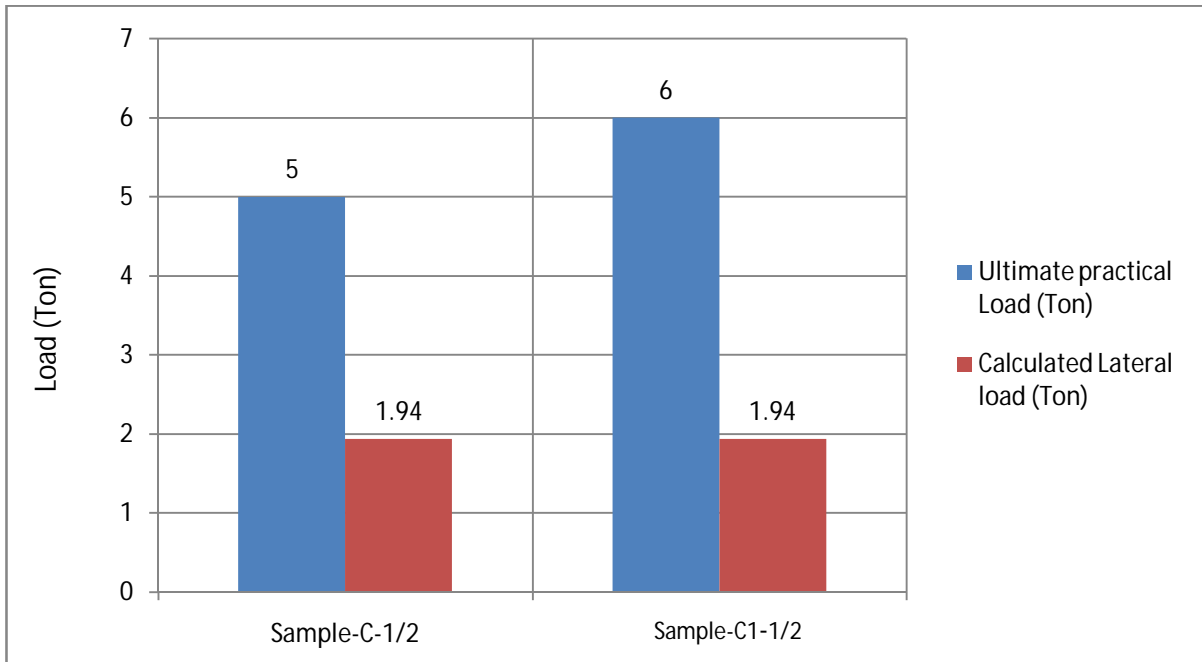
There is relationship developed between calculated lateral load of the wall vs practical Shear force capacity of the walls are shown in figure 4.78

From the figure 4.78a it is observed that, the specimen made of clay burnt brick with mortar thickness 1/2" (specimens-C-1/2 and C1-1/2), the average theoretical shear force is 35.3% of average tested lateral load. The lateral capacity of the specimen wall made of clay burnt brick with mortar thickness 1/2" was performed by 3 ton vertical loads.

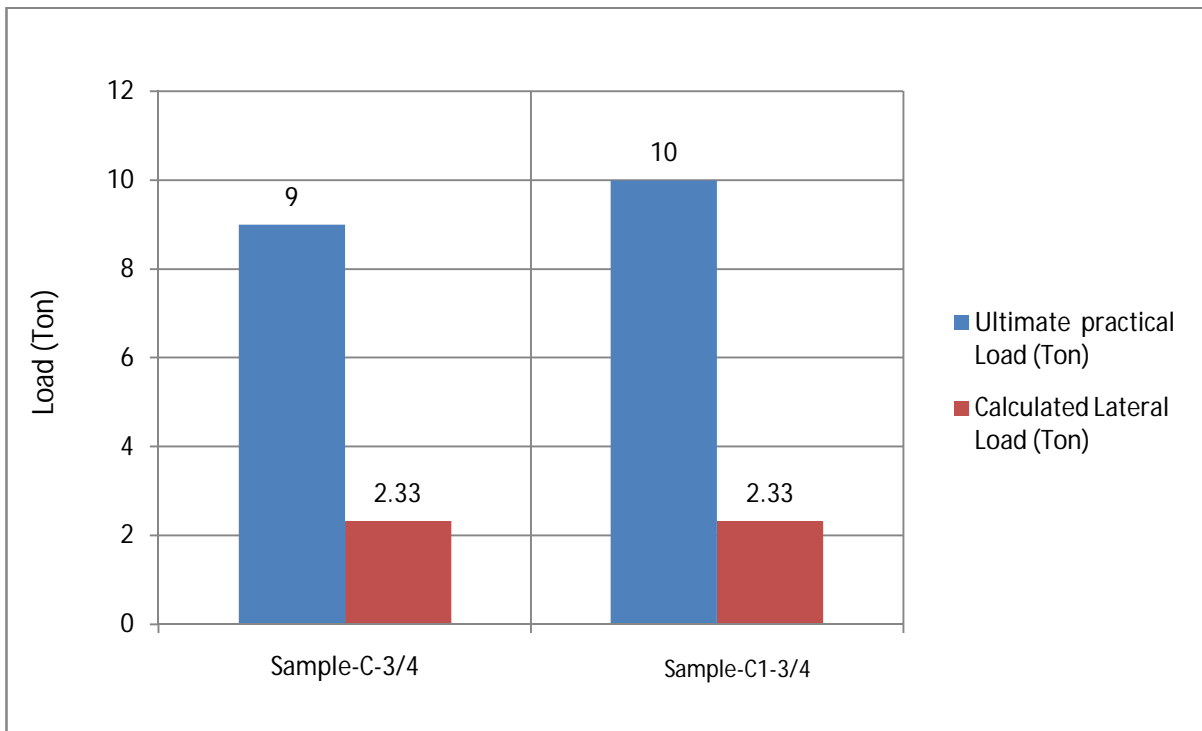
From the figure 4.78b it is observed that, the specimen made of clay burnt brick with mortar thickness 3/4" (specimens-C-3/4 and C1-3/4), the average theoretical shear force is 24.5% of average tested lateral load. The lateral capacity of the specimen wall made of clay burnt brick with mortar thickness 3/4" was performed by 6 ton vertical loads.

From the figure 4.78c it is observed that, the specimen made of machine made brick with mortar thickness 1/2" (specimens-M-1/2 and M1-1/2), the average theoretical shear force is 43.2% of average tested lateral load. The lateral capacity of the specimen wall made of machine made brick with mortar thickness 1/2" was performed by 6 ton vertical loads.

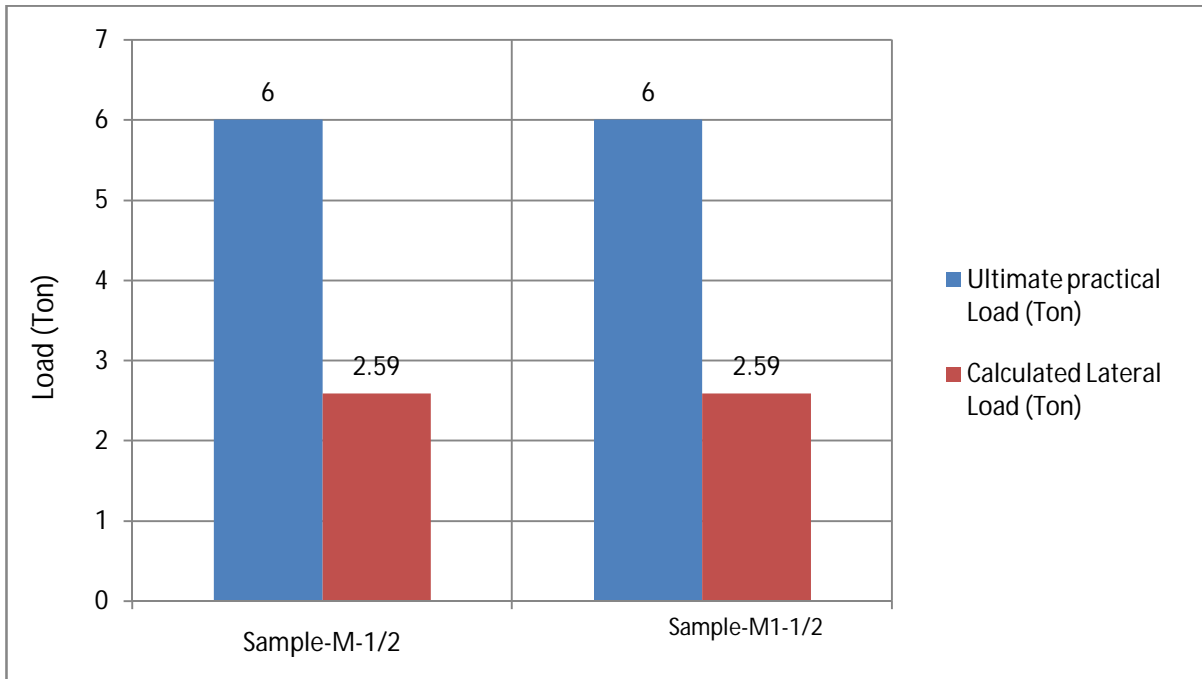
From the figure 4.78d it is observed that, the specimen made of machine made brick with mortar thickness 3/4" (specimens-M-3/4 and M1-3/4), the average theoretical shear force is 44.5% of average tested lateral load. The lateral capacity of the specimen wall made of machine made brick with mortar thickness 3/4" was performed by 6 ton vertical loads.



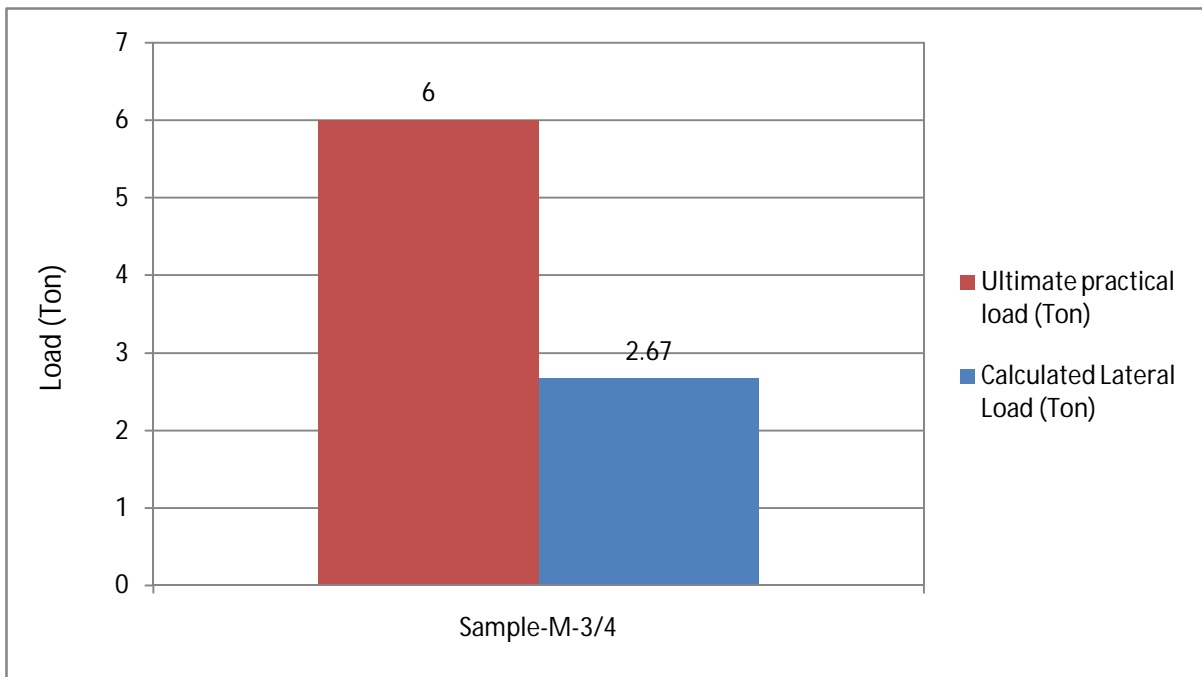
a. Tested load vs calculated lateral load of clay burnt brick wall with mortar thickness 1/2"



b. Tested load vs calculated lateral load of clay burnt brick wall with mortar thickness 3/4"



c. Tested load vs calculated lateral load of machine made brick wall with mortar thickness 1/2"



d. Tested load vs calculated lateral load of machine made brick wall with mortar thickness 3/4"

Figure 4.78: Relationship between Calculated Lateral Load vs Tested Lateral Load of Different Types of Wall

CHAPTER 5

SUMMARY, CONCLUSIONS AND RECOMMENDATIONS

5.1 Summary

The aim of this study was to find out the shear behavior of URM wall and the variables that affect the shear capacity of URM wall such as the thickness of masonry wall, and a relation between compressive strength measured by prism test and shear strength measured by shear test of clay burnt brick with frog mark and machine made brick without frog mark. To achieve the objectives, eight prisms and eight URM walls were constructed and tested. Eight (8) prisms were constructed of two different bricks. Out of eight prisms four (4) prisms were made of Clay burnt brick two with mortar thicknesses 1/2" and another two with mortar thickness 3/4". Four (4) prisms were made of machine made bricks two with mortar thicknesses 1/2" and another two with mortar thickness 3/4". Eight (10 inch) URM wall with a size of 5'× 3' were constructed for shear test and wall stiffness test. Out of eight URM walls four walls were made of clay burnt brick and another four walls were made of machine made bricks with two mortar thicknesses 1/2" and 3/4".

Preparations of wall consist of two steps, at first slab were made and then brick wall constructed on the slab. At every different step different wall and prisms were constructed following the usual construction practices. Prisms compressive strength was tested by compressive loading and shear test were tested on 5" wall with constant vertical loads. Walls were tested under incremental horizontal cyclic loading along with constant vertical load. Tests were conducted under load controlled cyclic loading.

During testing one dial gauges were used to determine the horizontal deflections of the wall. Dial gauges was installed at the top of the wall to determine the horizontal deflection of the wall. From these tests the displacement corresponding to each cyclic load was recorded. With this recorded data load- displacement response curves were prepared to compare the results of test specimens of different walls and a relationship between prism strength and shear strength. Finally some conclusions were drawn regarding the use of clay burnt brick with frog mark and machine made brick without frog mark considering the effects of mortar thicknesses.

5.2 Observations

Behavior of the walls under cyclic loading, the prism and shear test specimens experimented in the study were investigated. Based on the results obtained from the experiments of the specimens, the following observations can be drawn:

- a. Increasing mortar thickness prism cracking strength and ultimate strength increases in both types of brick i.e clay burnt brick with frog mark and machine made brick without frog mark.
- b. Increasing mortar thickness cracking shear strength and ultimate shear strength decreases in both types of brick i.e clay burnt brick with frog mark and machine made brick without frog mark.
- c. In clay burnt brick cracking prism strength is more than machine made brick.
- d. In machine made brick ultimate prism strength is more than clay burnt brick.
- e. In clay burnt brick shear strength is more than machine made brick.
- f. The specimen made of clay burnt brick with mortar thickness 1/2", the average cracking shear strength is 62.6% of average cracking prism strength and average ultimate shear strength is 54.4% of average ultimate prism strength.
- g. The specimen made of clay burnt brick with mortar thickness 3/4", the average cracking shear strength is 53.9% of average cracking prism strength and average ultimate shear strength is 31.0% of average ultimate prism strength.
- h. The specimen made of machine made brick with mortar thickness 1/2", the average cracking shear strength is 72.7% of average cracking prism strength and average ultimate shear strength is 25.9% of average ultimate prism strength.

- i. The specimen made of machine made brick with mortar thickness 3/4", the average cracking shear strength is 59.9% of average cracking prism strength and average ultimate shear strength is 20.7% of average ultimate prism strength.
- j. Increasing mortar thickness of both types of specimen's wall ductility decreases.
- k. The average stiffness degradation of clay burnt brick with mortar thickness 1/2" and 3/4" are 20.0% and 13.93% per cycle respectively. The average stiffness degradation of machine made brick with mortar thickness 1/2" and 3/4" are 18.68% and 18.21% per cycle.
- l. Energy absorbed by machine made brick wall with mortar thickness 3/4" is 58.1% of energy absorbed by machine made brick wall with mortar thickness 1/2".
- m. The specimens made of clay burnt brick with mortar thickness 1/2" (Specimens- C-1/2 and C1-1/2), the average cracking lateral load is 2.90% of average cracking shear force and the average ultimate lateral load is 5.77% of average ultimate shear force. Also specimens made of clay burnt brick with mortar thickness 3/4" (Specimens- C-3/4 and C1-3/4), the average cracking lateral load is 4.77% of average cracking shear force and the average ultimate lateral load is 12.09% of average ultimate shear force.
- n. The specimens made of machine brick with mortar thickness 1/2" (Specimens- M-1/2), the cracking lateral load is 4.28% of cracking shear force and the ultimate lateral load is 7.81% of ultimate shear force. Also specimens made of machine made brick with mortar thickness 3/4" (Specimens- M-3/4), the cracking lateral load is 3.78% of cracking shear force and the ultimate lateral load is 8.62% of ultimate shear force.
- o. For Specimens-C-1/2 and C1-1/2, the average cracking horizontal load is 62% of average cracking prism strength and average ultimate prism strength is 93.3% of average ultimate horizontal load and For Specimens-C-3/4 and C1-3/4, the average cracking horizontal load is 88.5% of average cracking prism strength and average ultimate prism strength is 77.6% of average ultimate horizontal load.

- p. For Specimens-M-1/2, the cracking prism strength is 85.6% of average cracking horizontal load and ultimate horizontal load is 70.5% of average ultimate prism strength. For Specimens-M-3/4, the cracking horizontal load is 85.8% of cracking prism strength and ultimate horizontal load is 67.0% of ultimate prism strength.
- q. For Specimens-C-1/2 and C1-1/2, the average cracking horizontal load is 99% of average cracking shear strength and average ultimate shear strength is 50.8% of average ultimate horizontal load. For Specimens-C-3/4 and C1-3/4, the average cracking shear strength is 61.3% of average horizontal load and average ultimate shear strength is 24.1% of average ultimate horizontal load.
- r. For Specimens-M-1/2, the cracking shear strength is 66.8% of average cracking horizontal load and ultimate shear strength is 33.8% of average ultimate horizontal load. For Specimens-M-3/4, the cracking shear strength is 73.0% of cracking horizontal load and ultimate shear strength is 32.0% of ultimate horizontal load.

5.3 Conclusions

Based on the results obtained from the experiments of the specimens, the following conclusions can be drawn:

- a. Increasing mortar thickness prism ultimate strength increases 18.0% for clay burnt brick and with increasing mortar thickness prism ultimate strength increases 1.3% for machine made brick.
- b. Increasing mortar thickness ultimate shear strength decreases 9.6% for clay burnt brick with frog mark and with increasing mortar thickness ultimate shear strength decreases 8.0% for machine made bricks without frog mark.
- c. In clay burnt brick shear strength is 12.5% more than machine made brick.
- d. Increasing mortar thickness ductility decreases 22.0% for clay burnt brick and 20.0% for machine made bricks.
- e. The average stiffness degradation of clay burnt brick with mortar thickness 1/2" and 3/4" are 20.0% and 13.93% per cycle respectively. The average stiffness degradation of

machine made brick with mortar thickness 1/2" and 3/4" are 18.68% and 18.21% per cycle.

- f. Energy absorbed by machine made brick wall with mortar thickness 3/4" is 58.1% of energy absorbed by machine made brick wall with mortar thickness 1/2".
- g. For specimen (C-1/2 & C1-1/2) and specimen (C-3/4 & C1-3/4), the average theoretical shear forces are 35.0% and 25.0% of average tested lateral load. Also for specimen (M-1/2 & M1-1/2) and specimen (M-3/4 & M1-3/4), the average theoretical shear forces are 43.0% and 45.0% of average tested lateral load
- h. In terms of load bearing, ductility and stiffness clay burnt brick performed better than machine made brick.
- i. No relation between prism strength, shear strength and wall stiffness was obtained since the failure mode of the wall is combination of sliding and rocking.

5.4 Recommendations

This research suggests following recommendations for further investigation.

- a. The experimental results may be verified by finite element analysis.
- b. Full scale specimens may be investigated to get more accurate result.
- c. More parameters may be considered to achieve more specified result.
- d. Bond wrench test may be performed to compare with shear test result.

REFERENCES

- ASTM C 1197, "Standard Test Method for In Situ Measurement of Masonry Deformability Properties Using the Jack Method," American Society for Testing Materials, 2004.
- ASTM C1314, "Standard Test Method for Compressive Strength of Masonry Prism," American Society for Testing Materials, 2004.
- ASTM C 1531, "Standard Test Method for In Situ Measurement of Masonry Mortar Joint Shear Strength," American Society for Testing Materials, 2003.
- Drysdale, R.G. and Hamid, A.A., "Concrete masonry under combined shear and compression along the mortar joints," American Concrete Institute Journal, Proceedings, Vol. 77, No. 5, pp 314-320, 1980.
- Drysdale R.G., Hamid, A.A. and Heidebrecht, A.C., "Tensile strength of concrete Masonry," Journal of the Structural Division, Vol. 105, No. 7, pp. 1261-1276, 1979.
- Drysdale, R.G., Hamid A.A., and Baker L.R., "Masonry Structures, Behavior and Design," Prentice Hall Inc., Englewood Cliffs, pp. 784, 1994.
- Deepa A & Joshi R.K., "Evaluation of Compressive Strength and Basic Compressive Stress of Clay Brick Unreinforced Masonry by Prism Test," International Journal of Science and Research (IJSR), May, 2015.
- Hegemier, G.A., Krishnamoorthy, G., Nunn, R.O. and Moorthy, T.V., "Prism tests for the compressive strength of concrete masonry," Proceedings of the North American Masonry Conference, No. 18, pp. 18-1 – 18-17, 1978.
- Ida A. M. B., "Experimental Compressive Strength and Modulus of Elasticity of Masonry," Jurnal Ilmiah Teknik Sipil, Vol. 13, No. 1, January, 2009.
- Isidoros C., "An investigation into the shear bond strength of masonry," M.Sc Thesis, University of the Witwatersrand, Johannesburg, 2014.
- Khalaf, F.M., "Block work masonry compressed in two orthogonal directions," Journal of Structural Engineering, Vol. 123, No. 5, pp. 591-596, 1997.
- Lee, R., Longworth, J. and Warwaruk J., "Concrete masonry prism response due to loads parallel and perpendicular to bed joint," M.Sc Thesis, Department of Civil Engineering, University of Alberta. 1984.
- Ludovikus S. W., "Seismic Assessment of Unreinforced Masonry Walls," PhD Thesis, University of Canterbury Christchurch, New Zealand, December, 2007.

Mohamed A., Elgwady, Pierino L. & Marc B., "Dynamic in-plane Behavior of URM Wall Upgraded With Composites," Swiss Federal Institute of Technology, Lausanne, Switzerland, 2000.

Maheri M. R., Najafgholipour M. A. & Rajabi A. R., "The Influence of Mortar Head Joints on the in-plane and out-of-plane Seismic Strength of Brick Masonry Walls," The 14th World Conference on Earthquake Engineering , Beijing, China , October, 2008.

Mahmoud R., Maheri M. A. "Shear Strength of Brick Walls in Iran; Evaluation of Field Test Data," 6th International Conference on Seismology and Earthquake Engineering, SEE6/1/IIIES, 2003.

Qaisar A., Yasir I. B., Naveed A., Bashir A., Shahzad R., & Farhat A. S. B., "Experimental Investigation on the Characterization of Solid Clay Brick Masonry for Lateral Shear Strength Evaluation," International Journal of Earth Science and Engineering, Vol. 5, No. 4, ISSN 0974-5904, 2012.

Reddy, V. B., "Influence of shear bond strength on compressive strength and stress–strain characteristics of masonry," Materials and Structures, Vol. 41, pp. 1697–1712, 2008.

Shahid N., "Studies on the Failure of Unreinforced Masonry Shear Walls," PhD Thesis, Queensland University of Technology, Australia, 2015.

Saman A. A., "Statistical Analysis of Compressive Strength of Clay Brick Masonry Prisms," M.Sc Thesis, The University of Texas at Arlington, 2006.

Soon, S., "In-plane behavior and capacity of concrete masonry infills bounded by steel Frames," M.S. thesis, Dalhousie University. 2011.

Tamara K., "Behavior and Strength of Masonry Prisms Loaded in Compression," M.Sc Thesis, Dalhousie University Halifax, Nova Scotia, 2013.

Voon, K. and J. Ingham., "Experimental In-Plane Shear Strength Investigation of Reinforced Concrete Masonry Walls," Journal of Structural Engineering Vol. 132, No. 3, pp. 400-408, 2008.

Wong, H.E. and Drysdale, R.G., "Compression Characteristics of Concrete Block Masonry Prisms," Masonry: Research, Application, and Problems, ASTM STP 871, pp. 167-177, 1985.

Woon H. Y., Sang H. O., & Jung H. L., "Shear Capacity Assessment of Unreinforced Masonry Wall," 13th World Conference on Earthquake Engineering, Vancouver, B.C., No. 1698, Canada August, 2004.

Yael D. H. & Frieder S., "Performance Evaluation Database for Concrete Bridge Components and Systems under Simulated Seismic Loads," PEER Report 1999/11, Nov, 1999.

APPENDIX-A

The axial compressive stress and shear stress are calculated according to BNBC.

a) Compressive Stress, Axial

i) Unreinforced masonry walls,

$$F_a = f'_m/5[1-(h'/42t)^3]$$

Where, f'_m = specified compressive strength of masonry at the age of 28 days

h' = effective height of a wall

t = effective thickness of a wall

For clay burnt brick with mortar thickness 1/2"

$$f'_m = 5.11 \text{ Mpa}$$

$$h' = 3 \text{ ft} = 0.91 \text{ m}$$

$$t = 10 \text{ inch} = 0.25 \text{ m}$$

$$L = 53 \text{ inch} = 1.35 \text{ m}$$

$$A = 1.35 * 0.25 = 0.3375 \text{ m}^2 = 337500 \text{ mm}^2$$

$$\text{So, } F_a = 5.11/5[1-(0.91/42*0.25)^3]$$

$$= 1.021 \text{ N/mm}^2$$

$$= 1.021 * 337500 = 344588 \text{ N} = 35126 \text{ kg} = 35.12 \text{ ton}$$

For clay burnt brick with mortar thickness 3/4"

$$f'_m = 7.36 \text{ Mpa}$$

$$h' = 3 \text{ ft} = 0.91 \text{ m}$$

$$t = 10 \text{ inch} = 0.25 \text{ m}$$

$$L = 53 \text{ inch} = 1.35 \text{ m}$$

$$A = 1.35 * 0.25 = 0.3375 \text{ m}^2 = 337500 \text{ mm}^2$$

$$\text{So, } F_a = 7.36/5[1-(0.91/42*0.25)^3]$$

$$= 1.47 \text{ N/mm}^2$$

$$= 1.47 * 337500 = 496125 \text{ N} = 50573 \text{ kg} = 50.57 \text{ ton}$$

For machine made brick with mortar thickness 1/2"

$$f'_m = 8.2 \text{ Mpa}$$

$$h' = 3.1 \text{ ft} = 0.95 \text{ m}$$

$$t = 10 \text{ inch} = 0.25 \text{ m}$$

$$L = 56 \text{ inch} = 1.42 \text{ m}$$

$$A = 1.42 * 0.25 = 0.355 \text{ m}^2 = 355000 \text{ mm}^2$$

$$\text{So, } F_a = 8.2/5[1-(0.95/42*0.25)^3]$$

$$= 1.639 \text{ N/mm}^2$$

$$= 1.639 * 355000 = 581845 \text{ N} = 59311 \text{ kg} = 59.3 \text{ ton}$$

For machine made brick with mortar thickness 3/4"

$$f'm = 8.7 \text{ Mpa}$$

$$h' = 3.1 \text{ ft} = 0.95\text{m}$$

$$t = 10 \text{ inch} = 0.25\text{m}$$

$$L = 56 \text{ inch} = 1.42\text{m}$$

$$A = 1.42 * 0.25 = 0.355 \text{ m}^2 = 355000 \text{ mm}^2$$

$$\text{So, } F_a = 8.7/5 [1 - (0.95/42 * 0.25)^3]$$

$$= 1.739 \text{ N/mm}^2$$

$$= 1.739 * 355000 = 617345\text{N} = 62930\text{kg} = 62.9 \text{ ton}$$

b) Shear Stress for Shear Walls,

Unreinforced masonry walls,

$$\text{For clay units } F_v = 0.025 \sqrt{f'm} \leq 0.40 \text{ N/mm}^2$$

For clay burnt brick with mortar thickness 1/2"

$$F_v = 0.025 \sqrt{f'm}$$

$$= 0.025 * \sqrt{5.11} = 0.0565 \text{ N/mm}^2 = 0.0565 * 337500 = 19073.22\text{N} = 1944.3\text{kg}$$

$$= 1.94 \text{ ton}$$

For clay burnt brick with mortar thickness 3/4"

$$F_v = 0.025 \sqrt{f'm}$$

$$= 0.025 * \sqrt{7.36} = 0.0678 \text{ N/mm}^2 = 0.0678 * 337500 = 22890.4\text{N} = 2333.4\text{kg}$$

$$= 2.33 \text{ ton}$$

For machine made brick with mortar thickness 1/2"

$$F_v = 0.025 \sqrt{f'm}$$

$$= 0.025 * \sqrt{8.2} = 0.0716 \text{ N/mm}^2 = 0.0716 * 355000 = 25414.1\text{N} = 2590.6\text{kg}$$

$$= 2.59 \text{ ton}$$

For machine made brick with mortar thickness 3/4"

$$F_v = 0.025 \sqrt{f'm}$$

$$= 0.025 * \sqrt{8.7} = 0.0737 \text{ N/mm}^2 = 0.0737 * 355000 = 26177.5\text{N} = 2668.4\text{kg}$$

$$= 2.67 \text{ ton}$$

APPENDIX-B

Table A.1: Load-Deflection Value for Specimen C-1/2

Load (Ton)	Displacement (mm)	Load (Ton)	Displacement (mm)
Cycle-I		Cycle-II	
0.0	0	0.0	-0.1
0.5	0.03	0.5	-0.03
1.0	0.11	1.0	0.08
1.5	0.22	1.5	0.19
2.0	0.4	2.0	0.34
1.5	0.37	2.5	0.47
1.0	0.31	3.0	0.68
0.5	0.25	2.5	0.67
0.0	0.12	2.0	0.6
-0.5	0.02	1.5	0.51
-1.0	-0.11	1.0	0.41
-1.5	-0.32	0.5	0.33
-2.0	-0.72	0.0	0.17
-1.5	-0.7	-0.5	0.07
-1.0	-0.51	-1.0	-0.08
-0.5	-0.22	-1.5	-0.21
0.0	-0.1	-2.0	-0.45
Cycle-III		-2.5	-0.81
0.0	-0.41	-3.0	-2.93
0.5	-0.24	-2.5	-2.62
1.0	-0.15	-2.0	-2.34
1.5	-0.03	-1.5	-1.77
2.0	0.14	-1.0	-1.23
2.5	0.32	-0.5	-0.84
3.0	0.56	0.0	-0.41
3.5	0.88	Cycle-IV	
4.0	4.27	0.0	-0.66

3.5	4.09	0.5	-0.6
3.0	3.39	1.0	-0.55
2.5	2.86	1.5	-0.25
2.0	2.39	2.0	0.01
1.5	1.79	2.5	0.16
1.0	1.47	3.0	0.36
0.5	0.67	3.5	0.84
0.0	0.31	4.0	4.25
-0.5	0.21	4.5	6.35
-1.0	-0.04	5.0	8.65
-1.5	-0.34	4.5	8.14
-2.0	-1.26	4.0	6.67
-2.5	-1.96	3.5	6.06
-3.0	-2.94	3.0	5.49
-3.5	-3.91	2.5	5.12
-4.0	-5.96	2.0	4.22
-3.5	-5.66	1.5	3.54
-3.0	-5.02	1.0	2.82
-2.5	-4.07	0.5	1.92
-2.0	-3.53	0.0	0.61
-1.5	-2.74	-0.5	0.49
-1.0	-2.05	-1.0	0.19
-0.5	-1.12	-1.5	-0.16
0.0	-0.66	-2.0	-1.21
		-2.5	-1.87
		-3.0	-3.36
		-3.5	-4.28
		-4.0	-7.3
		-4.5	-10.97
		-5.0	-13.77

		-4.5	-13.11
		-4.0	-12.22
		-3.5	-9.87
		-3.0	-8.57
		-2.5	-7.22
		-2.0	-6.18
		-1.5	-4.8
		-1.0	-3.3
		-0.5	-2.28

Table A.2: Load-Deflection Value for Specimen C1-1/2

Load (Ton)	Displacement (mm)	Load (Ton)	Displacement (mm)
Cycle-I		Cycle-II	
0.0	0	0.0	-0.06
0.5	0.11	0.5	0.06
1.0	0.26	1.0	0.33
1.5	0.38	1.5	0.53
2.0	0.54	2.0	0.66
1.5	0.5	2.5	0.84
1.0	0.42	3.0	1.08
0.5	0.29	2.5	1.06
0.0	0.21	2.0	1
-0.5	0.09	1.5	0.91
-1.0	-0.15	1.0	0.8
-1.5	-0.35	0.5	0.65
-2.0	-0.57	0.0	0.43
-1.5	-0.51	-0.5	0.31
-1.0	-0.41	-1.0	0.04
-0.5	-0.21	-1.5	-0.44

0.0	-0.06	-2.0	-0.64
Cycle-III		-2.5	-1.03
0.0	-0.26	-3.0	-1.44
0.5	-0.16	-2.5	-1.39
1.0	0.32	-2.0	-1.24
1.5	0.53	-1.5	-1.06
2.0	0.68	-1.0	-0.84
2.5	0.95	-0.5	-0.64
3.0	1.16	Cycle-IV	
3.5	1.4	0.0	-0.37
4.0	1.66	0.5	-0.2
3.5	1.64	1.0	0.26
3.0	1.57	1.5	0.4
2.5	1.46	2.0	0.58
2.0	1.31	2.5	0.82
1.5	1.09	3.0	1.07
1.0	1	3.5	1.28
0.5	0.81	4.0	1.46
0.0	0.6	4.5	1.74
-0.5	0.32	5.0	2.16
-1.0	-0.2	4.5	2.1
-1.5	-1	4.0	2.06
-2.0	-1.23	3.5	1.96
-2.5	-1.56	3.0	1.78
-3.0	-1.78	2.5	1.62
-3.5	-2.15	2.0	1.48
-4.0	-3.01	1.5	1.26
-3.5	-2.85	1.0	1.04
-3.0	-2.6	0.5	0.9
-2.5	-2.45	0.0	0.57

-2.0	-2.26	-0.5	0.13
-1.5	-2.02	-1.0	-0.5
-1.0	-1.7	-1.5	-1.31
-0.5	-1.26	-2.0	-1.73
0.0	-0.37	-2.5	-2.03
Cycle-V		-3.0	-2.26
0.0	-0.79	-3.5	-2.61
0.5	-0.61	-4.0	-2.98
1.0	-0.26	-4.5	-3.37
1.5	0.3	-5.0	-5.43
2.0	0.62	-4.5	-5.03
2.5	0.99	-4.0	-4.63
3.0	1.38	-3.5	-4.13
3.5	1.64	-3.0	-3.73
4.0	1.97	-2.5	-3.13
4.5	2.74	-2.0	-2.59
5.0	3.78	-1.5	-2.29
5.5	9.64	-1.0	-2.02
6.0	14.89	-0.5	-1.46
5.5	14.35	0.0	-0.79
5.0	13.99		
4.5	13.31		
4.0	12.44		
3.5	12.02		
3.0	11.05		
2.5	8.96		
2.0	7.21		
1.5	4.49		
1.0	3.33		
0.5	2.23		

0.0	0.99		
-----	------	--	--

Table A.3: Load-Deflection Value for Specimen C-3/4

Load (Ton)	Displacement (mm)	Load (Ton)	Displacement (mm)
Cycle-I		Cycle-II	
0.0	0	0.0	-0.1
0.5	0.02	0.5	-0.07
1.0	0.07	1.0	0.05
1.5	0.17	1.5	0.12
2.0	0.3	2.0	0.23
1.5	0.28	2.5	0.36
1.0	0.22	3.0	0.51
0.5	0.14	2.5	0.5
0.0	0.07	2.0	0.46
-0.5	-0.05	1.5	0.37
-1.0	-0.14	1.0	0.27
-1.5	-0.28	0.5	0.16
-2.0	-0.52	0.0	0.09
-1.5	-0.51	-0.5	-0.01
-1.0	-0.45	-1.0	-0.06
-0.5	-0.37	-1.5	-0.36
0.0	-0.1	-2.0	-0.87
Cycle-III		-2.5	-0.81
0.0	-0.38	-3.0	-1.65
0.5	-0.33	-2.5	-1.6
1.0	-0.22	-2.0	-1.4
1.5	-0.1	-1.5	-1.29
2.0	0.02	-1.0	-0.93
2.5	0.14	-0.5	-0.72

3.0	0.3	0.0	-0.38
3.5	0.45	Cycle-IV	
4.0	0.74	0.0	-0.55
3.5	0.73	0.5	-0.47
3.0	0.66	1.0	-0.34
2.5	0.57	1.5	-0.21
2.0	0.46	2.0	-0.03
1.5	0.38	2.5	0.12
1.0	0.31	3.0	0.26
0.5	0.25	3.5	0.42
0.0	0.19	4.0	0.61
-0.5	-0.08	4.5	0.79
-1.0	-0.22	5.0	1.31
-1.5	-0.43	4.5	1.29
-2.0	-0.93	4.0	1.22
-2.5	-1.33	3.5	1.12
-3.0	-1.74	3.0	0.98
-3.5	-2.05	2.5	0.82
-4.0	-2.57	2.0	0.62
-3.5	-2.41	1.5	0.47
-3.0	-2.18	1.0	0.37
-2.5	-1.83	0.5	0.29
-2.0	-1.57	0.0	0.22
-1.5	-1.4	-0.5	0.11
-1.0	-1.04	-1.0	-0.21
-0.5	-0.87	-1.5	-0.44
0.0	-0.55	-2.0	-1.02
Cycle-V		-2.5	-1.47
0.0	-0.67	-3.0	-1.82
0.5	-0.55	-3.5	-2.65

1.0	-0.42	-4.0	-3.18
1.5	-0.34	-4.5	-3.54
2.0	-0.14	-5.0	-3.98
2.5	0.03	-4.5	-3.94
3.0	0.19	-4.0	-3.83
3.5	0.36	-3.5	-3.57
4.0	0.5	-3.0	-3.22
4.5	0.67	-2.5	-2.83
5.0	0.88	-2.0	-2.36
5.5	1.1	-1.5	-1.83
6.0	1.37	-1.0	-1.35
6.5	1.65	-0.5	-1.16
7.0	2.92	0.0	-0.67
6.5	2.81	Cycle-VI	
6.0	2.67	0.0	-0.94
5.5	2.45	1.0	-0.67
5.0	2.1	2.0	-0.36
4.5	1.78	3.0	-0.06
4.0	1.57	4.0	0.31
3.5	1.44	5.0	0.67
3.0	1.04	6.0	1.55
2.5	0.86	7.0	3.03
2.0	0.56	8.0	5.32
1.5	0.47	9.0	6.91
1.0	0.39	8.0	6.81
0.5	0.31	7.0	6.32
0.0	0.16	6.0	5.68
-0.5	0.02	5.0	5.22
-1.0	-0.28	4.0	4.95
-1.5	-0.62	3.0	3.83

-2.0	-0.81	2.0	2.83
-2.5	-1.22	1.0	1.56
-3.0	-2.21	0.0	0.59
-3.5	-2.67	-1.0	0.13
-4.0	-3.26	-2.0	-0.49
-4.5	-3.72	-3.0	-2.4
-5.0	-4.07	-4.0	-3.24
-5.5	-4.61	-5.0	-4.44
-6.0	-5.33	-6.0	-5.39
-6.5	-5.85	-7.0	-6.52
-7.0	-6.13	-8.0	-8.88
-6.5	-6.11	-9.0	-12.52
-6.0	-6.05	-8.0	-11.97
-5.5	-5.87	-7.0	-11.02
-5.0	-5.69	-6.0	-10.47
-4.5	-5.42	-5.0	-9.77
-4.0	-5.11	-4.0	-8.83
-3.5	-4.54	-3.0	-7.69
-3.0	-4.12	-2.0	-5.89
-2.5	-3.56	-1.0	-2.69
-2.0	-2.95	0.0	-1.07
-1.5	-2.31		
-1.0	-1.79		
-0.5	-1.52		
0.0	-0.94		

Table A.4: Load-Deflection Value for Specimen C1-3/4

Load (Ton)	Displacement (mm)	Load (Ton)	Displacement (mm)
Cycle-I		Cycle-II	
0.0	0	0.0	-0.04
0.5	0.01	0.5	-0.02
1.0	0.06	1.0	0.05
1.5	0.13	1.5	0.08
2.0	0.33	2.0	0.15
1.5	0.24	2.5	0.21
1.0	0.2	3.0	0.38
0.5	0.15	2.5	0.33
0.0	0.11	2.0	0.26
-0.5	0.06	1.5	0.22
-1.0	0	1.0	0.16
-1.5	-0.13	0.5	0.11
-2.0	-0.38	0.0	0.06
-1.5	-0.3	-0.5	-0.03
-1.0	-0.17	-1.0	-0.11
-0.5	-0.11	-1.5	-0.18
0.0	-0.04	-2.0	-0.26
Cycle-III		-2.5	-0.81
0.0	-0.18	-3.0	-1.12
0.5	-0.15	-2.5	-1.1
1.0	-0.12	-2.0	-0.91
1.5	-0.06	-1.5	-0.78
2.0	0	-1.0	-0.63
2.5	0.06	-0.5	-0.46
3.0	0.15	0.0	-0.18
3.5	0.31	Cycle-IV	
4.0	0.61	0.0	-0.24

3.5	0.6	0.5	-0.21
3.0	0.59	1.0	-0.17
2.5	0.55	1.5	-0.09
2.0	0.5	2.0	0.01
1.5	0.44	2.5	0.06
1.0	0.37	3.0	0.12
0.5	0.32	3.5	0.21
0.0	0.27	4.0	0.28
-0.5	0.16	4.5	0.36
-1.0	0.06	5.0	0.63
-1.5	0.02	4.5	0.62
-2.0	-0.1	4.0	0.57
-2.5	-0.68	3.5	0.49
-3.0	-1.23	3.0	0.45
-3.5	-1.94	2.5	0.4
-4.0	-3.24	2.0	0.34
-3.5	-3.14	1.5	0.29
-3.0	-2.81	1.0	0.24
-2.5	-2.27	0.5	0.19
-2.0	-1.55	0.0	0.07
-1.5	-0.89	-0.5	-0.02
-1.0	-0.52	-1.0	-0.12
-0.5	-0.41	-1.5	-0.22
0.0	-0.24	-2.0	-0.39
Cycle-V		-2.5	-1.47
0.0	-0.65	-3.0	-1.11
0.5	-0.61	-3.5	-1.21
1.0	-0.55	-4.0	-1.61
1.5	-0.48	-4.5	-3.81
2.0	-0.41	-5.0	-4.96

2.5	-0.32	-4.5	-4.91
3.0	-0.24	-4.0	-4.63
3.5	-0.14	-3.5	-4.16
4.0	-0.09	-3.0	-3.71
4.5	0.01	-2.5	-3.06
5.0	0.07	-2.0	-2.16
5.5	0.36	-1.5	-1.73
6.0	0.51	-1.0	-1.21
6.5	1.66	-0.5	-0.96
7.0	2.88	0.0	-0.65
6.5	2.86	Cycle-VI	
6.0	2.8	0.0	-0.74
5.5	2.67	0.5	-0.69
5.0	2.34	1.0	-0.64
4.5	2.06	1.5	-0.57
4.0	1.85	2.0	-0.5
3.5	1.73	2.5	-0.4
3.0	1.45	3.0	-0.32
2.5	1.32	3.5	-0.24
2.0	1.14	4.0	-0.15
1.5	1.02	4.5	-0.04
1.0	0.91	5.0	0.16
0.5	0.68	5.5	0.65
0.0	0.34	6.0	0.84
-0.5	0.22	6.5	1.45
-1.0	0.15	7.0	3.08
-1.5	0.06	7.5	4.18
-2.0	-0.07	8.0	4.51
-2.5	-0.68	8.5	5.23
-3.0	-1.28	9.0	5.98

-3.5	-2.31	9.5	13.11
-4.0	-3.22	10.0	15.06
-4.5	-4.44	9.5	14.9
-5.0	-5	9.0	14.31
-5.5	-5.5	8.5	13.81
-6.0	-5.82	8.0	13.46
-6.5	-6.38	7.5	12.61
-7.0	-6.84	7.0	12.03
-6.5	-6.7	6.5	11.71
-6.0	-6.52	6.0	11.11
-5.5	-6.29	5.5	10.64
-5.0	-6.04	5.0	10.01
-4.5	-5.69	4.5	9.06
-4.0	-5.4	4.0	8.53
-3.5	-5.14	3.5	7.5
-3.0	-4.63	3.0	6.98
-2.5	-3.99	2.5	6.34
-2.0	-3.49	2.0	5.65
-1.5	-3.18	1.5	3.96
-1.0	-2.49	1.0	3.12
-0.5	-1.39	0.5	2.03
0.0	-0.74	0.0	0.89

Table A.5: Load-Deflection Value for Specimen M-1/2

Load (Ton)	Displacement (mm)	Load (Ton)	Displacement (mm)
Cycle-I		Cycle-II	
0.0	0	0.0	-0.05
0.5	0.07	0.5	0.04
1.0	0.11	1.0	0.09

1.5	0.2	1.5	0.19
2.0	0.36	2.0	0.31
1.5	0.35	2.5	0.4
1.0	0.3	3.0	0.53
0.5	0.21	2.5	0.46
0.0	0.13	2.0	0.42
-0.5	-0.03	1.5	0.34
-1.0	-0.1	1.0	0.26
-1.5	-0.21	0.5	0.18
-2.0	-0.3	0.0	0.05
-1.5	-0.28	-0.5	-0.09
-1.0	-0.22	-1.0	-0.18
-0.5	-0.14	-1.5	-0.29
0.0	-0.05	-2.0	-0.35
Cycle-III		-2.5	-0.46
0.0	-0.07	-3.0	-0.56
0.5	0.01	-2.5	-0.52
1.0	0.09	-2.0	-0.48
1.5	0.17	-1.5	-0.39
2.0	0.31	-1.0	-0.33
2.5	0.43	-0.5	-0.19
3.0	0.57	0.0	-0.07
3.5	0.73	Cycle-IV	
4.0	1.01	0.0	-0.13
3.5	0.99	0.5	-0.03
3.0	0.91	1.0	0.08
2.5	0.83	1.5	0.18
2.0	0.69	2.0	0.29
1.5	0.55	2.5	0.46
1.0	0.44	3.0	0.62

0.5	0.28	3.5	0.81
0.0	0.19	4.0	1.16
-0.5	0.11	4.5	2.21
-1.0	-0.04	5.0	8.52
-1.5	-0.17	4.5	7.92
-2.0	-0.26	4.0	7.44
-2.5	-0.38	3.5	6.97
-3.0	-0.47	3.0	6.76
-3.5	-0.59	2.5	6.06
-4.0	-0.8	2.0	5.15
-3.5	-0.77	1.5	3.7
-3.0	-0.71	1.0	2.74
-2.5	-0.6	0.5	1.94
-2.0	-0.48	0.0	0.82
-1.5	-0.4	-0.5	0.67
-1.0	-0.28	-1.0	0.57
-0.5	-0.2	-1.5	0.4
0.0	-0.13	-2.0	0.21
Cycle-V		-2.5	0.0
0.0	-0.42	-3.0	-0.23
0.5	-0.25	-3.5	-0.47
1.0	0.04	-4.0	-1.57
1.5	0.1	-4.5	-3.19
2.0	0.68	-5.0	-5.44
2.5	1.34	-4.5	-5.34
3.0	2.33	-4.0	-5.06
3.5	2.96	-3.5	-4.67
4.0	3.44	-3.0	-4.29
4.5	4.55	-2.5	-3.7
5.0	8.79	-2.0	-2.81

5.5	11.38	-1.5	-2.27
6.0	14.98	-1.0	-1.87
5.5	14.52	-0.5	-1.22
5.0	13.68	0.0	-0.42
4.5	13.21		
4.0	12.74		
3.5	12.17		
3.0	11.64		
2.5	10.04		
2.0	8.24		
1.5	6.44		
1.0	4.94		
0.5	3.44		
0.0	1.14		

Table A.6: Load-Deflection Value for Specimen M1-1/2

Load (Ton)	Displacement (mm)	Load (Ton)	Displacement (mm)
Cycle-I		Cycle-II	
0.0	0	0.0	-0.11
0.5	0.03	0.5	0.12
1.0	0.21	1.0	0.64
1.5	0.4	1.5	0.73
2.0	0.75	2.0	0.96
1.5	0.71	2.5	1.24
1.0	0.58	3.0	1.71
0.5	0.43	2.5	1.66
0.0	0.26	2.0	1.48
-0.5	-0.03	1.5	1.25
-1.0	-0.12	1.0	1.07

-1.5	-0.42	0.5	0.72
-2.0	-0.7	0.0	0.51
-1.5	-0.68	-0.5	-0.06
-1.0	-0.6	-1.0	-0.45
-0.5	-0.39	-1.5	-0.77
0.0	-0.11	-2.0	-1.08
Cycle-III		-2.5	-1.37
0.0	-0.13	-3.0	-1.71
0.5	0.11	-2.5	-1.68
1.0	0.59	-2.0	-1.58
1.5	0.96	-1.5	-1.4
2.0	1.22	-1.0	-1.07
2.5	1.53	-0.5	-0.72
3.0	1.95	0.0	-0.13
3.5	2.29	Cycle-IV	
4.0	2.81	0.0	-0.29
3.5	2.71	0.5	-0.18
3.0	2.51	1.0	0.42
2.5	2.13	1.5	0.9
2.0	1.8	2.0	1.22
1.5	1.51	2.5	1.59
1.0	1.23	3.0	2.02
0.5	1.05	3.5	2.51
0.0	0.6	4.0	3.1
-0.5	0.27	4.5	3.52
-1.0	-0.15	5.0	4.15
-1.5	-0.87	4.5	4.1
-2.0	-1.17	4.0	3.92
-2.5	-1.45	3.5	3.62
-3.0	-1.74	3.0	3

-3.5	-2.07	2.5	2.42
-4.0	-2.77	2.0	1.96
-3.5	-2.67	1.5	1.64
-3.0	-2.6	1.0	1.32
-2.5	-2.48	0.5	0.76
-2.0	-2.27	0.0	0.5
-1.5	-1.96	-0.5	-0.2
-1.0	-1.55	-1.0	-0.68
-0.5	-1.15	-1.5	-1.08
0.0	-0.29	-2.0	-1.4
Cycle-V		-2.5	0.0
0.0	-0.81	-3.0	-2
0.5	-0.21	-3.5	-2.08
1.0	0.08	-4.0	-2.39
1.5	0.38	-4.5	-3.9
2.0	0.58	-5.0	-4.38
2.5	1.37	-4.5	-4.31
3.0	1.58	-4.0	-4.12
3.5	1.89	-3.5	-3.89
4.0	2.28	-3.0	-3.6
4.5	2.91	-2.5	-3.32
5.0	3.57	-2.0	-3
5.5	3.97	-1.5	-2.58
6.0	4.39	-1.0	-2.1
5.5	4.23	-0.5	-1.43
5.0	4.07	0.0	-0.81
4.5	3.94		
4.0	3.46		
3.5	2.93		
3.0	2.47		

2.5	2.06		
2.0	1.67		
1.5	1.38		
1.0	1.03		
0.5	0.65		
0.0	0.18		
-0.5	-0.57		
-1.0	-0.97		
-1.5	-1.37		
-2.0	-1.62		
-2.5	-1.89		
-3.0	-2.21		
-3.5	-2.83		
-4.0	-3.21		
-4.5	-4.19		
-5.0	-4.81		
-5.5	-8.11		
-6.0	-13.29		
-5.5	-12.25		
-5.0	-11.19		
-4.5	-10		
-4.0	-8.8		
-3.5	-7.5		
-3.0	-7.21		
-2.5	-5.83		
-2.0	-4.49		
-1.5	-3.31		
-1.0	-2.41		
-0.5	-1.7		
0.0	-1.21		

Table A.7: Load-Deflection Value for Specimen M-3/4

Load (Ton)	Displacement (mm)	Load (Ton)	Displacement (mm)
Cycle-I		Cycle-II	
0.0	0	0.0	-0.09
0.5	0.05	0.5	-0.02
1.0	0.24	1.0	0.19
1.5	0.38	1.5	0.36
2.0	0.74	2.0	0.7
1.5	0.7	2.5	0.98
1.0	0.62	3.0	2.06
0.5	0.46	2.5	1.84
0.0	0.25	2.0	1.57
-0.5	0.21	1.5	1.05
-1.0	0.04	1.0	0.59
-1.5	-0.07	0.5	0.38
-2.0	-0.45	0.0	0.24
-1.5	-0.39	-0.5	0.19
-1.0	-0.29	-1.0	0.01
-0.5	-0.18	-1.5	-0.13
0.0	-0.09	-2.0	-0.52
Cycle-III		-2.5	-0.67
0.0	-0.11	-3.0	-1.79
0.5	-0.02	-2.5	-1.64
1.0	0.18	-2.0	-1.34
1.5	0.3	-1.5	-1.01
2.0	0.71	-1.0	-0.61
2.5	1.1	-0.5	-0.31
3.0	2.18	0.0	-0.11
3.5	2.71	Cycle-IV	
4.0	4.9	0.0	-0.19

3.5	4.56	0.5	-0.07
3.0	4.09	1.0	0.13
2.5	3.31	1.5	0.24
2.0	2.56	2.0	0.65
1.5	1.8	2.5	1.36
1.0	1.51	3.0	2.67
0.5	0.61	3.5	3.76
0.0	0.4	4.0	5.1
-0.5	0.32	4.5	6.7
-1.0	0.2	5.0	11.6
-1.5	-0.03	4.5	11.4
-2.0	-0.41	4.0	11.04
-2.5	-0.59	3.5	10.58
-3.0	-1.5	3.0	9.83
-3.5	-1.97	2.5	9.0
-4.0	-2.89	2.0	7.06
-3.5	-2.8	1.5	5.46
-3.0	-2.66	1.0	3.38
-2.5	-2.49	0.5	1.57
-2.0	-1.94	0.0	0.93
-1.5	-1.4	-0.5	0.72
-1.0	-0.83	-1.0	0.49
-0.5	-0.44	-1.5	0.44
0.0	-0.19	-2.0	0.09
Cycle-V		-2.5	-0.56
0.0	-0.64	-3.0	-1.71
0.5	-0.51	-3.5	-2.05
1.0	-0.3	-4.0	-2.66
1.5	-0.24	-4.5	-3.12
2.0	0.22	-5.0	-7.01

2.5	1.1	-4.5	-6.61
3.0	1.98	-4.0	-6.41
3.5	3.7	-3.5	-6.06
4.0	5.5	-3.0	-5.81
4.5	6.45	-2.5	-5.51
5.0	11.25	-2.0	-4.75
5.5	12.57	-1.5	-4.01
6.0	20.25	-1.0	-3.11
5.5	19.15	-0.5	-1.65
5.0	18.65	0.0	-0.64
4.5	17.65		
4.0	16.45		
3.5	14.55		
3.0	13.35		
2.5	11.85		
2.0	9.55		
1.5	6.65		
1.0	4.78		
0.5	2.4		
0.0	1.33		